AD_____

Award Number: W81XWH-10-2-0088

TITLE: Advanced MRI in Acute Military TBI

PRINCIPAL INVESTIGATOR: David Brody, M.D., Ph.D.

CONTRACTING ORGANIZATION: Washington University
Saint Louis, MO 63130

REPORT DATE: September 2013

TYPE OF REPORT: Annual

PREPARED FOR: U.S. Army Medical Research and Materiel Command
Fort Detrick, Maryland 21702-5012

DISTRIBUTION STATEMENT: Approved for public release; distribution unlimited

REPORT DOCUMENTATION PAGE

Form Approved
OMB No. 0704-0188

1. REPORT DATE *(DD-MM-YYYY)*	2. REPORT TYPE	3. DATES COVERED *(From - To)*
September 2013	Annual	1 September 2012 - 31 August 2013

4. TITLE AND SUBTITLE

Advanced MRI in Acute Military TBI

5a. CONTRACT NUMBER

5b. GRANT NUMBER
W81XWH-10-2-0088

5c. PROGRAM ELEMENT NUMBER

6. AUTHOR(S)

David L. Brody, M.D., Ph.D.

E-Mail: brodyd@neuro.wustl.edu

5d. PROJECT NUMBER

5e. TASK NUMBER

5f. WORK UNIT NUMBER

7. PERFORMING ORGANIZATION NAME(S) AND ADDRESS(ES)

Washington University
Saint Louis, MO 63130

8. PERFORMING ORGANIZATION REPORT NUMBER

9. SPONSORING / MONITORING AGENCY NAME(S) AND ADDRESS(ES)

U.S. Army Medical Research and Materiel Command
Fort Detrick, Maryland 21702-5012

10. SPONSOR/MONITOR'S ACRONYM(S)

11. SPONSOR/MONITOR'S REPORT NUMBER(S)

12. DISTRIBUTION / AVAILABILITY STATEMENT

Approved for Public Release; Distribution Unlimited

13. SUPPLEMENTARY NOTES

14. ABSTRACT

The objective of the project is to test two advanced MRI methods, DTI and resting-state fMRI correlation analysis, in military TBI patients acutely after injury and correlate findings with TBI-related clinical outcomes 6-12 months later. An additional objective is to test the interaction of candidate genetic vulnerability factors with patterns of injury. These combined methods may add clinically useful predictive information following traumatic brain injury that could be of assistance in standardizing diagnostic criteria for TBI, making return-to-duty triage decisions, guiding post-injury rehabilitation, and developing novel therapeutics. The overarching hypothesis is that traumatic axonal injury, interacting with genetic vulnerability factors, is a principal cause of impaired brain function following blast-related and non-blast-related TBI. The study is a prospective longitudinal study with subject enrollment and initial evaluation at Landstuhl Regional Medical Center in Landstuhl Germany and at 2 sites in Afghanistan. Follow-up evaluations are performed at Washington University in St Louis. We have closed enrollment in all sites as of June 1, 2013. 255 subjects were enrolled at LRMC and 230 subjects were enrolled in Afghanistan. 177 subjects enrolled at LRMC and 70 subjects enrolled in Afghanistan have completed follow-up evaluations There have been no adverse events.

15. SUBJECT TERMS

Traumatic Brain Injury. Blast. MRI. Diffusion Tensor Imaging. Post-traumatic Stress Disorder

16. SECURITY CLASSIFICATION OF:			17. LIMITATION OF ABSTRACT	18. NUMBER OF PAGES	19a. NAME OF RESPONSIBLE PERSON
a. REPORT	b. ABSTRACT	c. THIS PAGE			USAMRMC
U	U	U	UU	66	19b. TELEPHONE NUMBER *(include area code)*

Standard Form 298 (Rev. 8-98)
Prescribed by ANSI Std. Z39.18

Table of Contents

Page

Introduction……..... **4**

Body…… **5**

Key Research Accomplishments…….. **7**

Reportable Outcomes…… **7**

Conclusion…… **7**

References…… **7**

Appendices……... **7**

Introduction

The objective of the project is to test two advanced MRI methods, DTI and resting-state fMRI correlation analysis, in military TBI patients acutely after injury and correlate findings with TBI-related clinical outcomes 6-12 months later. The interaction of candidate genetic vulnerability factors with patterns of injury will be evaluated. These combined methods may add clinically useful predictive information following traumatic brain injury that could be of assistance in standardizing diagnostic criteria for TBI, making return-to-duty triage decisions, guiding post-injury rehabilitation, and developing novel therapeutics.
The overarching hypothesis is that traumatic axonal injury, interacting with genetic vulnerability factors, is a principal cause of impaired brain function following blast-related and non-blast-related TBI.

The specific aims of the proposal are as follows:

Aim 1) To determine whether DTI and fcMRI will noninvasively reveal abnormalities that are not present on CT or conventional MRI acutely following blast-related and non-blast-related TBI. For this aim, the goal was to enroll a total of 200 participants with TBI, 100 with blast-related injuries and 100 with non-blast-related injuries, at LRMC.

Aim 2) To assess the frequency of clinically occult traumatic axonal injury resulting from blast and non-blast mechanisms that is detectible using DTI, fcMRI, and conventional MRI. For this aim, the goal was to enroll a total of 200 participants without TBI but with other injuriesat LRMC during the same 2 year period: 100 with blast-related injuries and 100 with non-blast-related injuries.

Aim 3) To use DTI and fcMRI to clarify the principal similarities and differences between blast-related TBI and TBI due to other mechanisms (e.g. motor vehicle accidents, falls, and direct blows to the head). This will be analyzed using the same 4 groups of participants described above in aims 1 and 2.

Aim 4) To test the hypothesis that specific pattern of injuries detected with these methods will predict specific longer-term neurological and neuropsychological deficits. We will collect detailed clinical information on TBI-related outcomes 6-12 months after injury at Washington University. This will include standardized neurobehavioral assessments, neuropsychological testing, and structured interviews for depression and post-traumatic stress disorder. Several pre-specified hypotheses based on known brain anatomical-clinical correlations will be tested. Also, exploratory approaches will be used as the structural bases for many post-traumatic deficits and disorders are not well understood.

Aim 5) To test the hypothesis that specific genetic factors interact with patterns of injuries to further increase the risk of specific neurological, neuropsychological, and psychiatric deficits and disorders. At follow-up, blood will be drawn for genetic testing. Genetic testing will be performed for *GABRA2* and *FKBP5* polymorphisms associated with PTSD, *5-HTTLPR* polymorphisms associated with increased risk of depression and PTSD following stressors, and *APOE* and *IL1β* genotypes associated with poor recovery from TBI.

Since the last report, the additional funding from DARPA supported the analysis of DTI and clinical data acquired in Afghanistan using MRI scanners installed in that country at 3 US military bases. The hypothesis guiding the studies in Afghanistan is that acute DTI abnormalities after blast-related TBI will reveal axon injury not apparent at later times, and help guide early return-to-duty decisions.

Body

During the third year of the project, we have made substantial progress towards these aims. We have worked closely with clinical coordinators and MRI technologists at Landstuhl regional medical center (LRMC). We have enrolled a total of 255 subjects at LRMC and 230 subjects in Afghanistan. (**Table 1**). The studies are now closed to enrollment as of June 4, 2013.

Group	Number of Subjects Enrolled
LRMC A: Blast exposed active-duty US military controls (no TBI)	35
LRMC B: Blast-related active-duty US military TBI subjects	79
LRMC C: Non-blast-exposed active-duty US military controls (no TBI)	97
LRMC D: Non-blast-related active-duty US military TBI subjects	44
AFG E: Blast-related active-duty US military acute TBI subjects	115
AFG F: Control active-duty US military subjects with other injuries (no TBI)	115

There have been no adverse events. All acute DTI, fcMRI and conventional MRI scans performed using the new Siemens 3T scanner at LRMC have been of good quality. We have successfully transferred MRI data and clinical information to Washington University without breaches of HIPAA regulations or other disclosure of confidential information using our Medweb server.

Dr. David Zonies has served as site PI at LRMC.
Ms. Tess Stewart, RN has continued at LRMC to serve as a research coordinator for our study. In addition Ms Elizabeth Kasten, RN has joined team as a research coordinator. Dr. Mac Donald has trained both coordinators.
The PI and Dr. Mac Donald performed a site visit at LRMC in June, 2013. No concerns were raised.
Dr. Mac Donald has accepted a research faculty position at the University of Washington starting Jan 1, 2014 and will not be supported by the grant after that date.

Dr. Octavian Adam is the PI for the Afghanistan study. Our role at WashU is to perform the DTI analysis, perform 6-12 month clinical evaluations, genetic analyses, and repeat the scans at 6-12 months. This work is supported by additional funds from DARPA transferred to CDMRP and combined with the current grant funds.

At Washington University, our clinical coordinators have performed telephone-based monthly clinical assessments and scheduled in-person follow-up evaluations in St Louis. We have continued to work with our excellent team of psychometricians and clinical psychologists to perform the in-person neuropsychological and psychiatric evaluations. We have performed 247 of these in-person evaluations as of September 2013, 177 on subjects enrolled at LRMC and 70 in Afghanistan. Others have been scheduled through 11/17/2013. There have been no complications arising from the evaluations. All subjects have been able to complete transportation in and out of St. Louis. No adverse effects of repeat MRI scans, neuropsychological testing, and psychiatric evaluations have been observed.

We have continued to use an automated DTI analysis method called DTIStudio. This had yielded excellent and consistent results when compared to hand-drawn region-of-interest analyses. It has substantial advantages in terms of time savings, and covers 130 regions of the brain rather than the 12 regions we were previously analyzing.
We have also begun collaborating with Dr. Carlo Pierpaoli at NIH to determine whether more advanced pre-processing of DTI will improve the data quality.
We have a large, stable excel-based database with all of the data entered and up-to-date.

Dr. Kihwan Han, a post-doctoral fellow in the group, has published a detailed manuscript describing analysis of the fcMRI data (Han et al. 2013). Dr. Han has completed his post-doc and taken a position at UT Southwestern.

Our team has begun preparing several manuscripts detailing our findings.

1) A report comparing the DTI findings across the 4 groups of subjects enrolled at LRMC
2) A report comparing the clinical findings across the 4 groups of subjects enrolled at LRMC
3) A report on the acute clinical status in the subjects enrolled in Afghanistan
4) A report on the imaging findings in the subjects enrolled in Afghanistan
5) A report on the genetic effects on outcomes across both the LRMC and Afghanistan cohorts.

Of these, #2 is the furthest along. A draft is appended to the end of this report.
The major findings so far have been as follows:

1) Clinical outcomes after blast-related TBI and non-blast-related TBI do not substantially differ. Both groups have worse global outcomes than controls, and both groups have similarly high rates of PTSD and depression.
2) Blast-exposed controls had slightly but not significantly worse global outcomes than non-blast-exposed controls, but far better than blast-related TBI subjects
3) Headache severity and PTSD symptom severity were the two major correlates of adverse global outcomes. Neuropsychological test performance, neurological exam findings, self-reported alcohol and drug use were not strongly associated with global outcomes.
4) Self-reported combat exposure intensity was higher in the blast-related TBI and blast-exposed control groups than in the non-blast-related TBI and non-blast-exposed control groups. Combat exposure intensity did not correlated with either global outcome or PTSD severity.

5) **Key Research Accomplishments:**

-Enrollment of 255 subjects at LRMC from all 4 planned groups and 230 subjects in Afghanistan.
-Completion of 247 in-person follow-up evaluations in St Louis.
-Initial Genetic analyses
-Publication of fcMRI analyses

Reportable Outcomes from the Current Project:
Han et al NeuroImage 2013.

Abstracts and Presentations:
The PI and Dr. Mac Donald presented aspects of the results at several meetings and seminars:

1. 2013 MHSRS meeting.
2. 2013 Workshop on Genetic Disease Models of Psychiatric and Neurological Diseases, Utrecht, NL
3. 2013 American Society for Neural Therapy and Repair, Clearwater, FL
4. 2013 Academy of Sciences, St Louis
5. 2013 Toronto Sick Kids Head Injury in Sport meeting
6. 2013 Johns Hopkins University TBI conference

Conclusion:

The study has closed enrollment with approximately 5/8 of the projected total at LRMC but an extra cohort from Afghanistan. During the next period, we expect to complete the 6-12 month follow-ups and fully analyze the acquired imaging, clinical, and genetic data.

References:

1 Han, K., Mac Donald, C. L., Johnson, A. M., Barnes, Y., Wierzechowski, L., Zonies, D., Oh, J., Flaherty, S., Fang, R., Raichle, M. E. and Brody, D. L. (2013). "Disrupted modular organization of resting-state cortical functional connectivity in U.S. military personnel following concussive 'mild' blast-related traumatic brain injury." Neuroimage **84C**: 76-96. http://www.ncbi.nlm.nih.gov/pubmed/23968735

Appendices:
Mac Donald et al, in preparation.
Han et al NeuroImage 2013.

NeuroImage 84 (2014) 76–96

Contents lists available at ScienceDirect

NeuroImage

journal homepage: www.elsevier.com/locate/ynimg

Disrupted modular organization of resting-state cortical functional connectivity in U.S. military personnel following concussive 'mild' blast-related traumatic brain injury ☆

Kihwan Han [a], Christine L. Mac Donald [a], Ann M. Johnson [b], Yolanda Barnes [c], Linda Wierzechowski [c], David Zonies [c], John Oh [c], Stephen Flaherty [c], Raymond Fang [c], Marcus E. Raichle [a,d,e,f,g], David L. Brody [a,*]

[a] Department of Neurology, Washington University School of Medicine, St. Louis, MO, USA
[b] Center for Clinical Studies, Washington University School of Medicine, St. Louis, MO, USA
[c] Department of Trauma and Critical Care, Landstuhl Regional Medical Center, Landstuhl, Germany
[d] Department of Radiology, Washington University School of Medicine, St. Louis, MO, USA
[e] Department of Neurobiology, Washington University School of Medicine, St. Louis, MO, USA
[f] Department of Biomedical Engineering, Washington University School of Medicine, St. Louis, MO, USA
[g] Department of Psychology, Washington University School of Medicine, St. Louis, MO, USA

ARTICLE INFO

Article history:
Accepted 9 August 2013
Available online 20 August 2013

Keywords:
Functional connectivity
Traumatic brain injury
Graph theory
Modularity
Functional magnetic resonance imaging (fMRI)
Blast injury

ABSTRACT

Blast-related traumatic brain injury (TBI) has been one of the "signature injuries" of the wars in Iraq and Afghanistan. However, neuroimaging studies in concussive 'mild' blast-related TBI have been challenging due to the absence of abnormalities in computed tomography or conventional magnetic resonance imaging (MRI) and the heterogeneity of the blast-related injury mechanisms. The goal of this study was to address these challenges utilizing single-subject, module-based graph theoretic analysis of resting-state functional MRI (fMRI) data. We acquired 20 min of resting-state fMRI in 63 U.S. military personnel clinically diagnosed with concussive blast-related TBI and 21 U.S. military controls who had blast exposures but no diagnosis of TBI. All subjects underwent an initial scan within 90 days post-injury and 65 subjects underwent a follow-up scan 6 to 12 months later. A second independent cohort of 40 U.S. military personnel with concussive blast-related TBI served as a validation dataset. The second independent cohort underwent an initial scan within 30 days post-injury. 75% of the scans were of good quality, with exclusions primarily due to excessive subject motion. Network analysis of the subset of these subjects in the first cohort with good quality scans revealed spatially localized reductions in the participation coefficient, a measure of between-module connectivity, in the TBI patients relative to the controls at the time of the initial scan. These group differences were less prominent on the follow-up scans. The 15 brain areas with the most prominent reductions in the participation coefficient were next used as regions of interest (ROIs) for single-subject analyses. In the first TBI cohort, more subjects than would be expected by chance (27/47 versus 2/47 expected, $p < 0.0001$) had 3 or more brain regions with abnormally low between-module connectivity relative to the controls on the initial scans. On the follow-up scans, more subjects than expected by chance (5/37, $p = 0.044$) but fewer subjects than on the initial scans had 3 or more brain regions with abnormally low between-module connectivity. Analysis of the second TBI cohort validation dataset with no free parameters provided a partial replication; again more subjects than expected by chance (8/31, $p = 0.006$) had 3 or more brain regions with abnormally low between-module connectivity on the initial scans, but the numbers were not significant (2/27, $p = 0.276$) on the follow-up scans. A single-subject, multivariate analysis by probabilistic principal component analysis of the between-module connectivity in the 15 identified ROIs, showed that 31/47 subjects in the first TBI cohort were found to be abnormal relative to the controls on the initial scans. In the second TBI cohort, 9/31 patients were found to be abnormal in identical multivariate analysis with no free parameters. Again, there were not substantial differences on the follow-up scans. Taken together, these results indicate that single-subject, module-based graph theoretic analysis of resting-state fMRI provides potentially useful information for concussive blast-related TBI if high quality scans can be obtained. The underlying biological mechanisms and consequences of disrupted between-module connectivity are unknown, thus further studies are required.

☆ The views and opinions expressed in this article are those of the authors and do not reflect the official policy or position of the Department of the Army, Department of the Air Force, Department of Defense or United States Government.

* Corresponding author at: Department of Neurology, Washington University in St. Louis, 660 South Euclid Avenue, Box 8111, St. Louis, MO 63110, USA. Fax: +1 314 362 3279.
E-mail address: brodyd@neuro.wustl.edu (D.L. Brody).

1053-8119/$ – see front matter © 2013 Elsevier Inc. All rights reserved.
http://dx.doi.org/10.1016/j.neuroimage.2013.08.017

Introduction

Traumatic brain injury (TBI) has been called a "signature injury" in the wars of Iraq and Afghanistan (Okie, 2006). As of the first quarter of 2012, the total incidence of TBI in U.S. military personnel since 2000 is 244,217 with 76.8% of these incidents concussive or 'mild' TBI (Defense Medical Surveillance System and Theater Medical Data Store, http://www.health.mil/Libraries/TBI-Numbers-Current-Reports/dod-tbi-worldwide-2000-2012Q1-as-of-120516.pdf). Concussive or 'mild' TBI is characterized by loss of consciousness up to 30 min, altered consciousness and mental state up to 24 h, post-traumatic amnesia up to 24 h and the absence of abnormalities in computed tomography or conventional magnetic resonance imaging (MRI) (Casscells, 2007). However, utilizing advanced neuroimaging techniques such as functional magnetic resonance imaging (fMRI), diffusion tensor imaging (DTI), magnetoencephalography and electroencephalography, reports have described abnormalities in concussive TBI subjects (e.g., fMRI: Scheibel et al. (2012), Shumskaya et al. (2012), Slobounov et al. (2011), Tang et al. (2011); DTI: Levin et al. (2010), Mac Donald et al. (2011), Niogi et al. (2008), Niogi and Mukherjee (2010), Shenton et al. (2012); fMRI and DTI: Mayer et al. (2011); magnetoencephalography: Castellanos et al. (2010, 2011); electroencephalography and DTI: Sponheim et al. (2011)).

Most of these previous functional neuroimaging studies in TBI have focused on group comparisons and have adopted hypothesis-driven approaches with predefined regions of interest, seed, or networks of interests. However, high individual variability of functional topology (van Essen and Dierker, 2007) is a major source of variability in group analysis in healthy normal subjects. In TBI populations, the heterogeneity of injury types and locations (Doppenberg and Bullock, 1997; Saatman et al., 2008) further increases between-subject variability. In blast-related TBI (bTBI), the heterogeneity is further increased by the variety of blast-related injury mechanisms. Blast-related injuries may occur by (1) blast overpressure inducing mechanical damage to the brain, (2) having the head struck by debris or other objects set in motion by the blast, (3) being thrown to the ground or against another stationary object or (4) inhaling toxic fumes, smoke or dust (Finkel, 2006; Warden, 2006). Different combinations of these injury types and other variables such as direction, distance and open field versus enclosed space associated with the blast exposures may make group analysis insufficient for the assessment of bTBI. The aforementioned heterogeneity of concussive bTBI also increases the chance for hypothesis-driven approaches with predefined regions or networks of interest to miss regions or networks with alterations of functional connectivity in concussive bTBI patients. Thus, single-subject based, data-driven approaches would be more meaningful in these heterogeneous concussive bTBI populations.

Recently, graph theory has become increasingly popular in neuroimaging research (see Rubinov and Sporns (2010) and Bullmore and Sporns (2009) for reviews), offering new insights into the understanding of the brain as a complex network. Several studies (Achard et al., 2006; He et al., 2007; Salvador et al., 2005; van den Heuvel et al., 2008) have found that the brain network has economical 'small world' properties having high levels of clustering and a short path length for efficient global and local communications (Latora and Marchiori, 2001; Watts and Strogatz, 1998). Early studies of graph theoretic analysis in clinical populations have demonstrated disrupted 'small world' properties in patients with dementia of the Alzheimer's type (Stam et al., 2006), schizophrenia (Micheloyannis et al., 2006) and epilepsy (Ponten et al., 2007). Taking advantage of the 'small world' properties of the brain network, subsequent studies (Chen et al., 2008; Hagmann et al., 2008; He et al., 2009; Power et al., 2011; Valencia et al., 2009; Yeo et al., 2011b) have identified a modular or community structure of the normal, healthy human brain. With regard to clinical populations, Valencia et al. (2009) raised the possibility that characterizing the modular structure of the brain may be important to understand the brain organization during different pathological or cognitive states. Indeed, graph theoretic analysis of magnetoencephalography data has revealed a disrupted modular structure in patients with dementia of the Alzheimer's type (de Haan et al., 2012).

Another advantage of graph theoretic analyses over simple network approaches is that they do not require assumptions regarding hypothesized (thus predefined) seed regions or networks of interest. Thus, in this regard, graph theoretic analyses are useful in heterogeneous populations. With this advantage in heterogeneous populations over simple network approaches, recent studies (Caeyenberghs et al., 2012; Castellanos et al., 2011; Nakamura et al., 2009; Pandit et al., 2013) have utilized graph theoretic analyses to provide a more comprehensive understanding of abnormal functional connectivity in TBI patients. In particular, Nakamura et al. (2009) demonstrated disrupted 'small worldness', defined as the level of clustering relative to path length, of functional networks in patients with moderate to severe TBI. To our knowledge, there are no previous studies that have investigated modular structure in resting-state functional connectivity MRI in patients with bTBI or any other concussive 'mild' TBI populations (though Pandit et al. (2013) included a wide range of injury severities).

In this study, we posited that module-based connectivity in patients with concussive bTBI may be disrupted. In our previous report (Mac Donald et al., 2011), we demonstrated DTI 'abnormalities' in white matter integrity of active duty U.S. military personnel with concussive bTBI relative to controls who had blast exposure but no diagnosis of TBI. At the time of the DTI and structural MRI collections in each of these subjects, resting-state blood oxygenation level dependent (BOLD) fMRI scans were also acquired. Here, we assessed modular organization of these active duty U.S. military personnel with concussive bTBI, utilizing whole brain, module-based graph theoretic analysis of these resting-state BOLD fMRI scans. Because of the heterogeneity of the concussive bTBI patients, we investigated module-based resting-state network properties at both the group and single-subject levels.

Materials and methods

Subjects

Three groups (controls and two TBI cohorts) of active duty U.S. military personnel deployed to the wars in Iraq and Afghanistan participated in this study. All of them had been exposed to blasts in a combat environment. The two TBI cohorts had sustained clinically diagnosed bTBI. The 21 controls (20 males; 19–49 years old with median = 29; 11–17.5 years of education with median = 12.5) had other injuries but screened negative for TBI (Dempsey et al., 2009). The first TBI cohort (TBI I cohort) consisted of a subset of the subjects about which we have reported previously (Mac Donald et al., 2011). Screening, enrollment, and initial scans were performed at the Landstuhl Regional Medical Center (LRMC), a U.S. Military hospital in Landstuhl, Germany. 63 TBI patients (all males; 19–57 years old with median = 25; 8–17 years of education with median = 12) were diagnosed with mild, uncomplicated traumatic brain injury based on the criteria from the Department of Defense (Casscells, 2007), marked by less than 30 min of loss of consciousness and the absence of abnormalities in conventional MRI and CT. Post blast exposure time on the initial scans at LRMC were within 90 days (median = 14). After 6–12 months from their initial scans, 65 of these subjects traveled to Washington University in St. Louis for follow-up scans. More details and demographics of this cohort are in Mac Donald et al. (2011).

The same screening criteria as on the TBI I cohort and controls allowed the second TBI cohort (TBI II cohort) to comprise 40 additional concussive bTBI patients (37 males; 19–44 years old with median = 23; 9–16 years of education with median = 12). The TBI II cohort underwent the initial scans within 30 days (median = 7) after the blast exposure. After 6–12 months from their initial scans, 32 out of these subjects underwent follow-up scans at Washington University in St. Louis. The first cohort

underwent initial scans in 2008–2009 whereas the second cohort was scanned in 2010–2011.

All subjects participated in this study after obtaining written informed consent and this study was approved by the Human Research Protection Office at Washington University in St. Louis, the Institutional Review Board for LRMC at Brooke Army Medical Center, and the Clinical Investigation Regulatory and Human Research Protection Offices of the U.S. Army Medical Research and Materiel Command. This study was also registered at clinicaltrials.gov (NCT00785304).

MRI data acquisition

Both initial scans at LRMC and follow-up scans in St. Louis were acquired using Siemens Magnetom Avanto 1.5 T MRI scanners (Siemens, Germany) with identical imaging protocols. In each imaging session, three 412.5-second runs (total 1237.5 s) of resting-state BOLD fMRI were acquired using a 12-channel phase-arrayed head coil supplied by the manufacturer with T_2^*-weighted blipped EPI sequence (TR/TE = 2500/50 ms; flip angle (FA) = 90°; field of view (FOV) = 25.6 × 25.6 cm; matrix = 64 × 64) to obtain 165 images of each of 30 axial slices (4.0 mm thick) of the whole cerebrum. During resting-state fMRI acquisition, the subjects were asked to remain still during the scan, but no specific requests were made regarding eyes open versus eyes closed and no specific attempts were made to keep subjects awake. In the setting of acute injury, this was not feasible as some subjects had orbital injuries and extracranial injuries and analgesic medications after enrollment. See the Discussion for the relevant limitations of the study findings due to these constraints.

For surface reconstruction and alignment to resting-state BOLD fMRI of each subject, the same head coil was used with one high resolution T_1-weighted sagittal magnetization prepared rapid acquisition gradient echo (MPRAGE) image of the whole brain (TR/TE = 2000/2.92 ms; FA = 8°; FOV = 25.6 × 25.6 cm; matrix = 256 × 256; 176 slices, 1.0 mm thick).

MRI preprocessing

Briefly, our analyses consisted of cortical surface reconstruction of structural MRI, preprocessing of resting-state BOLD fMRI, projection of BOLD fMRI onto the reconstructed cortical surface, network construction and finally graph theoretic analysis (see Fig. 1). We used Freesurfer (Dale et al., 1999; Fischl et al., 1999a, 2002) for cortical surface reconstruction of structural MRI, AFNI (Cox, 1996) for fMRI preprocessing and SUMA (Saad et al., 2004) for surface mapping and surface-based analysis of fMRI time series. fMRI data were preprocessed in the three dimensional subject-native space of each participant.

Surface reconstruction of structural imaging

Cortical surface reconstruction (Figs. 1(a) to (b)) was performed with the Freesurfer image analysis suite (version 5.1.0), online documented and freely available for download (http://surfer.nmr.mgh.harvard.edu/). The technical details of these procedures are described in previous publications (Dale and Sereno, 1993; Dale et al., 1999; Fischl et al., 1999a,b, 2001, 2002, 2004a,b; Jovicich et al., 2006; Segonne et al., 2004). Cortical surface reconstruction results for each image of the subjects were visually inspected to ensure the accuracy of skull stripping, Talairach transformation, gray/white matter boundary (white surface), gray matter/cerebrospinal fluid boundary (pial surface) and cerebral cortex labeling. When necessary, manual intervention was performed in order for Freesurfer to correctly reconstruct the cortical surface. The surface reconstruction was performed unblinded to group membership. See the Discussion for the limitation of this study related to manual intervention and unblindness to group membership.

fMRI preprocessing

Volumetric BOLD fMRI data were preprocessed (Figs. 1(c) to (d)) with standard methods using a modified version of a shell script generated by *afni_proc.py* (http://afni.nimh.nih.gov/pub/dist/doc/program_help/afni_proc.py.html) from AFNI (Cox, 1996). Each subject's whole-brain structural images were first skull-stripped and coregistered (affine transform with 12 parameters) to the fifth time point of the first fMRI run. For each fMRI run, the initial four time points were discarded to allow T_1 magnetization saturation. Standard preprocessing methods were then used, including despiking, slice timing correction, motion correction, normalization to whole brain mode of 1000, linear regression and band-pass filtering ($0.009 < f < 0.08$ Hz). At the motion correction stage, the 6 rigid body motion profiles were obtained for the linear regression. After the motion correction, subject masks indicating voxels that have an fMRI signal were obtained for each of the subjects. In the linear regression, several sources of signal fluctuation unlikely to be of neuronal origin were regressed out as the nuisance variables: (1) six parameters for the rigid body head motion acquired from the motion correction (Johnstone et al., 2006), (2) the signal averaged over the lateral ventricles, (3) the signal averaged over a region centered in the deep cerebral white matter, (4) the signal averaged over the whole brain (Fox et al., 2005; see the control analyses and their results for the effects of global signal regression on graph theoretic analysis) and (5) the first temporal derivatives of aforementioned parameters. After the band-pass filtering, motion 'scrubbing' (Power et al., 2012) was performed with a frame-to-frame head movement rate of 0.12 mm/s and a standardized DVARS (http://www2.warwick.ac.uk/fac/sci/statistics/staff/academic-research/nichols/scripts/fsl/DVARS.sh) of 1.49 to prevent potential motion artifacts (Power et al., 2012; Satterthwaite et al., 2012; van Dijk et al., 2012). To prevent the introduction of artificial correlations in the fMRI signal between voxels (1) adjacent to each other in space, but distant in terms of cortical surface topology (e.g., voxels on opposite sides of the midline) or (2) that were located near the boundary of functional subdivisions unrelated to each other in functional connectivity (e.g., primary motor versus primary somatosensory cortex), spatial smoothing was not applied at this preprocessing step (van den Heuvel et al., 2008).

Inter-subject alignment and surface mapping of volumetric fMRI

The total number of mesh nodes in the reconstructed cortical surface by Freesurfer varies across subjects. To allow for cross-subject analysis while preserving the geometry of sulcal and gyral patterns in the original surface of each individual and minimizing unnecessary interpolation artifacts (Argall et al., 2006), we used SUMA (Saad et al., 2004) to standardize surface meshes (i.e., coordinates) of each individual (i.e., the total number of mesh nodes is the same across subjects and each mesh node corresponds to the same anatomical location in each surface of the subjects). When calculating new coordinates, SUMA allowed us to set the total number of mesh nodes in the standard mesh surface of each subject (Fig. 1(e)) to be 11,524 so that the average distance between two nodes (3.7 mm) is close to the spatial resolution of original volumetric fMRI data (4 mm isotropic) while maintaining topology shown in the original high resolution (1 mm isotropic) structural MRI.

Volumetric functional time series were then projected onto the standard mesh surfaces of each subject by interpolating the time series located along the line between two matching nodes of the white and pial surfaces. For each mesh node, five equally-spaced coordinates were sampled between corresponding white and pial surfaces. At each time point, functional data were projected by averaging across the unique 3D voxels belonging to these coordinates. Consequently, surface-based functional time series (Fig. 1(f)) contained signals only from voxels within the cortical gray matter. In the same way, the voxel-based subject masks were converted to surface-based subject masks. For more technical details of the surface mapping procedure, readers are referred to Saad et al. (2004). Due to susceptibility artifacts (Ojemann et al., 1997) and inclusion of only cortical surface areas (i.e., exclusion of the surface areas of the amygdala, putamen, hippocampus,

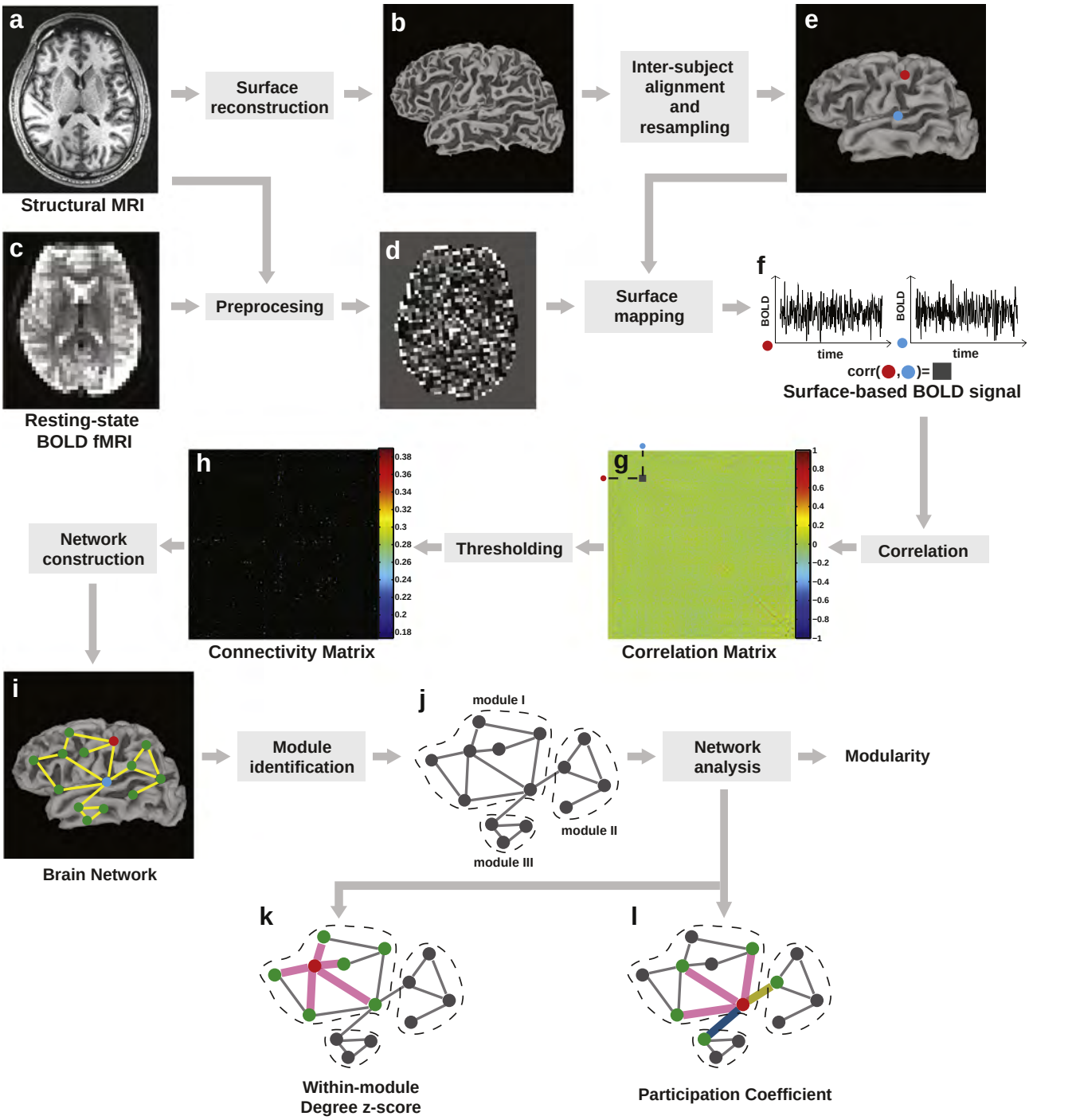

Fig. 1. An illustration of the analysis procedure. For each subject, with volumetric structural MRI data (a), cortical surface (b) was reconstructed. Subsequently, the surface underwent the inter-subject alignment and spatial resampling close to the spatial resolution of resting-state BOLD fMRI (c) to allow surface-based, node-by-node cross-subject analyses. The preprocessed resting-state BOLD fMRI data (d) were converted to surface-based BOLD signal data (f) aligned to the individual cortical surface (e). BOLD fluctuation correlation coefficients between every pair of nodes in the brain (e.g., the gray square from red and cyan nodes in (e)) were obtained to yield a correlation matrix (g). A connectivity matrix (h) was derived by thresholding the correlation matrix, and a brain network (i) was constructed. In this illustration, yellow lines indicate connection between nodes. With the identified modules (three modules delineated by dashed lines in this example) in (j), modularity, within-module degree z-score (e.g., five magenta lines for the red-colored node in (k)) and participation coefficient (e.g., the distribution of magenta, cyan and olive lines for the red-colored node in (l)) were obtained for each node.

caudate, ventricles and corpus callosum), not all nodes had an fMRI signal, and surface-based subject masks indicating existence of an fMRI signal on mesh nodes were different across the subjects. Thus, to make a comparison across subjects, further analyses on network measures considered only the mesh nodes (8977 nodes) having an fMRI signal across all subjects. This was performed by obtaining a subject-intersection mask and subsequently applying the intersection mask to surface-based functional time series of each of the subjects.

Quality assurance

We restricted our analysis to the subjects whose data quality was reliable within a tolerable range. In the cortical surface reconstruction

step, the quality of T_1 images was visually inspected to determine if surface reconstruction was feasible. In fMRI preprocessing, the quality of preprocessed data was visually inspected at each step. After visual inspection, a subset of subjects' data was excluded for the following reasons: (1) a superior part of the functional images did not fall within the prescribed FOV due to substantial run-to-run change of head position, (2) intensity variation artifacts of low spatial frequency presumably due to constant oscillating head movement in a certain direction, (3) substantial susceptibility artifacts (Ojemann et al., 1997) in inferior frontal and inferior temporal regions, (4) motion correction failure due to a large amount of abrupt motion and (5) lack of fMRI frames due to subject's refusal to stay in the scanner. After motion 'scrubbing', additional subjects' data were excluded if the total length of remaining volumes after the 'scrubbing' was less than 4 min, the minimum length required to reliably estimate functional connectivity (van Dijk et al., 2010). See Table 1 for the details of the number of datasets excluded by this quality assurance procedure.

Visual inspection on each module of the subjects identified by the Louvain algorithm allowed us to verify that, in 1 control, 4 TBI I and 2 TBI II subjects on the initial scans and 1 control and 1 TBI II subjects on the follow-up scans, the total number of modules was too few (less than 3) or module assignments were severely scattered yielding failure to identify major modules shown in group module assignment maps (Fig. 2). Thus, we conservatively excluded datasets with unidentifiable major modules in subsequent analyses as we could not be sure whether these module assignments were results of subjects' condition or merely failures of the module identification algorithm (Table 2).

After quality assurance exclusion, we analyzed functional images of 12/21 control subjects on the initial scans, 12/18 control subjects on the follow-up scans, 47/63 TBI I subjects on the initial scans, 37/47 TBI I subjects on the follow-up scans, 31/40 TBI II subjects on the initial scans and 27/32 TBI II subjects on the follow-up scans for the subsequent network analyses. Thus, 75% of all subjects' data acquired as described above were of sufficient quality for further analyses. Note that we included subjects' data if the data passed the quality assurance procedure for each scan separately. In other words, after the quality assurance procedure, included subjects on the follow-up scan analyses were no longer an exact subset of subjects included on the initial scan analyses.

Network analysis

Network construction

Weighted and undirected networks were constructed (Figs. 1(g)–(i)) for module-based graph theoretic analysis. For the network analysis, a node, a basic element of graph theoretic analysis, was defined as a mesh node in the cortical surface. An edge of the graph was defined from the correlation matrix (Fig. 1(g)) whose components are Pearson correlation coefficients of time series at each pair of the mesh nodes in the brain. In other words, the weights of the edges were the correlation coefficients. An alternative to Pearson correlation coefficients would be the partial correlation coefficients. The partial correlation coefficients control for the influence of correlations from the other nodes on a correlation between two nodes of interest, which could replace global signal regression. Unfortunately, it was not feasible to use partial correlation coefficients in this study since the inversion of the covariance matrix to obtain the partial correlations was numerically unstable. More specifically, the total number of frames has to be greater than total number of nodes to ensure a numerically stable estimation of the inverse covariance matrix. However, total number of frames (at most 495 frames) was far less than the total number of nodes (8977 nodes) in our case. Thus, we proceeded with the use of Pearson product moment correlations as edge weights.

Correlation coefficients between time series at short-distance nodes (20 mm in Euclidean distance), presumably associated with non-biological origins such as increased correlation by preprocessing and subject motion, were excluded in selecting edges of the graph (Power et al., 2011). The remaining correlation coefficients were thresholded at 3% tie density, i.e., the density of the retained strongest correlations, to define edges of the graph (a colored dot and a yellow line in Figs. 1(h) and (i), respectively) for most analyses. Sparse tie densities were selected since module identification algorithms perform reliably when graphs are sparse (Fortunato, 2010). Further, inclusion of weak correlation coefficients (i.e., high tie density) could yield less reliable module-based graph measures due to artificial correlations between noise time courses. In addition, we explored the effects of 2% and 1.5% tie densities. For less than 1.5% tie densities, the TBI patients had excessive numbers of 'trivial' modules making it difficult to fairly compare the remaining major modules of the TBI groups with those of the controls. These 'trivial' modules were defined as <1% of brain nodes; most generally had a single node without connection to other nodes. In these thresholding procedures, only positive correlation coefficients were considered for the network connections, as there is ongoing debate about the meaning of negative correlations assessed after global signal regression (Anderson et al., 2011; Chai et al., 2012; Chang and Glover, 2009; Fox et al., 2009; Murphy et al., 2009; Saad et al., 2012).

Module identification and module-based network properties

With the constructed weighted and undirected brain networks, module-based graph theoretic analysis was performed using brain connectivity toolbox in MATLAB (Rubinov and Sporns, 2010) freely available online (http://www.brain-connectivity-toolbox.net) after applying the previously described subject-intersection mask for the nodes having functional times series across all subjects. First, the modules were identified (Fig. 1(j)). After module identification, global and node-specific module-based network properties were obtained.

Identification of modules is a complex and computationally demanding problem. For the module identification, the modularity of a weighted and undirected network, Q_M^w, was defined:

$$Q_M^w = \sum_{s=1}^{M} \left[l_s/L - (d_s/2L)^2 \right],$$

Table 1
Excluded datasets after the quality assurance procedure.

Criteria	Ctrl		TBI I		TBI II		Total
	Initial	Follow-up	Initial	Follow-up	Initial	Follow-up	
Poor T_1 image quality	0	0	1	0	0	0	1
Brain outside FOV	1	0	1	0	3	1	6
Motion correction failure	1	0	1	0	0	0	2
Lack of frames	0	0	1	0	0	0	1
Intensity distortion	0	0	1	0	0	0	1
Susceptibility artifacts	1	1	0	1	0	0	3
<4 min of data after motion scrubbing	5	4	7	9	4	3	32
Unidentifiable major modules	1	1	4	0	2	1	9
Total	9	6	16	10	9	5	55

Note: FOV, field of view; Ctrl, control; TBI I, TBI I cohort; TBI II, TBI II cohort.

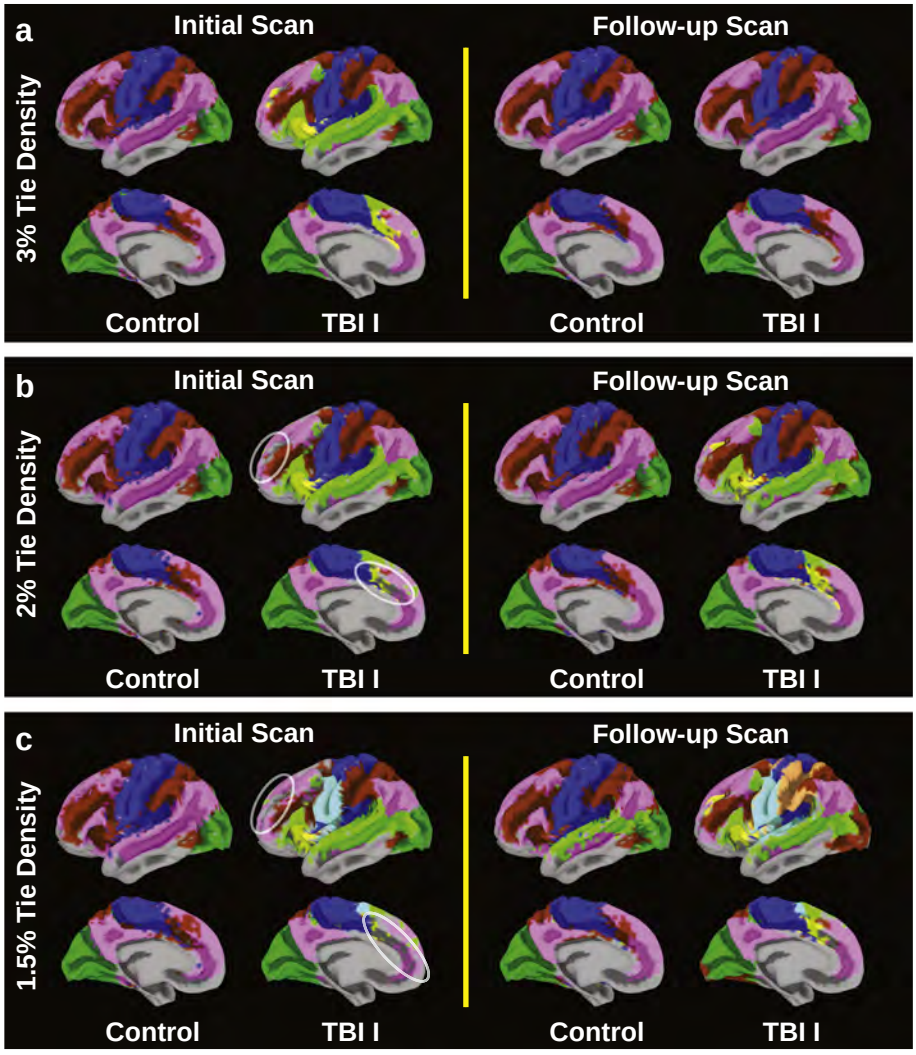

Fig. 2. Group module assignments of each of the controls and the first TBI (TBI I) cohort. The identified modules from group averaged correlation matrices were color-coded as a function of tie densities (densities of the retained strongest correlations): 3% (a), 2% (b) and 1.5% (c). Only modules of sizes greater than 1% of the total number of nodes were displayed.

where M is the number of modules, l_s is the sum of the weights of all within-module connections in the module s, L is the total sum of all weights in the network, d_s is the sum of the strength at each node in the module s and the strength of a node is the sum of the weights of all edges associated with the given node (Guimera and Amaral, 2005; Newman, 2004). In theory, Q_M^w is bounded between 0 and 1 (Guimera and Amaral, 2005; Newman, 2004). $Q_M^w = 0$ when nodes are randomly partitioned or all nodes belong to the same module. Thus, higher modularity means deviations from random networks with no community structure. In practice, the modularity of typical networks with a strong modular structure ranges from 0.3 to 0.7, and higher values are rare (Newman and Girvan, 2004). Assuming the brain network has a modular structure (i.e., many within-module connections whereas few between-module connections), a module identification algorithm optimizes the total number of modules and the associated module membership of nodes for maximum modularity. For the implementation of our analysis, we used the Louvain algorithm (Blondel et al., 2008), a fast and relatively accurate algorithm, suitable for large networks. Due to the

Table 2
Demographics of the controls, TBI I cohort and TBI II cohort.

Demographics[a]	Ctrl, all (N = 21)	Ctrl, subset[b] (N = 14)	TBI I, all (N = 63)	TBI I, subset[b] (N = 54)	TBI II, all (N = 40)	TBI II, subset[b] (N = 38)
Age (years)[c]	19–49, 29	20–49, 29	19–57, 25	19–44, 24	19–44, 23	19–44, 23
Gender (males, females)	20, 1	14, 0	63, 0	54, 0	37, 3[e]	35, 3[f]
Education (years)[c]	11–17.5, 12.5	11–16, 12	8–17, 12	8–17, 12	9–16, 12	9–16, 12
Post-injury time (days)[c, d]	N/A	N/A	0–90, 14	0–90, 14	0–30, 7	0–30, 7

[a] Demographics of the controls and TBI I cohort were reproduced from Table 1 in Mac Donald et al. (2011).
[b] Subsets of subjects that were included in graph theoretic analyses of either the initial scans, the follow-up scans, or both.
[c] Range and median values were reported.
[d] Post-injury time on the day of the initial scan.
[e] $p < 0.05$ (chi-square) vs. TBI I, all.
[f] $p < 0.05$ (chi-square) vs. TBI I, included subset.

"heuristic" nature of this algorithm (i.e., a 'good enough' approximation of the exact solution is implemented, resulting in faster execution time), the module identification algorithm was executed ten times. Then, we selected a single module identification result from among the 10 executions that yielded the highest modularity to report modularity and assess subsequent module-based network measures. Overall, the variation of modularity over the executions was negligible, as in Blondel et al. (2008). For comparison, we additionally identified modules using the Infomap algorithm (Rosvall and Bergstrom, 2008), another module identification algorithm (see Supplemental Figs. S2, S3).

Given the identified modules, weighted within-module degree *z*-score (Fig. 1(k); Guimera and Amaral, 2005) and weighted participation coefficient (Fig. 1(l); Guimera and Amaral, 2005) were measured at each node of the individual brain network. In calculating within-module degree *z*-scores and participation coefficients, we excluded trivial modules whose sizes were less than 1% of the total number of nodes.

Briefly, weighted within-module degree *z*-score of node *i*, z_i^w, measures the normalized strength of connections from a node within the corresponding module *s*. z_i^w can be written as:

$$z_i^w = \left(k_i^w(s_i) - \overline{k^w}(s_i)\right)/\sigma_{k^w(s_i)},$$

where s_i is the module containing node *i*, $k_i^w(s_i)$, within-module strength, is the total sum of weights of edges connecting node *i* and all other nodes within s_i, $\overline{k^w}(s_i)$ and $\sigma_{k^w(s_i)}$ are the respective mean and standard deviation of the $k_j^w(s_i)$ for all nodes $j \in s_i$. So, high weighted within-module degree *z*-score of a node means that the node has a larger than expected strength within its own module.

The weighted participation coefficient of node *i*, PC_i^w, is defined as:

$$PC_i^w = 1 - \sum_{s=1}^{M} \left(k_i^w(s)/k_i^w\right)^2,$$

where $k_i^w(s)$ is the total sum of weights of edges connecting node *i* and all other nodes in module *s* and k_i^w,strength of node *i*, is the total sum of weights of edges connecting between node *i* and all other nodes in the entire network. The weighted participation coefficient shows how well a node communicates with other modules. The weighted participation coefficient is close to 1 if the distribution of connections at a node across modules is uniform. The weighted participation coefficient becomes 0 if there is no inter-module connection. A high value of the weighted participation coefficient means nodes' inter-module connections are 'well-distributed' over multiple modules, thus are likely to span more modules.

Each node-specific measure was then spatially smoothed (10 mm full-width-at-half-maximum (FWHM)) on the cortical surface of each individual to increase signal-to-noise ratio as in van den Heuvel et al. (2008). To identify 'abnormal' regions in the TBI patients, we counted the number of patients whose network measures were outside two standard deviations from the mean of the controls.

Region of interest analysis

In the region of interest (ROI) analysis, the TBI I cohort served as an exploratory dataset to identify functional ROIs exhibiting a noticeable difference in node-specific network measures between the controls and TBI patients from the TBI I cohort. The TBI II cohort served as a validation dataset with no free parameters with regard to ROI selection. Surface-based ROIs were selected on the standard mesh template in reference to the Destrieux surface atlas (Destrieux et al., 2010) using SUMA (Saad et al., 2004) to define the center of each ROI. Similar to the method described in Hagler et al. (2006), we slid a threshold level between $p_{uncorr} = 0.05$ and 0.01 from the group comparison map for participation coefficients to identify functional ROIs. We first identified ROI candidates with cluster area (white matter surface) greater than 150 mm^2 at $p_{uncorr} = 0.05$. Then we subdivided large clusters in reference to the Destrieux atlas (Destrieux et al., 2010) and slid the threshold level up to $p_{uncorr} = 0.01$. With peaks that survived at $p_{uncorr} = 0.01$, we selected ROIs comprising nodes within 15 mm geodesic distance (along the white matter surface) from the peaks and whose $p_{uncorr} < 0.05$. If nodes within 15 mm geodesic distance from the peaks of these preliminary ROIs were part of 2 neighboring ROIs such that there was overlap, the boundaries of these ROIs were determined by sliding the threshold down from $p_{uncorr} = 0.01$ towards 0.05 allowing the clusters to grow until the ROIs reached the edge of the neighboring clusters. With these identified ROIs from the first dataset (i.e., the controls versus TBI I cohort), we performed ROI analysis on the second dataset (i.e., the controls versus TBI II cohort). For each ROI, we defined that a TBI patient had an 'abnormal' network measure relative to the controls in the ROI if the average network measure of the patient in the ROI was outside the mean plus or minus two-standard deviation band of the control group. This procedure to identify TBI patients with 'abnormal' network measure in ROIs was carried out after the normality test of the controls' ROI-specific network measures.

Multivariate region of interest analysis

A multivariate approach was then used to decide which TBI patients had 'abnormal' measures relative to the controls over all ROIs by aggregating average node-specific measures within each of the ROIs. After confirming that controls' network measure at each ROI passed the normality test, multivariate Gaussian distribution of the network measures for the controls was estimated. Since the sample size of the controls after the module identification was small compared to the number of ROIs, estimating the covariance structure was challenging. In order to circumvent this 'curse of dimensionality' issue (Duda et al., 2001), the vector dimension was reduced using probabilistic principal component analysis (PPCA; Minka, 2000). PPCA automatically estimates the number of reduced components preserving the variability of the original high dimensional vector while eliminating spurious and noisy components. Based on reduced components of ROI-based network measures via PPCA, we defined relatively 'abnormal' TBI patients whose components were located within the lower and upper tails (less than the 2.5th percentile and greater than the 97.5th percentile) of the estimated multivariate normal distribution from the controls.

Statistical analyses

All statistical analyses were assessed in MATLAB. First, we performed the Shapiro–Wilk test at $\alpha = 0.05$ to assess the normality of distributions of each group's demographics (age, years of education and post-injury time at the initial scan) and each network measure. The aforementioned demographics did not pass the Shapiro–Wilk normality test. Thus, the Mann–Whitney *U* test was used to compare the demographics between each pair of groups: (1) the controls versus TBI I cohort, (2) control versus TBI II cohort and (3) TBI I cohort versus TBI II cohort. Chi-square tests were used to compare the gender distributions between each pair of groups.

All network measures for the control group passed the Shapiro–Wilk normality test, but some measures for the TBI groups did not. Thus, for group comparison of the network measures, two sided hypothesis tests were taken using permutation tests (10,000 permutations; Nichols and Holmes, 2001) on group means of each measure by permuting group membership. For global and region-specific network properties, permutation tests were performed on the *t*-statistics.

We performed the one-sided *z*-test (TBI > control) to compare the distributions of the number of TBI patients with more than two relatively 'abnormal' regions versus those expected. To calculate the expected number of TBI patients with relatively 'abnormal' regions, the binomial distribution was used with the probability that a region is relatively 'abnormal.' This probability was calculated from both upper and lower tails

(i.e., two-standard deviations ± mean) of the normal distribution. More specifically, the estimated number of TBI patients with m 'abnormal' regions out of the total n ROIs was:

$$|S| \times C_m^n p^m (1-p)^{(n-m)},$$

where $|S|$ is total number of TBI patients, C_m^n is n choose m and p is the probability that one region is 'abnormal' by chance. The number of 'abnormal' regions expected to occur by chance in each TBI patient was estimated based on the assumption that the ROIs are statistically independent (see Mac Donald et al. (2011) for the details of this statistical test procedure).

To minimize potential bias from possible non-independence across ROIs in the single-subject analyses, we additionally performed one-sided z-tests (TBI > control) on the distributions of the number of TBI patients as a function of the proportion of 'abnormal' nodes versus those expected. The expected distributions were obtained by permuting group memberships (10,000 permutations) and redefining abnormality based on permuted 'controls'.

Control analyses

To assess effects of motions on module-based graph theoretic measures obtained from our cohorts, each subject's average frame-to-frame head movement after censoring was first calculated and compared between cohorts. To compare the average frame-to-frame head movement after motion censoring between cohorts, subjects whose images passed all quality assurance procedures up to the motion censoring criterion were included (see Table 1). To assess effects of motion on module-based graph theoretic measures, i.e., average participation coefficients within each cohort and the number of 'abnormal' ROIs in each TBI cohort, subjects whose images passed all quality assurance procedures were included. We also assessed the effect of thresholds on our findings by applying two different threshold levels at 2% and 1.5% tie densities to the correlation matrices and subsequently performing group and ROI analyses of participation coefficients. To assess the effect of global signal regression on our results, we additionally preprocessed our data without global signal regression and constructed a correlation and connectivity matrix. ROI analyses after group comparisons were then performed for participation coefficients. Lastly, we selected a different version of ROIs comprising nodes within 20 mm geodesic distance from the peaks, and we repeated the ROI analyses to verify effects of different sizes of ROIs on our results.

Results

Demographics comparisons between the groups

There were no statistically significant differences in age, education, gender, or post-injury time between the subjects whose scans were included in graph theoretic analyses and their respective whole cohorts (Table 2). The whole cohorts did not show statistically significant differences in age, education and post-injury time comparing the control vs. TBI I, control vs. TBI II, and TBI I vs. TBI II cohorts. There were differences in gender that were significant only between the two TBI cohorts ($p = 0.03$; chi-square test) as only the TBI II cohort had females (Table 2). For the subjects whose scans (initial or follow-up scans) were included in graph theoretic analyses, there were no statistically significant differences in the demographics between each cohort except gender between the two TBI cohorts ($p = 0.04$; chi-square test).

Seed-based approach results for the default mode network

To ensure that the preprocessed resting-state BOLD fMRI had acceptable data quality for the further network analyses, we obtained the seed-based correlation maps from the left posterior cingulate cortex (−7, −55, 27) per each subject dataset that passed the quality assurance procedure prior to checking module assignment results. Group statistic maps (Fig. S1) for the seed-based correlation maps of each control and TBI I group on both scans showed the default mode network (see Fig. S1 legend for the detailed methods for the seed-based approach we used).

Module identification results

Color maps for identified modules from a group averaged correlation matrix (Fig. 2) allowed us to compare major modules (comprising more than 1% of the total number of nodes) between groups at each tie density. In the control group, there were typically 4 major modules identified (except at 1.5% tie density on the follow-up scans, where there were 5). The identified 4 major modules in the control group corresponded to the default mode (Greicius et al., 2002; Raichle et al., 2001), executive control (Seeley et al., 2007; Vincent et al., 2008), visual (Lowe et al., 1998) and somatosensory–motor (Biswal et al., 1995) networks. In contrast, the TBI I cohort generally had more than 4 modules (except at 3% tie density on the follow-up scans). These module identification results were consistent with modular organization maps from young healthy subjects reported elsewhere (Liang et al., 2013) using the same module identification algorithm. At 3% tie density, subdivided modules (light green and yellow modules) in the TBI I cohort on the initial scans reorganized (merged to other modules) on the follow-up scans and their module assignments became similar to modular structures of the control groups. At 2% and 1.5% tie densities, many subjects in the TBI I cohort had substantial numbers of trivial modules in the lateral prefrontal cortex and anterior cingulate cortex (white circles) on the initial scans, whereas fewer trivial modules were observed on the follow-up scans (Figs. 2b, c). Further assessment revealed that these trivial modules were disconnected from major modules and most of them consisted of single node, i.e., a node with no connections to other nodes.

An alternative module identification algorithm (Infomap) also demonstrated a large number of trivial modules and increased total number of major modules in the TBI I cohort on the initial scans (Fig. S3). For the controls, module assignments were largely similar to the results of Power et al. (2011), but direct comparisons at the same tie densities were not feasible as other parameters were different. Specifically, definition of nodes (i.e., modified voxel or large functional areas versus vertex of surface) and brain regions that involved the analyses (i.e., whole-brain including subcortical versus cortex only) were different. Note that we did not further compare Louvain algorithm results with those obtained by the Infomap algorithm as the Infomap algorithm did not reliably identify modules in some of our cohorts at the single-subject level (e.g., see Fig. S3).

Global network properties

Group differences in modularity (Fig. 3) were statistically significant at $\alpha = 0.05$ on the initial scans, but not on the follow-up scans. The TBI I cohort had higher modularity on the initial scans than the controls. Modularity in both groups passed the Shapiro–Wilk normality test. Modularity of the controls ranged from 0.3 to 0.55 (Fig. 3). This range is slightly low, especially on the initial scans, but the range is comparable to the modularity range (0.4 to 0.6) previously described in healthy normal subjects (Meunier et al., 2009a,b; Valencia et al., 2009). At the single subject level, 14 TBI patients on the initial scans had 'abnormally' high modularity and 2 had 'abnormally' low modularity (Fig. 3). Note that by chance only 2 subjects out of 47 (4.8%) would be expected to be outside of the 2-standard deviation range; 1 above and 1 below. With regard to trivial modules observed in the TBI patients (Fig. 2), the effect of excluding trivial modules on the modularity value was negligible ($<10^{-6}$) since most of the trivial modules comprised of single

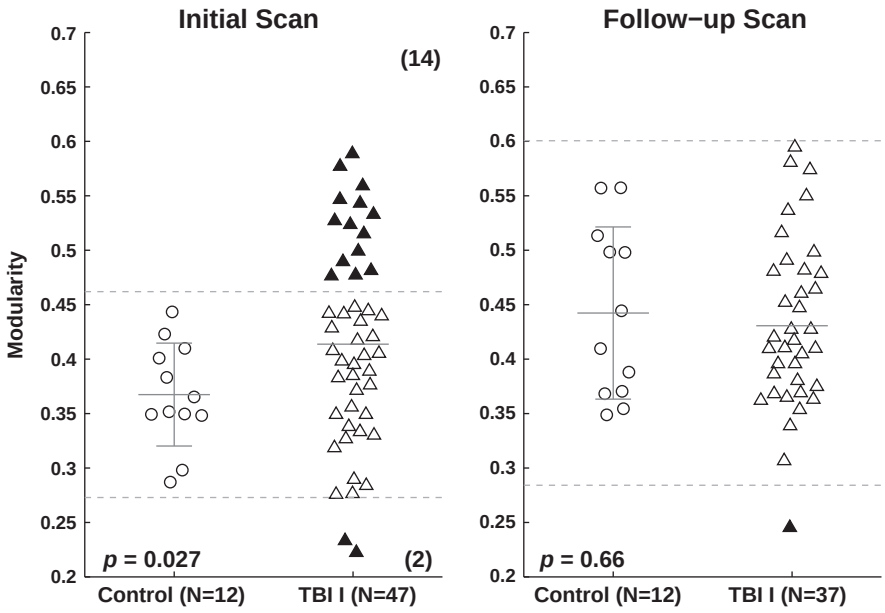

Fig. 3. Whole brain modularity of the controls and the first TBI (TBI I) cohort. Each symbol represents a single individual's modularity. The I bars indicate the means and standard deviation of the control, the dotted horizontal bar is two standard deviations from the mean of the control and the solid horizontal bar in the TBI I cohort is the mean of the TBI I cohort. Filled triangles represent TBI patients with relatively 'abnormal' modularity, located outside of the dotted horizontal bars. The number of relatively 'abnormal' TBI patients for modularity was labeled in parentheses, and the *p*-values were obtained from permutation tests (10,000 permutations) on group mean difference. Because the quality control procedures for inclusion or exclusion were performed on each scan individually, the subjects whose modularity data is shown for the follow-up scans were not an exact subset of subjects whose data is shown for the initial scans.

nodes (see the modularity equation in the Materials and methods section).

Higher modularity in the TBI cohort on the initial scans was associated with a lower average participation coefficient, a measure of between-module connectivity, in these subjects. Modularity and the average participation coefficient were highly inversely correlated on both scans (Figs. S4a, b), and the average participation coefficient was lower in the TBI I cohort than in the controls on the initial scans (Fig. S4c).

When the modularities were compared across the initial and follow-up scans at each group, the modularities were apparently changed in the controls whereas they appeared to remain stable on average in the TBI I cohort (Fig. 3). However, the interpretation of this result is not straightforward for two reasons: 1) we acquired MRIs at a different site for the follow-up scans and 2) the subjects on the follow-up scans included in the analyses were not an exact subset of subjects on the initial scans due to the quality assurance procedures. In other words, longitudinal comparisons between each group should not be made until unknown amounts of (1) effects of different sites on the module-based network properties and (2) inter-subject variability of the module-based network properties are clarified. Therefore, to further investigate if the modularities of TBI patients remained stable while those of controls changed over the two scans at each subject, we performed additional, direct comparisons between the initial and follow-up scans with subjects who underwent both scans at the single-subject level (see Fig. S5). At the group level, the overall result was unchanged: there was increased modularity in the control group over time and stable modularity in the TBI I group (Fig. S5, 1st, 2nd columns). However, single subject analyses demonstrated a wide variety of changes (both increases and decreases) in modularity over time in both controls and the TBI I cohort (Fig. S5, 3rd column). See Discussion for the limitations of this study relevant to this observation. Further, notable group differences in longitudinal changes in these measures were mainly due to TBI patients with 'abnormal' modularities (Fig. S4, 4th column). More specifically, it was the 'abnormal' TBI patients on the initial scans that shifted the group average of longitudinal changes toward zero. Without these 'abnormal' TBI patients, average longitudinal changes in the TBI I (dotted horizontal bar in Fig. S4, 4th column) were increased as well, making group differences in longitudinal changes no longer statistically significant at $\alpha = 0.05$. Thus, the most likely explanation is that there were systematic differences between the two scanners as well as changes in the most abnormal subjects over time.

Node-specific network properties

Node-specific analysis allowed us to identify localized patterns of module-based network measures that differed between TBI and control subjects (Figs. 4, 5). Overall, the spatial pattern of group comparisons (Fig. 4) and the number of TBI patients with 'abnormal' network measures relative to the controls (Fig. 5) were clear on the initial scans but less prominent on the follow-up scans. On the initial scans, the TBI I cohort had small areas of increased and decreased within-module connectivity relative to the controls (Fig. 4a). On the contrary, the TBI subjects had an extensive and more markedly decreased participation coefficient (Fig. 4b) compared with the controls. Maps for the count of the TBI patients with 'abnormal' node-specific measures relative to the controls were similar to the corresponding group comparison maps (Fig. 5).

Group comparisons

The spatial pattern of group differences in within-module connectivity changed over time. At the time of the initial scan, within-module connectivity in the TBI I cohort was slightly elevated, on average, compared with the controls in the right precentral gyrus, right medial superior frontal gyrus, and right dorsomedial superior frontal gyrus (R G_precentral, R G_front_sup-*medial* and R G_front_sup-*dorsomedial* in Fig. 4a left panel). Subtle decreases in within-module connectivity of the TBI patients compared with the controls were also observed in the right supramarginal gyrus and right opercular part of the inferior frontal gyrus (R G_pariet_inf-Supramar and R G_front_inf-Opercular in Fig. 4a left panel). Though there were trends in group differences on the initial scans, none of the group differences were statistically significant at $q_{FDR} < 0.05$ (FDR: false discovery rate; Genovese et al., 2002). At

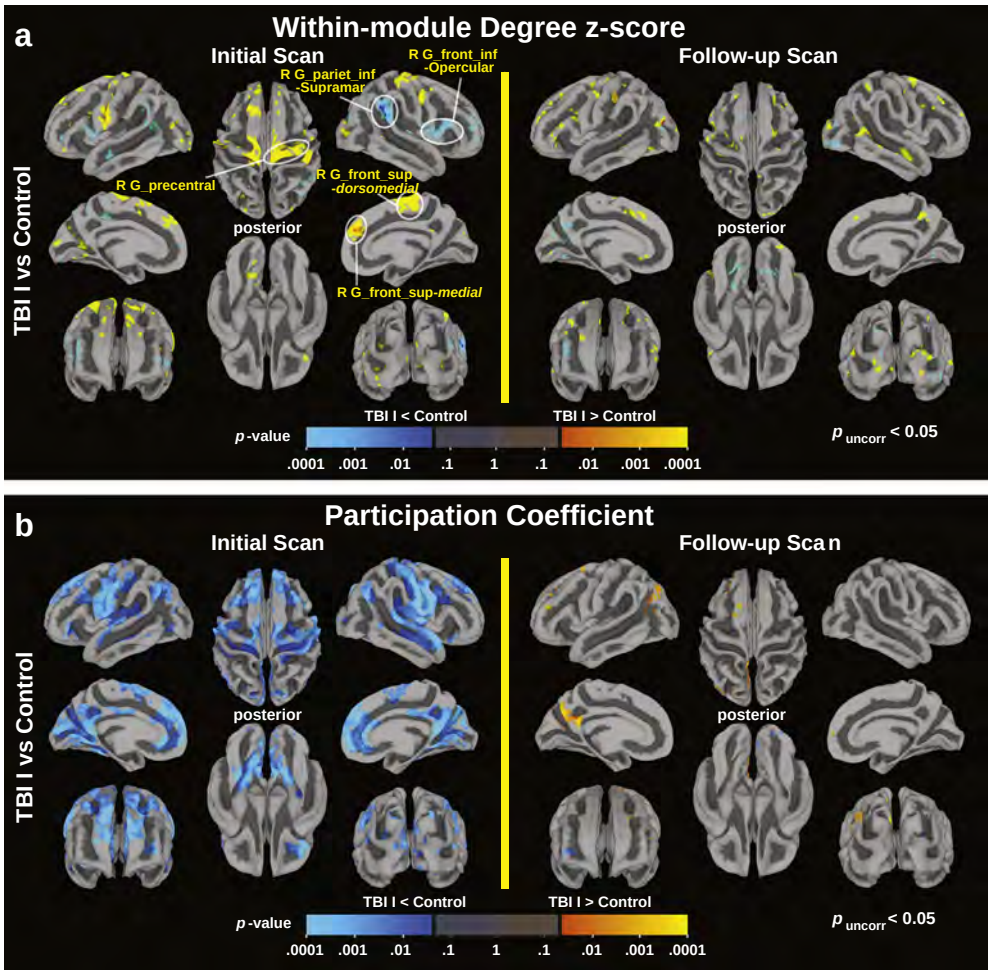

Fig. 4. Node-specific network properties of the controls and TBI I cohort. Group mean comparison maps ($p_{uncorr} < 0.05$) of within-module degree *z*-score (a) and participation coefficient (b), respectively. All color maps were superimposed on the averaged cortical surface from all participants in the controls and TBI I cohort. R G_precentral: right precentral gyrus, R G_pariet_inf-Supramar: right supramarginal gyrus, R G_front_inf-Opercular: right opercular part of the inferior frontal gyrus, R G_front_sup-*medial*: right medial superior frontal gyrus, R G_front_sup-*dorsomedial*: right dorsomedial superior frontal gyrus.

the time of the follow-up scan, such disturbances in within-module connectivity became less prominent (Fig. 4a, right panel).

In contrast to the scattered subtle increases and decreases in the within-module connectivity, the group comparison maps for the participation coefficient (Fig. 4b left panel) exhibited more widespread decreases in the TBI I cohort compared with the controls. At the time of the initial scan, such patterns were localized over the central sulcus, left anterior transverse temporal gyrus, right long insular gyrus and central sulcus of the insula, superior frontal gyrus and sulcus, anterior part of the cingulate gyrus and sulcus, right superior part of the precentral sulcus, right superior temporal sulcus, right orbital gyri, posterior-ventral part of the cingulate gyrus near the calcarine sulcus, lingual gyrus, right parieto-occipital sulcus and left cuneus. These differences on the initial scans were significant based on uncorrected *p*-values. However, such group differences on the initial scans did not survive after correction for multiple comparisons at $q_{FDR} < 0.05$. At the time of the second scan, the widespread group differences in the participation coefficient mostly became less prominent (Fig. 4b, right panel).

Counts of the numbers of TBI patients with relatively 'abnormal' node-specific network measures

Color maps for the number of TBI patients with 'abnormal' network measures relative to the controls in each of the nodes (Fig. 5) allowed us to identify regions where functional connectivity appeared most vulnerable to bTBI. Here, 'abnormal' was defined if a network measure of a patient was outside two standard deviations from the mean of the controls. Though abnormalities revealed on group comparison maps did not survive at $q_{FDR} < 0.05$, the 'abnormality' maps demonstrated that substantial portions of the TBI patients (up to 25%) had an 'abnormally' low participation coefficient relative to the controls (Fig. 5c). None had an 'abnormally' high participation coefficient. These findings are notable in that by chance 2.4% of the TBI I cohort would be expected to be lower than the mean of the controls minus the 2-standard deviations.

ROI analysis results

Since the participation coefficient was the most prominent among the module-based network measures in the group-wide node-specific analysis, we focused on the participation coefficient in further analyses. From the group comparison map in the participation coefficient (Fig. 4b), we identified 15 regions (Fig. 6) for ROI analysis using the Destrieux atlas (Destrieux et al., 2010), a standard surface-based atlas available from Freesurfer. See the Discussion section for an explanation of utilizing structural parcellations as opposed to functional parcellations in this ROI analysis. The identified ROIs were (1) the central sulcus (S_central), (2) left anterior transverse temporal gyrus (L G_temp_sup-G_T_transv), (3) right long insular gyrus and central sulcus of the insula (R G_Ins_lg_and_S_cent_ins), (4) superior frontal sulcus (S_front_sup), (5) the medial portion of the superior frontal

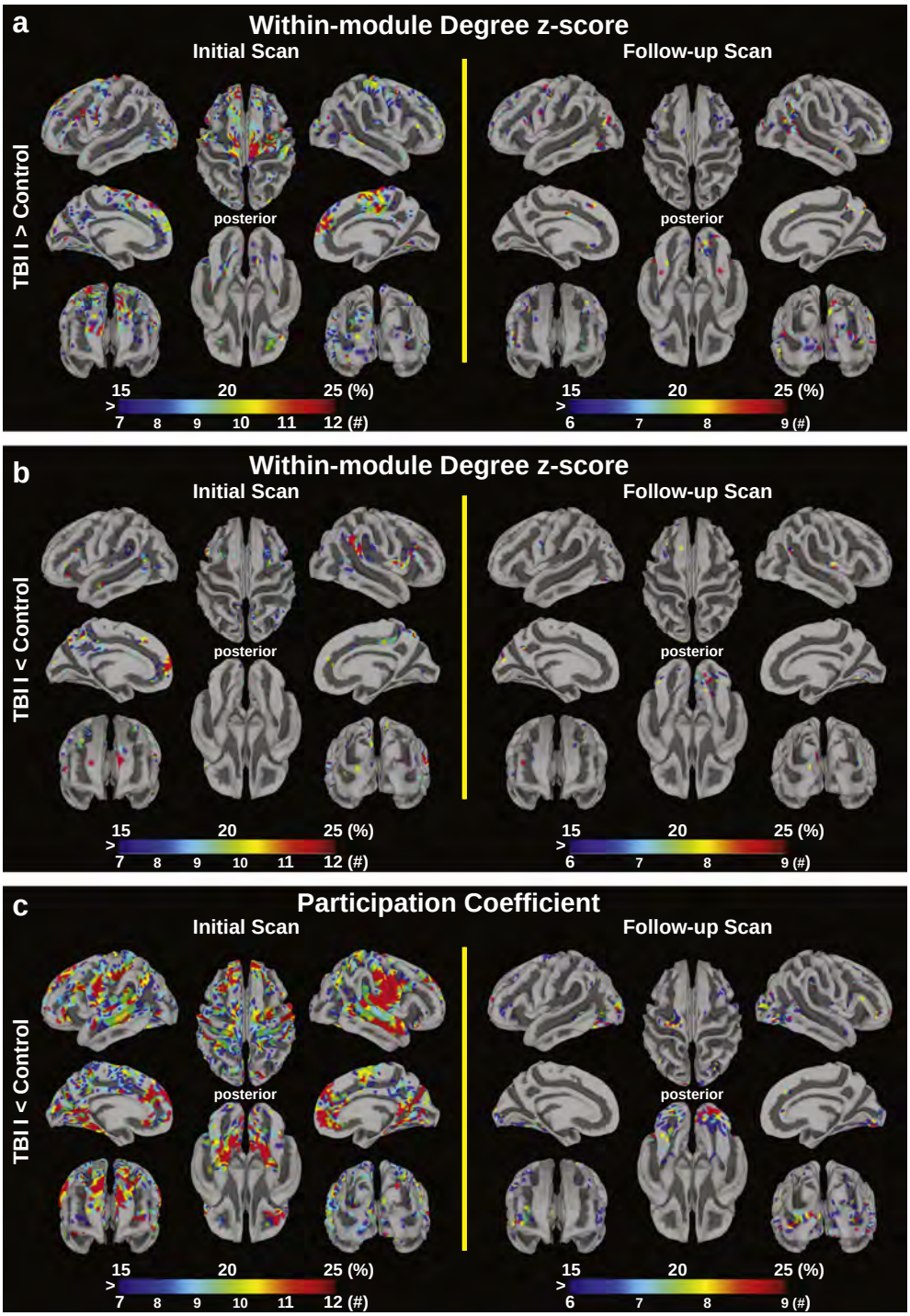

Fig. 5. Count of the TBI patients from the TBI I cohort with 'abnormal' node-specific network properties relative to the controls. Color maps of the number of TBI patients whose measures (within-module degree *z*-score and participation coefficient, respectively) were outside two standard deviations from the mean of the control. All color maps were superimposed on the averaged cortical surface from all participants in the controls and TBI I cohort.

gyrus (G_front_sup-*medial*), (6) the anterior portion of the superior frontal gyrus (G_front_sup-*anterior*), (7) deep anterior part of the cingulate gyrus and sulcus (G_and_S_cingul-Ant-*deep*), (8) superficial anterior part of the cingulate gyrus and sulcus (G_and_S_cingul-Ant-*superficial*), (9) right superior part of the precentral sulcus (R S_precentral-sup-part), (10) right superior temporal sulcus (R S_temporal_sup), (11) right orbital gyri (R G_orbital), (12) posterior-ventral part of the cingulate gyrus (G_cingul-Post-ventral) near the calcarine sulcus, (13) lingual gyrus (G_oc-temp_med-Lingual), (14) right parieto-occipital sulcus (R S_parieto_occipital) and (15) left cuneus (L G_cuneus). For detailed locations and surface areas of these ROIs, see Fig. 6 and Table 3.

Scatter plots were made (Fig. 7) to examine the distributions of the average participation coefficient of each subject in three ROIs (G_and_S_cingul-Ant-*superficial* (left: (−8, 56, 3), right: (9, 55, 2)), G_cingul-Post-ventral (left: (−8, −52, 3), right: (12, −53, 5)) and R S_parieto_occipital (18, −81, 38)). These three ROIs were representative of all 15 ROIs analyzed (see Table 4 for the complete list of the

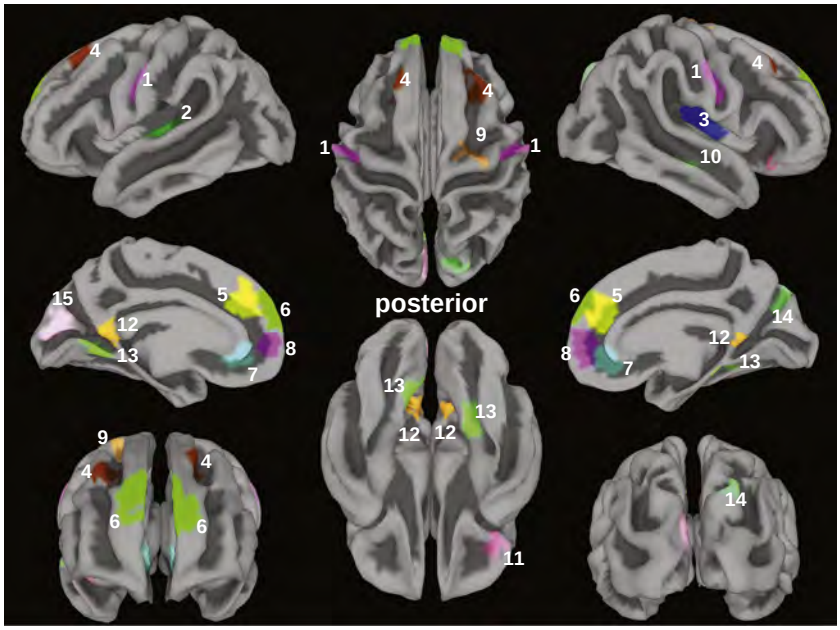

Fig. 6. Regions of interest (ROIs) for participation coefficient. 15 ROIs are colored and labeled (1: central sulcus, 2: left anterior transverse temporal gyrus, 3: right long insular gyrus and central sulcus of the insula, 4: superior frontal sulcus, 5: medial superior frontal gyrus, 6: anterior superior frontal gyrus, 7: deep anterior part of the cingulate gyrus and sulcus, 8: superficial anterior part of the cingulate gyrus and sulcus, 9: right superior part of the precentral sulcus, 10: right superior temporal sulcus, 11: right orbital gyri, 12: posterior-ventral part of the cingulate gyrus, 13: lingual gyrus, 14: right parieto-occipital sulcus and 15: left cuneus). See Table 3 for the coordinates and areas of these ROIs.

ROI analysis results). Similar to the trends observed in global and node-specific network measures, the TBI I cohort, on average, had lower participation coefficients than the controls on the initial scans, yielding up to 15 (36.6%) relatively 'abnormal' TBI patients (Figs. 7a–c left panel). Such group differences that were marked by many relatively 'abnormal' TBI patients became less prominent at the time of the follow-up scans (Figs. 7a–c right panel).

Subsequently, without free parameters with regard to ROI selection, we used the TBI II cohort as a validation dataset to test the hypotheses generated with the TBI I cohort. On the initial scans, in the three ROIs, relative 'abnormality' patterns in the TBI II cohort were less striking than those in the TBI I cohort, yielding up to 3 (9.6%) TBI patients with relatively 'abnormal' participation coefficients (Figs. 7d–f left panels). Table 4 indicates that the number of TBI patients from the TBI II cohort with relatively 'abnormal' ROI-specific participation coefficients on the initial scans was greater than the expected number by chance (0 above and 0 below). Relatively abnormal participation coefficients on the initial scans in TBI patients from the TBI II cohort were identified in all ROIs except in the G_front_sup-*medial* and L G_cuneus. However, there were fewer TBI patients with a relatively abnormal participation coefficient over the ROIs in the TBI II cohort compared with the TBI I cohort (Fig. 7 and Table 4).

Turning to multiple ROI single-subject analyses, we counted the number of relatively 'abnormal' ROIs in each individual TBI patient and tested if this observed distribution of 'abnormal' ROIs differed from the distribution expected by chance (Fig. 8). On the initial scans, the observed numbers of TBI patients with more than two 'abnormal' ROIs were markedly different from those expected by chance, and these differences were statistically significant at $\alpha = 0.05$ in both datasets (27/47 observed versus 2/47 expected in the TBI I cohort, $p < 0.0001$, one-sided z-test; 8/31 observed versus 1/31 expected in the TBI II cohort, $p = 0.006$, one-sided z-test). As expected considering the nature of these analyses, the proportion of TBI patients from the TBI II cohort with more than two relatively 'abnormal' ROIs was lower than those from the TBI I cohort: 44.9% reduction from the TBI I cohort to TBI II cohort on the initial scans (i.e., 57.4% = 27/47 versus 25.8% = 8/31).

On the follow-up scans, the proportion of patients in the TBI I cohort with more than two 'abnormal' ROIs was different than expected by chance with marginal statistical significance ($p = 0.044$). The proportion of patients in the TBI II cohort with more than two 'abnormal' ROIs on follow-up scans was not statistically significant ($p = 0.276$).

Multivariate analysis aggregating all 15 ROIs after dimensionality reduction via probabilistic principal component analysis (Fig. 9) demonstrated a similar reduction in the proportion of the TBI patients with relatively 'abnormal' ROIs from the TBI I cohort to the TBI II cohort. Specifically, 31/47 (66.0%) of the patients from the TBI I cohort (Fig. 9a) and 9/31 (29.0%) of the patients from the TBI II cohort (Fig. 9b) were deemed to be relatively 'abnormal' across the 15 ROIs on the initial scans. On the follow-up scans, 4/37 (10.8%) of the patients from the TBI I cohort (Fig. 9c) and 1/27 (3.7%) of the patients from the TBI II cohort (Fig. 9d) were found to be 'abnormal' using this multivariate analysis.

Permutation-based omnibus abnormality analysis results

We next asked whether the above results could have been biased by non-independence of the ROIs. Therefore, we counted the proportion of 'abnormal' nodes in each individual TBI patient and compared the observed distributions in TBI patients with those expected by chance using permutation of group membership (Fig. 10). Again, 'abnormal' was defined as the participation coefficient outside of 2 standard deviations of the mean of the controls. Overall, these omnibus nodal abnormality analysis results were consistent with the ROI analysis results shown in Fig. 8. Specifically, on the initial scans, the differences between the observed number of TBI patients with more than 15% 'abnormal' nodes in the TBI I cohort or more than 10% in the TBI II cohort vs. those expected by chance were statistically significant at $\alpha = 0.05$ in both datasets (19/47 observed versus 1/47 expected in the TBI I cohort, $p < 0.0001$, one-sided z-test; 7/31 observed versus 1/31 expected in the TBI II cohort, $p = 0.012$, one-sided z-test). Again, the trends on the follow-up scans shown in Fig. 10 were similar to those in Fig. 8. The

Table 3
Regions-of-interest (ROI) for participation coefficient analyses.

Index[a]	ROI name	MNI coordinates (x,y,z) of center[b]		Surface area (mm^2)[c]	
		Left	Right	Left	Right
1 (45)	S_central	(−51, −11, 28)	(51, −11, 30)	531.5	616.5
2 (33)	L G_temp_sup-G_T_transv	(−41, −20, 4)		419.0	
3 (17)	R G_Ins_lg_and_S_cent_ins		(39, −15, 10)		560.4
4 (54)	S_front_sup	(−21, 25, 46)	(28, 27, 41)	281.0	310.5
5 (16)	G_front_sup-*medial*	(−5, 39, 31)	(9, 41, 22)	409.3	411.5
6 (16)	G_front_sup-*anterior*	(−8, 63, 25)	(13, 57, 29)	490.9	473.2
7 (6)	G_and_S_cingul-Ant-*deep*	(−4, 37, −8)	(7, 38, −7)	262.3	356.0
8 (6)	G_and_S_cingul-Ant-*superficial*	(−8, 56, 3)	(9, 55, 2)	203.8	338.7
9 (69)	R S_precentral-sup-part		(23, −13, 61)		260.7
10 (73)	R S_temporal_sup		(55, −20, −12)		291.8
11 (24)	R G_orbital		(41, 28, −16)		237.3
12 (10)	G_cingul-Post-ventral	(−8, −52, 3)	(12, −53, 5)	300.0	199.5
13 (22)	G_oc-temp_med-Lingual	(−14, −60, 1)	(29, −41, −11)	441.9	381.2
14 (65)	R S_parieto_occipital		(18, −81, 38)		302.2
15 (11)	L G_cuneus	(−2, −85, 14)		465.1	

Note: S_central, central sulcus (Rolando's fissure); L G_temp_sup-G_T_transv, left anterior transverse temporal gyrus (of Heschl); R G_Ins_lg_and_S_cent_ins, right long insular gyrus and central sulcus of the insula, S_front_sup, superior frontal sulcus; G_front_sup-*medial*, medial superior frontal gyrus (F1); G_front_sup-*anterior*, anterior superior frontal gyrus (F1); G_and_S_cingul-Ant-*deep*, deep anterior part of the cingulate gyrus and sulcus; G_and_S_cingul-Ant-*superficial*, superficial anterior part of the cingulate gyrus and sulcus; R S_precentral-sup-part, right superior part of the precentral sulcus; R S_temporal_sup, right superior temporal sulcus (parallel sulcus); R G_orbital, right orbital gyri; G_cingul-Post-ventral, posterior-ventral part of the cingulate gyrus (vPCC, isthmus of the cingulate gyrus); G_oc-temp_med-Lingual, lingual gyrus, lingual part of the medial occipito-temporal gyrus (O5); R S_parieto_occipital, right parieto-occipital sulcus (or fissure); L G_cuneus, left cuneus (O6); MNI, Montreal Neurological Institute (Evans et al., 1993).

[a] Initial index numbers indicate regions of interest labeled in Fig. 6. Numbers in parentheses refer to the corresponding index numbers in Destrieux et al. (2010).

[b] MNI coordinates correspond to a midpoint between pial surface and white matter surface.

[c] Surface area of white matter surface.

observed proportion of patients in the TBI I cohort was statistically significant ($p = 0.0008$), but not in the TBI II ($p = 0.080$).

Control analysis results

Assessment of the effects of subtle head motion

Recently, the effects of subtle motion have been found to substantially influence resting-state functional connectivity MRI findings (Power et al., 2012; Satterthwaite et al., 2012; van Dijk et al., 2012). Our motion analysis (Fig. S6) revealed that there were no statistically significant group differences in average frame-to-frame movement in the analyzed data, after censoring and exclusion of scans with excessive motion (Table 1). There were no associations between the average participation coefficient and head motion (Fig. S7) in any of the groups. Furthermore, there was no relationship between the number of 'abnormal' ROIs and head motion (Fig. S8).

Assessment of the effects of network connectivity thresholds

The differences between TBI subjects and controls in the number of regions of interest with an 'abnormal' participation coefficient were replicated at 2 additional threshold levels for connectivity matrices (Figs. S9 and S10 for 2% and 1.5% tie densities, respectively).

Effects of global signal regression

Analyses of the number of ROIs with an abnormal participation coefficient in TBI patients vs. controls based on connectivity matrices created without global signal regression (Fig. S11) essentially replicated the results with global signal regression (Fig. 8). The only exception was that the number of TBI I patients with relatively 'abnormal' ROI values on the follow-up scans was not quite statistically significant at $\alpha = 0.05$.

Effects of region of interest size

To explore the effect of ROI size, we re-analyzed the data using all nodes within 20 mm rather than 15 mm geodesic distance of the local peaks of the participation coefficient difference between groups as the ROIs (Fig. S12). The analysis of the number of ROIs with an 'abnormal' participation coefficient in TBI patients versus controls using 20 mm geodesic distance ROIs (Fig. S13) again essentially replicate the results with 15 mm geodesic distance ROIs (Fig. 8).

Discussion

In summary, we found disrupted community organization of resting-state functional connectivity in a subset of U.S. military personnel following concussive bTBI using module-based graph theoretic analysis. Of the module-based graph theoretical measures studied, the participation coefficient, a measure of between-module connectivity, showed the most pronounced disruptions in the TBI patients relative to the controls. There were spatially localized 'abnormalities' over multiple brain regions in the TBI patients. Importantly, these abnormalities were detected in comparison with U.S. military controls that had blast-exposures but no clinical diagnosis of TBI. At the time of the initial scans, the distribution of the number of the 'abnormal' regions was different from the expected distribution by chance. Multivariate analysis aggregating the 15 ROI values of between-module connectivity consistently demonstrated that a substantial portion of TBI patients had relatively 'abnormal' between-module connectivity. The number of TBI patients with relatively 'abnormal' between-module connectivity was less prominent at the time of the follow-up scans. In an independent group of concussive bTBI patients, we were able to partially replicate these results with no free parameters.

Technological innovations effectively analyze heterogeneous concussive bTBI patients at the single subject level

The single-subject analyses performed in this study were useful to effectively analyze a heterogeneous group of bTBI patients in this report. Scatter plots (Figs. 3, 7) illustrate skewed distribution of the network measures in the TBI patients. The distributions of the TBI patients with multiple 'abnormal' regions or nodes (Figs. 8, 10) were consistently different from those expected by chance. The multivariate analysis (Fig. 9) also consistently revealed the TBI patients with relatively 'abnormal' regions over the two independent cohorts. Thus, we suggest that single-subject analysis should be considered along with group analysis for the identification of 'abnormalities' in heterogeneous subject populations such as concussive bTBI patients. Obviously, single-subject analyses have greater potential clinical applicability than group analyses.

We adopted a surface-based approach to reduce between-subject variability arising from brain anatomy. An advantage of the surface-

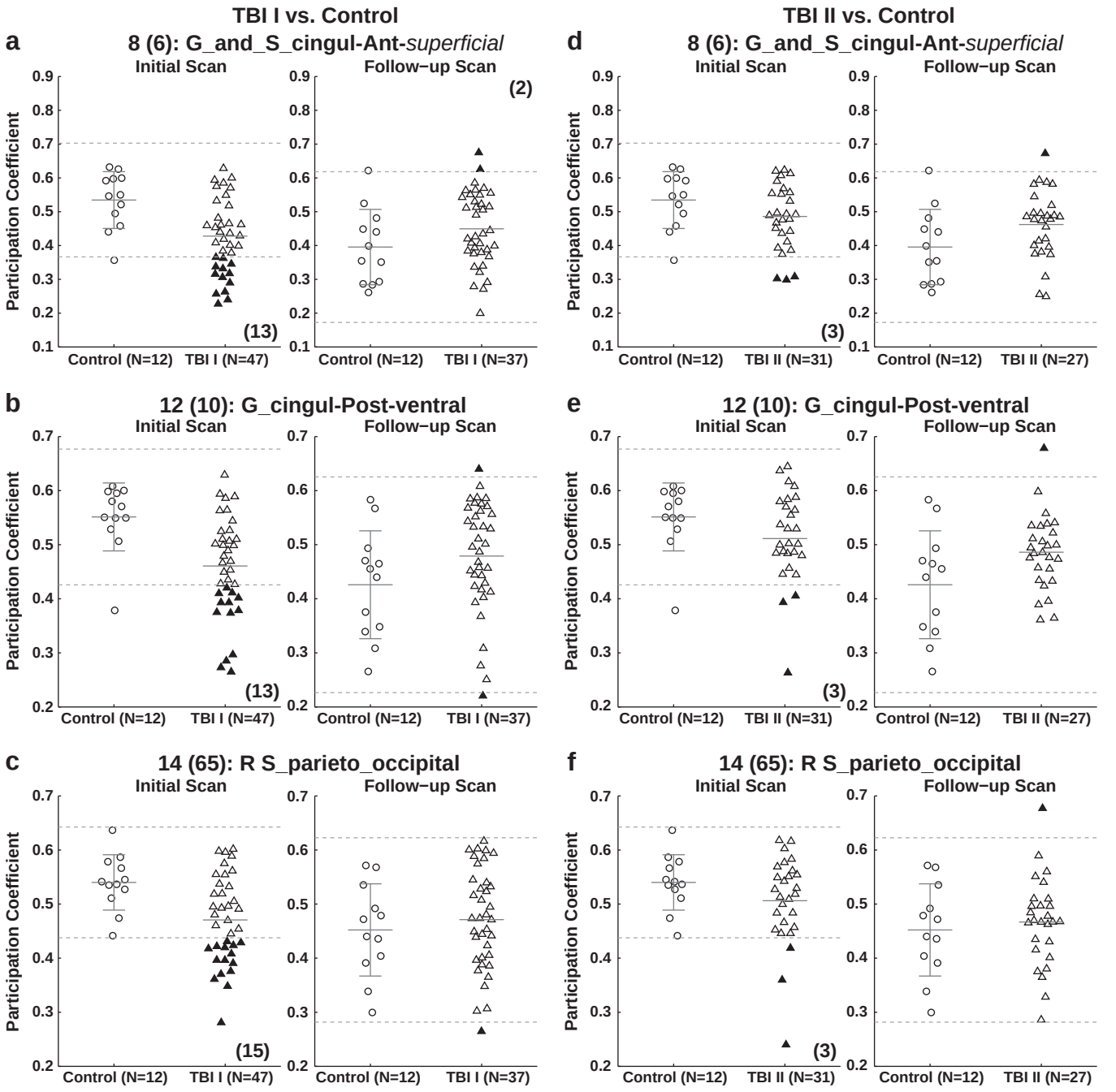

Fig. 7. ROI analysis of participation coefficient of the controls and patients with TBI. Scatter plots for averaged participation coefficients within each of the three selected ROIs. See Fig. 3 for the details of the scatter plots, Table 3 for abbreviations and Table 4 for results from all ROIs. Again, because the quality control procedures for inclusion or exclusion were performed on each scan individually, the subjects whose modularity data are shown for the follow-up scans were not an exact subset of subjects whose data are shown for the initial scans.

based approach is an increase in sensitivity by (1) matching sulcus-to-sulcus and gyrus-to-gyrus of cortical surface across subjects to circumvent the issues of improper registration and (2) utilizing spatial smoothing on the cortical surface rather than the voxel space (Jo et al., 2007, 2008; Tucholka et al., 2012). On the other hand, a disadvantage of the surface-based approach is that it does not represent the whole brain. The surface based approach does not assess cerebellum and subcortical regions such as the basal ganglia and thalamus.

Complex network analysis using the graph theory is advantageous in bTBI populations with heterogeneous injury mechanisms since it does not make assumptions regarding networks or regions of interest. Thus, our data-driven approach may provide a more 'comprehensive' view than hypothesis-driven approaches do in the studies of heterogeneous TBI populations. Disrupted between-module connectivity in the TBI patients over multiple regions (Figs. 4b, 5c, 7–10, Table 4) indicates that multiple regions or networks should be included to detect 'abnormalities' in TBI patients if hypothesis-driven approaches are adopted. Like complex network analysis using the graph theory, independent component analysis (ICA) is another data driven approach with potential to identify abnormalities in heterogeneous TBI populations. Indeed, Shumskaya et al. (2012) identified abnormalities of resting-state networks in concussive TBI patients utilizing the whole-brain ICA. However, Shumskaya et al. (2012) applied the ICA to a relatively more homogenous concussive TBI group including only patients with fronto-occipital injuries. Thus, the utility of whole brain ICA in heterogeneous concussive bTBI populations warrants further investigations.

Table 4
ROI analysis results of participation coefficients.

Index	ROI name	'Abnormal' TBI[a]			
		TBI I vs. control		TBI II vs. control	
		Initial	Follow-up	Initial	Follow-up
1 (45)	S_central	13/0	3/0	1/0	1/1
2 (33)	L G_temp_sup-G_T_transv	12/1	4/0	2/1	4/0
3 (17)	R G_Ins_lg_and_S_cent_ins	10/1	4/3	1/1	2/1
4 (54)	S_front_sup	10/0	2/1	1/0	0/1
5 (16)	G_front_sup-*medial*	11/0	1/1	0/0	0/1
6 (16)	G_front_sup-*anterior*	14/0	1/3	2/0	0/1
7 (6)	G_and_S_cingul-Ant-*deep*	12/0	1/2	3/0	0/1
8 (6)	G_and_S_cingul-Ant-*superficial*	13/0	0/2	3/0	0/1
9 (69)	R S_precentral-sup-part	11/0	1/0	1/0	1/1
10 (73)	R S_temporal_sup	13/0	2/0	3/0	1/0
11 (24)	R G_orbital	15/0	2/1	1/0	0/0
12 (10)	G_cingul-Post-ventral	13/0	1/1	3/0	0/1
13 (22)	G_oc-temp_med-Lingual	15/0	2/0	3/1	0/1
14 (65)	R S_parieto_occipital	15/0	1/0	3/0	0/1
15 (11)	L G_cuneus	8/0	2/0	0/0	0/1

Note: See Table 3 for the abbreviations of ROI names.
[a] The number of TBI patients with 'abnormally' low participation coefficients/the number of TBI patients with 'abnormally' high participation coefficients.

In contrast to other graph theoretic analyses on TBI populations (Castellanos et al., 2011; Nakamura et al., 2009), we exploited the spatial resolution of fMRI by defining each vertex of the cortical surface as a node. Network analyses with higher spatial resolution of nodes are beneficial over region-based network analyses in identifying network properties of interests with greater sensitivity and specificity and visualizing spatially localized network properties of interest (Hayasaka and Laurienti, 2010). Thus, we attempted to use a vertex as a node considering that the spatial extent of 'abnormalities' in concussive bTBI populations measured by the graph theoretic analysis in fMRI was unknown. Indeed, the utilization of high spatial resolution of fMRI allowed us to identify localized 'abnormalities' in the TBI patients in greater detail, which would be missed if a node was defined from coarse parcellations. However, a vertex itself is arguably less biologically meaningful than a functional brain region in the context of graph theoretic analysis (Wig et al., 2011). Unfortunately our current understanding of the functional subdivisions of the human brain is not yet sufficient for optimal prespecified ROI analyses. For the same reason, we selected the 15 ROIs in reference to the Destrieux atlas, a structural parcellation, as opposed to a functional parcellation.

Findings in relation to prior literature

Multiple regions with disrupted between-module connectivity as potential candidates for hypothesis-driven network-specific approaches

Most of the previous functional connectivity studies in fMRI on civilian TBI patients (Arenivas et al., 2012; Bonnelle et al., 2011; Caeyenberghs et al., 2012; Kasahara et al., 2010; Marquez de la Plata

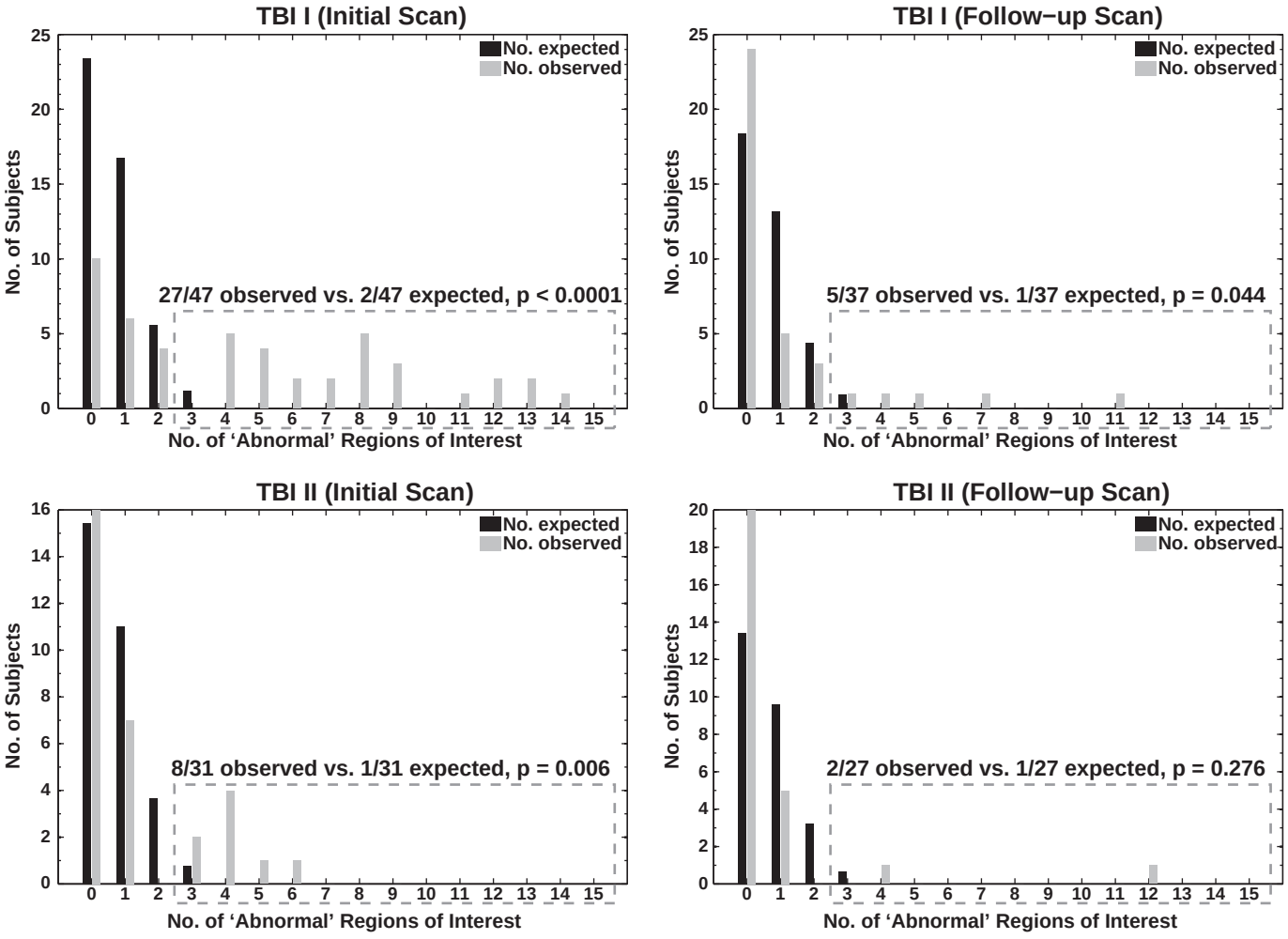

Fig. 8. Bar graphs for observed and expected 'abnormal' ROIs in the patients with TBI relative to the controls. The distribution of expected relatively 'abnormal' ROIs was calculated from the binomial distribution with the probability that one region deems 'abnormal' by chance (0.0455; the probability that participation coefficient for a TBI patient falls outside two standard deviations from the mean of the controls). The *p*-values were obtained by the one-sided *z*-test (TBI I > controls in the number of 'abnormal' ROIs).

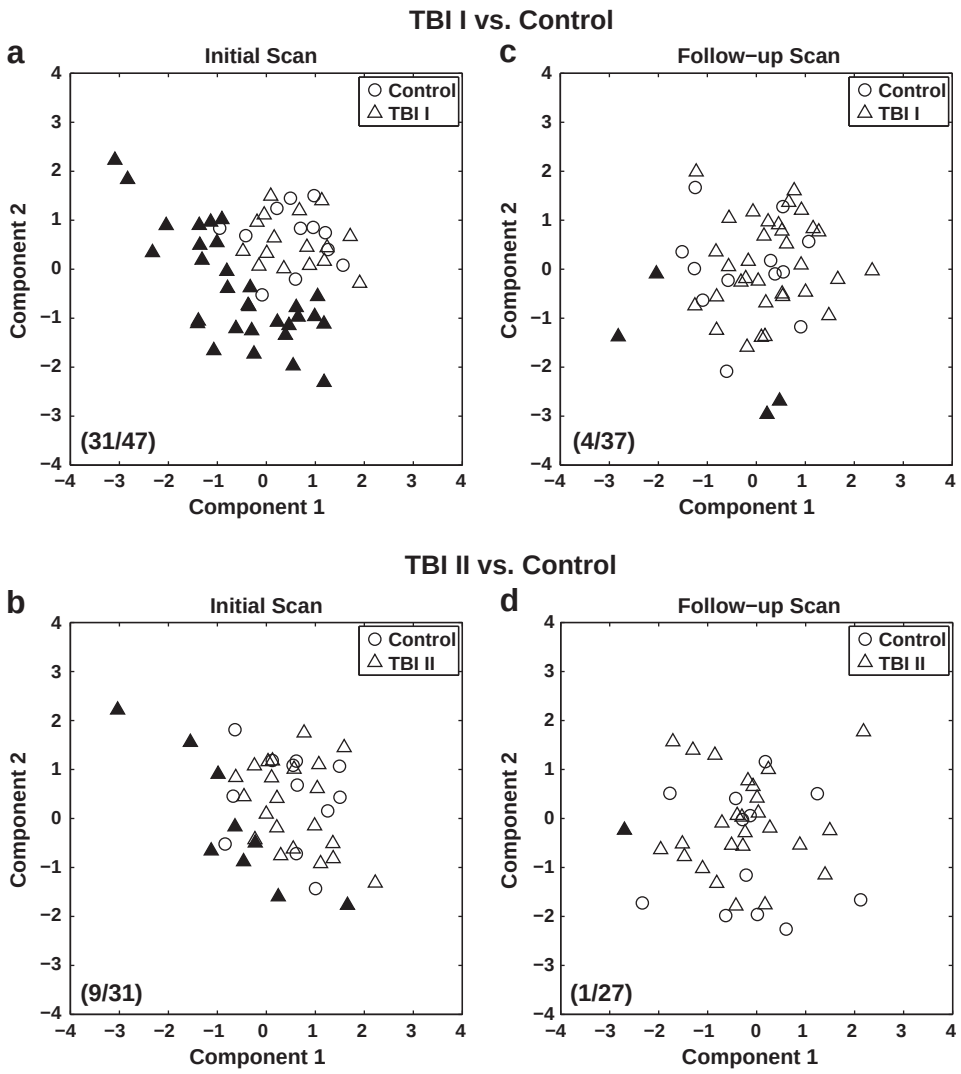

Fig. 9. Scatter plots for multivariate analysis of participation coefficients within the ROIs after dimensionality reduction by probabilistic principal component analysis. Solid triangles represent relatively 'abnormal' TBI patients whose values are located within the lower and upper tails, accounting for 2.5% in each tail, of the estimated multivariate normal distribution from the control. The label in each panel indicates the number of relatively 'abnormal' TBI patients and the number of TBI patients on the corresponding scan.

et al., 2011; Mayer et al., 2011; Sharp et al., 2011; Slobounov et al., 2011; Tang et al., 2011) used hypothesis-driven approaches within the default mode (Greicius et al., 2002; Raichle et al., 2001), executive control (Seeley et al., 2007; Vincent et al., 2008), motor (Biswal et al., 1995), thalamic (Zhang et al., 2008) and hippocampal (Rombouts et al., 2003) networks. However, to our knowledge, there are no current fMRI studies of resting-state functional connectivity in concussive bTBI patients using these networks. In this regard, future work based on the identified 'abnormal' regions in Figs. 4–7 could involve assessment of within-network and between-network connectivity in these specific resting-state networks.

Transient change of module-based organizations following concussive bTBI

A prevailing view on the plasticity of TBI patients based on functional neuroimaging studies (Castellanos et al., 2010, 2011; Mayer et al., 2011; Nakamura et al., 2009; Sponheim et al., 2011) is that the recovery of functional network at the chronic stage is incomplete. Even after 7 to 12 months of active rehabilitation treatments, it has been reported that many TBI patients had incomplete recovery of the graph-theory measures, associated with the incomplete reestablishment of cognitive function (Castellanos et al., 2011). Furthermore, concussive bTBI patients with 32 months of mean post-injury time demonstrated relatively reduced inter-hemispheric connectivity in the lateral frontal lobe despite no observed deficits in neuropsychological measures (Sponheim et al., 2011).

In contrast, in our study at the global, region- and node-specific levels (Figs. 3–5, 7–10), group differences in module-based connectivity observed on the initial scans were less prominent at the follow-up scan 6–12 months later. This transient change in module-based connectivity supports the utility of early scanning (if feasible) on bTBI patients to identify localized modular disruptions in brain networks. However, less prominent group differences in between-module connectivity at the follow-ups do not necessarily mean complete restoration of bTBI patients' network architectures to baseline.

Marginally perturbed within-module connectivity, but markedly unbalanced between-module connectivity with increased modularity

Node-specific analysis of the module-based network measures (Figs. 4, 5) demonstrates that the TBI patients had disrupted between-module connectivity with marginal change in within-module connectivity relative to the controls. Disrupted between-module connectivity in the TBI patients indicate that the blast-related injuries may interfere with integration across functional brain networks, as between-module connectivity may be necessary for complex tasks spanning multiple

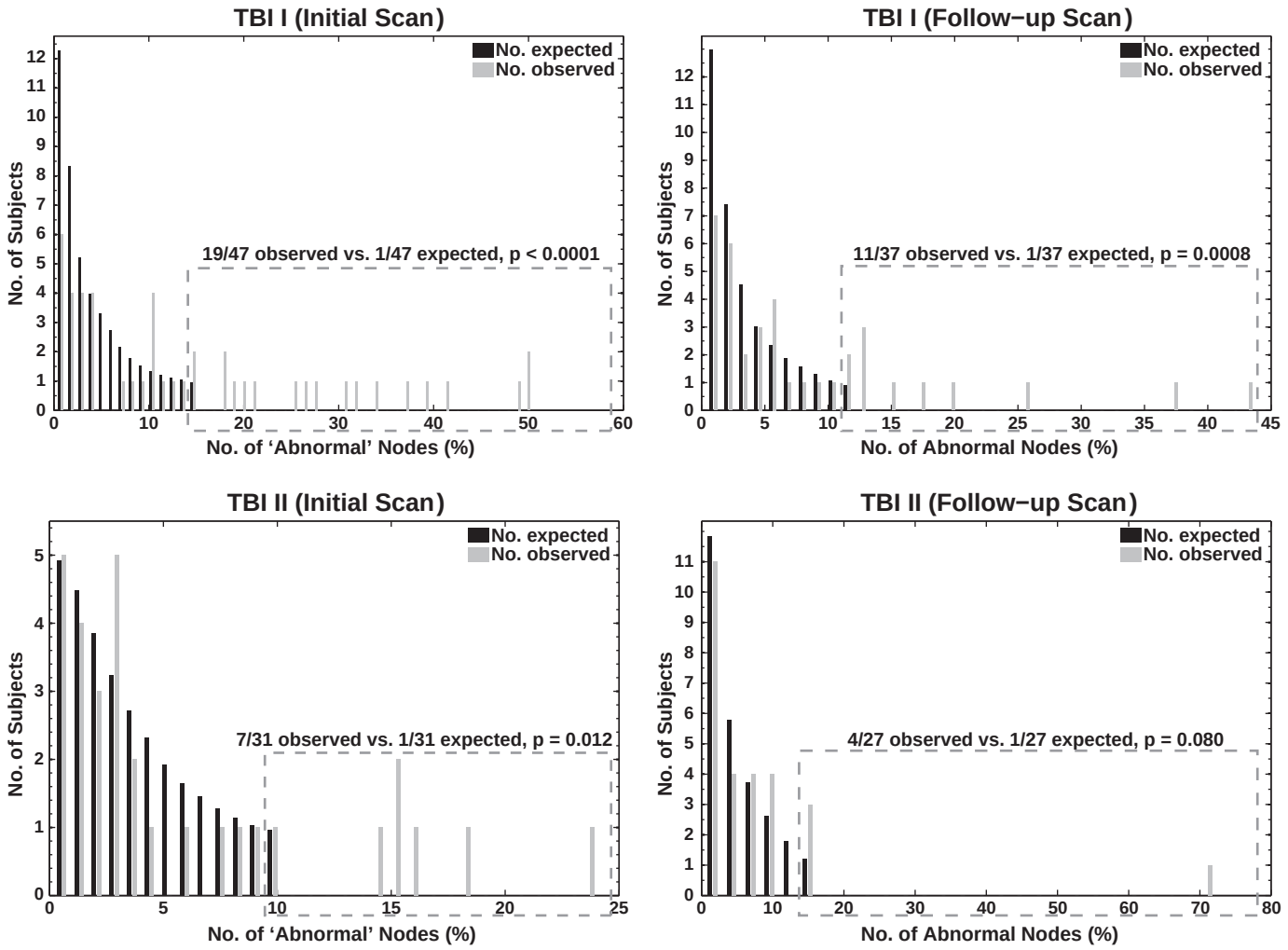

Fig. 10. Bar graphs for observed and expected proportion of 'abnormal' nodes in the patients with TBI relative to the controls without ROI selection. The distributions of expected relatively 'abnormal' ROIs were calculated from the permutation of group memberships (10,000 permutations). The *p*-values were obtained by the one-sided *z*-test (TBI I > controls in the proportion of 'abnormal' nodes).

modules. In healthy normal subjects, modules in the spontaneous brain network are closely associated with auditory, visual, somatosensory/motor, attention, sub-cortical and default mode networks (He et al., 2009). Though we did not directly assess in this study, traumatic axonal injuries in long range fibers mediating connections with multiple modules may lead to disruptions in between-module connectivity. In TBI patients, disrupted white matter integrity in the splenium of the corpus callosum has been correlated with PCC functional connectivity in the default mode network (Sharp et al., 2011). Our previous DTI study showed disrupted white matter integrity in the TBI I cohort relative to the controls (Mac Donald et al., 2011). However, it is too early to interpret the association of altered white matter integrity reported in Mac Donald et al. (2011) with disrupted between-module functional connectivity following bTBI without direct investigation of structural white matter connectivity at a subject by subject level. Since strong functional connectivity between regions is often maintained without monosynaptic connections between these regions (Honey et al., 2009), direct comparisons of functional and structural connectivity are not straightforward. Therefore, further studies on the association between structural and functional connectivity on these concussive bTBI patients are needed to understand the underlying mechanisms of disrupted between-module connectivity following bTBI. This will require further investigations that are beyond the scope of the current manuscript.

Technical limitations

The present study has several limitations due to data quality. First, our analysis results were from a subset (75% of all subjects' data; 62%, 76%, 81% of the controls, TBI I cohort and TBI II cohort, respectively) of the subjects' data to ensure data quality. Our study results may be more representative if more subjects' data had passed the quality assurance procedure. As such, the quality assurance procedure yielded a relatively small sample size (N = 12 for each scan) of controls. A small sample size could be an alternative explanation for the apparent resolution of the module-based graph measures in the TBI patients on follow-up scans. In other words, decreases in the numbers of relatively abnormal TBI patients could have been partially explained by the increased standard deviations of the module-based graph measures for the controls on the follow-up scans. The exclusion of a part of the subjects' data for data quality assurance may not be surprising to neuroimaging researchers, particularly in fMRI, considering the difference in subjects' conditions between clinical populations and healthy subjects. However, this is an important consideration clinically as it may not be feasible to collect reliable data from every patient to be used as early indicators of injury, disease, or for non-invasive monitoring of rehabilitation progress.

Second, moderate data quality of the T_1-weighted MRI due to subject motion was not sufficient for Freesurfer to reconstruct cortical surfaces

in fully automated fashion. Thus, following the well-documented instructions, a substantial amount of time was required for manual intervention during cortical surface reconstruction to compensate for the MRI data quality of our study. Cortical surface reconstruction would be more reliable (and require less manual intervention) if we increased the signal-to-noise ratio of the T_1-weighted MRI by acquiring two or more images as the Freesurfer instructions suggest. However, a practical limitation of studies of relatively acutely injured subjects is that time in the scanner must be kept relatively short for patient comfort and safety.

Third, we were not able to include much of the orbitofrontal cortex and inferior temporal cortex in our analysis due to signal loss by fMRI susceptibility artifacts (Ojemann et al., 1997) and low signal to noise due to distance from the MR receiver coils. Particularly, the orbitofrontal cortex was of interest based on a previous simulation study on the effect of blasts on the brain (Taylor and Ford, 2009) and our previous DTI study (Mac Donald et al., 2011) involving the TBI I cohort. An optimized pulse sequence to account for susceptibility artifacts (Domsch et al., 2012) would be beneficial in this regard for future studies.

Fourth, we did not include negative correlations for the network constructions as the meaning of negative correlations after global signal regression is still unclear (Anderson et al., 2011; Chai et al., 2012; Chang and Glover, 2009; Fox et al., 2009; Murphy et al., 2009; Saad et al., 2012). Assessment of anticorrelations in bTBI populations would be of interest if the meaning of negative correlations is clarified by future studies.

Finally, we did not make a direct comparison of the initial and follow-up scans even though we acquired MRI data at two time points. Instead, we performed only a cross-sectional study at two time points and observed change of modular organization of the TBI patients relative to the controls at each time point. Lack of quantification on the effects of the two different MRI scanners, medications between the time of the initial and follow-up scans and sleep deprivation at the time of the initial scans prevented us from directly analyzing our data in a subject-by-subject longitudinal fashion.

Interpretations

The underlying biological mechanisms and consequences of the findings in this study are not yet clear. Possible explanations for the relatively disrupted between-module functional connectivity in the TBI cohorts on initial scans may be related to white matter injury. This hypothesis is based on previous combined DTI and fMRI connectivity studies on TBI populations (Bonnelle et al., 2012; Mayer et al., 2011; Sharp et al., 2011). Several relevant investigations into the underlying biological mechanisms of concussive TBI in the context of white matter injury have been performed recently. In magnetic resonance spectroscopy (MRS) studies of concussive TBI (Gasparovic et al., 2009; Johnson et al., 2012; Yeo et al., 2011a), three main findings have been reported: (1) reduced N-acetylaspartate (NAA) in the white matter, reflective of disruptions in neuronal integrity, (2) increased creatine in the white matter, reflective of alterations in cellular energy metabolism, and (3) increased choline in the white matter, associated with injury and repair of myelin and/or inflammation. In particular, Johnson et al. (2012) demonstrated that altered metabolic integrity measured by NAA/choline in the splenium of the concussive TBI patients was associated with reduced functional inter-hemispheric connectivity following TBI.

Another possibility is unmeasured pathophysiology following TBI in the gray matter. Previous metabolic imaging studies in concussive TBI reported metabolic changes in the gray matter following TBI that might lead to changes in BOLD signals (see Lin et al., 2012 for a review). For example, single photon emission computed tomography (SPECT) identified reduced regional cerebral blood flow (rCBF) in concussive TBI patients (Jacobs et al., 1996). Positron emission tomography (PET) revealed a decreased cerebral glucose metabolic rate (CMR_{glu}) in veterans with repetitive concussive bTBI (Peskind et al., 2011). MRS studies (Gasparovic et al., 2009; Yeo et al., 2011a) demonstrated decreased glutamate–glutamine (Glx) in the gray matter of the concussive TBI group and reduced BOLD response following TBI. Taken together, future studies involving DTI, MRS, SPECT, PET and other methods sensitive to structural and metabolic derangements will be required to assess the underlying pathological mechanisms of findings in this study.

The biological mechanisms for apparent resolution of between-module functional connectivity in the TBI patients on the follow-up scans are not known. One possibility is that the TBI patients could have been subjected to more sleep deprivation at the time of initial scans; sleep deprivation has been shown to affect BOLD signals (Gujar et al., 2010). Medications used by TBI patients at the acute stage and during rehabilitation could also be partially accountable.

There are several alternative explanations for our findings:

1) It is possible that some of these results may have occurred by chance as group differences at the node- and region-specific levels were not statistically significant after correction for multiple comparisons ($q_{FDR} < 0.05$). We do not think that this is likely to be the case for all of our results since the analysis of the TBI II cohort was performed with no free parameters after we obtained the analysis results of the TBI I cohort. In other words, the TBI II cohort served as a validation dataset. Thus, the single-subject analyses of the initial scan (Figs. 7–9) should be regarded as the most solid.
2) Unmeasured systematic differences in the time spent in the scanner with eyes open versus closed or awake versus asleep could also be confounding factors. It has been reported that functional connectivity strength in the default mode network and attention network with eyes closed is decreased over network connectivity with eyes opened (van Dijk et al., 2010). Functional connectivity in the default mode, attention, executive control, motor, visual and auditory network is retained (Larson-Prior et al., 2009) during light sleep, but functional connectivity in the default mode network is partially changed during deep sleep (Horovitz et al., 2009). We were not able to control the extent of eyes-open vs. eyes closed time, nor assess sleep in the scanner due to the logistical challenges of obtaining scans in acutely injured U.S. military personnel.
3) The effects of analgesic medications could be another confounding factor. To our knowledge, immediate effects of analgesics on resting-state functional connectivity in fMRI are unknown, but alterations in regional synchrony of resting-state functional connectivity in fMRI in the right anterior cingulate cortex and left precentral frontal gyrus in chronic ketamine users has been reported (Liao et al., 2012).
4) Other, unmeasured differences in pre- and post-injury characteristics among the three groups could also provide alternative explanations for our findings. The initial scan data of the controls and TBI I cohort were acquired in 2008–2009 while those of the TBI II cohort were acquired in 2010–2011. During this period, the pace of the wars was changed and rehabilitation strategies and treatments may have improved (see van Wingen et al. (2012) for the effects of combat stress on functional connectivity). All these characteristics were unmeasured. Thus, it is unclear whether reduction in the proportion of TBI patients with a relatively 'abnormal' participation coefficient across ROIs (Figs. 7–9) from the TBI I cohort to the TBI II cohort was solely due to a different detection performance of the multivariate analysis over the two datasets or due to an intrinsic difference between the subjects in the 2 TBI cohorts.
5) Biases due to incomplete blinding during the manual portions of the Freesurfer analysis could also affect our results though the associated effects are not likely to be substantial considering the difference in spatial resolutions: 4^3 mm^3 in fMRI versus 1 mm^3 in structural MRI.
6) Test–retest reliability of our findings is still unknown. Two previous reports, one indicating moderately good reliability (Braun et al., 2012) and another indicating relatively low test–retest reliability for many graph theoretical measures (Wang et al., 2011) used coarser parcellation and less aggressive motion scrubbing than the current work.

Future directions

The most important future direction for this line of investigation is an assessment of the relationship between these graph-theoretically derived neuroimaging variables and clinical outcomes in these cohorts. This will be the topic of future communications. Further studies will be required to address the technical concerns discussed above and assess the mechanisms underlying these observed network properties.

Conclusions

In conclusion, we demonstrated a disrupted modular organization of the resting-state cortical functional network in U.S. military personnel with concussive bTBI. Module-based graph theoretic analysis revealed altered between-module connectivity in the TBI patients relative to the controls who had blast exposures without a diagnosis of TBI. Single-subject multivariate analysis fairly consistently detected the TBI patients with relatively 'abnormal' ROIs over two independent cohorts. Our single-subject analysis approach may be useful for heterogeneous populations and potentially complement hypothesis-driven approaches for these populations in future resting-state fMRI studies. Further studies are required to explain the underlying mechanisms and consequences of these phenomena.

Supplementary data to this article can be found online at http://dx.doi.org/10.1016/j.neuroimage.2013.08.017.

Acknowledgments

First of all, we would like to thank all participants, their families, the commanding officers and the clinical care providers that supported this study. Our thanks also go to Dr. Nico U. Dosenbach, Dr. Steven E. Petersen and Dr. Abraham Z. Snyder for their helpful comments. This work has been supported by Department of Defense CDMRP grants PT075299 and PT090444 to DLB. We also would like to thank the facilities of the Washington University Center for High Performance Computing, which were partially provided through grant NCRR 1S10RR022984-01A1 for providing computational resource for conducting this study. Finally, we would like to thank the two anonymous reviewers for their comments which substantially improved this manuscript.

Conflict of interest

The authors declare no conflict of interest.

References

Achard, S., Salvador, R., Whitcher, B., Suckling, J., Bullmore, E.T., 2006. A resilient, low-frequency, small-world human brain functional network with highly connected association cortical hubs. J. Neurosci. 26, 63–72.

Anderson, J.S., Druzgal, T.J., Lopez-Larson, M., Jeong, E., Desai, K., Yurgelun-Todd, D., 2011. Network anticorrelations, global regression, and phase-shifted soft tissue correction. Hum. Brain Mapp. 32, 919–934.

Arenivas, A., Diaz-Arrastia, R., Spence, J., Cullum, C.M., Krishnan, K., Bosworth, C., Culver, C., Kennard, B., Marquez de la Plata, C., 2012. Three approaches to investigating functional compromise to the default mode network after traumatic axonal injury. Brain Imaging Behav. 13, 1–13.

Argall, B.D., Saad, Z.S., Beauchamp, M.S., 2006. Simplified intersubject averaging on the cortical surface using SUMA. Hum. Brain Mapp. 27, 14–27.

Biswal, B., Yetkin, F.Z., Haughton, V.M., Hyde, J.S., 1995. Functional connectivity in the motor cortex of resting human brain using echo-planar MRI. Magn. Reson. Med. 34, 537–541.

Blondel, V.D., Guillaume, J., Lambiotte, R., Lefebvre, E., 2008. Fast unfolding of communities in large networks. J. Stat. Mech.: Theory Exp. 2008, P10008.

Bonnelle, V., Leech, R., Kinnunen, K.M., Ham, T.E., Beckmann, C.F., de Boissezon, X., Greenwood, R.J., Sharp, D.J., 2011. Default mode network connectivity predicts sustained attention deficits after traumatic brain injury. J. Neurosci. 31, 13442–13451.

Bonnelle, V., Ham, T.E., Leech, R., Kinnunen, K.M., Mehta, M.A., Greenwood, R.J., Sharp, D.J., 2012. Salience network integrity predicts default mode network function after traumatic brain injury. Proc. Natl. Acad. Sci. U. S. A. 109, 4690–4695.

Braun, Urs, Plichta, M.M., Esslinger, C., Sauer, C., Haddad, L., Grimm, O., Mier, D., et al., 2012. Test–retest reliability of resting-state connectivity network characteristics using fMRI and graph theoretical measures. Neuroimage 59, 1404–1412.

Bullmore, E.T., Sporns, O., 2009. Complex brain networks: graph theoretical analysis of structural and functional systems. Nat. Rev. Neurosci. 10, 186–198.

Caeyenberghs, K., Leemans, A., Heitger, M.H., Leunissen, I., Dhollander, T., Sunaert, S., Dupont, P., Swinnen, S.P., 2012. Graph analysis of functional brain networks for cognitive control of action in traumatic brain injury. Brain 135, 1293–1307.

Casscells, S.W., 2007. Traumatic Brain Injury: Definition and Reporting. Department of Defense, Washington, DC ((memorandum) (http://mhs.osd.mil/Content/docs/pdfs/policies/2007/07-030.pdf)).

Castellanos, N.P., Paul, N., Ordonez, V.E., Demuynck, O., Bajo, R., Campo, P., Bilbao, A., Ortiz, T., del-Pozo, F., Maestu, F., 2010. Reorganization of functional connectivity as a correlate of cognitive recovery in acquired brain injury. Brain 133, 2365–2381.

Castellanos, N.P., Leyva, I., Buldu, J.M., Bajo, R., Paul, N., Cuesta, P., Ordonez, V.E., et al., 2011. Principles of recovery from traumatic brain injury: reorganization of functional networks. Neuroimage 55, 1189–1199.

Chai, X.J., Castanon, A.N., Ongur, D., Whitfield-Gabrieli, S., 2012. Anticorrelations in resting state networks without global signal regression. Neuroimage 59, 1420–1428.

Chang, C., Glover, G.H., 2009. Effects of model-based physiological noise correction on default mode network anti-correlations and correlations. Neuroimage 47, 1448–1459.

Chen, Z.J., He, Y., Rosa-Neto, P., Germann, J., Evans, A.C., 2008. Revealing modular architecture of human brain structural networks by using cortical thickness from MRI. Cereb. Cortex 18, 2374–2381.

Cox, R.W., 1996. AFNI: software for analysis and visualization of functional magnetic resonance neuroimages. Comput. Biomed. Res. 29, 162–173.

Dale, A.M., Sereno, M.I., 1993. Improved localization of cortical activity by combining EEG and MEG with MRI cortical surface reconstruction: a linear approach. J. Cogn. Neurosci. 5, 162–176.

Dale, A.M., Fischl, B., Sereno, M.I., 1999. Cortical surface-based analysis. I. Segmentation and surface reconstruction. Neuroimage 9, 179–194.

de Haan, W., van der Flier, W.M., Koene, T., Smits, L.L., Scheltens, P., Stam, C.J., 2012. Disrupted modular brain dynamics reflect cognitive dysfunction in Alzheimer's disease. Neuroimage 59, 3085–3093.

Dempsey, K.E., Dorlac, W.C., Martin, K., Fang, R., Fox, C., Bennett, B., Williams, K., Flaherty, S., 2009. Landstuhl Regional Medical Center: traumatic brain injury screening program. J. Trauma Nurs. 16, 6–12.

Destrieux, C., Fischl, B., Dale, A.M., Halgren, E., 2010. Automatic parcellation of human cortical gyri and sulci using standard anatomical nomenclature. Neuroimage 53, 1–15.

Domsch, S., Linke, J., Heiler, P.M., Kroll, A., Flor, H., Wessa, M., Schad, L.R., 2012. Increased BOLD sensitivity in the orbitofrontal cortex using slice-dependent echo times at 3 T. Magn. Reson. Imaging 31, 201–211.

Doppenberg, E.M.R., Bullock, R., 1997. Clinical neuro-protection trials in severe traumatic brain injury: lessons from previous studies. J. Neurotrauma 14, 71–80.

Duda, R.O., Hart, P.E., Stork, D.G., 2001. Pattern Classification, 2nd ed. Wiley.

Evans, A.C., Collins, D.L., Mills, S.R., Brown, E.D., Kelly, R.L., Peters, T.M., 1993. 3D statistical neuroanatomical models from 305 MRI volumes. Proc IEEE Nucl Sci Symp Med Imaging Conf. IEEE, pp. 1813–1817.

Finkel, M.F., 2006. The neurological consequences of explosives. J. Neurol. Sci. 249, 63–67.

Fischl, B., Sereno, M.I., Dale, A.M., 1999a. Cortical surface-based analysis: II: Inflation, flattening, and a surface-based coordinate system. Neuroimage 9, 195–207.

Fischl, B., Sereno, M.I., Tootell, R.B.H., Dale, A.M., 1999b. High-resolution intersubject averaging and a coordinate system for the cortical surface. Hum. Brain Mapp. 8, 272–284.

Fischl, B., Liu, A., Dale, A.M., 2001. Automated manifold surgery: constructing geometrically accurate and topologically correct models of the human cerebral cortex. IEEE Trans. Med. Imaging 20, 70–80.

Fischl, B., Salat, D.H., Busa, E., Albert, M., Dieterich, M., Haselgrove, C., van der Kouwe, A.J.W., et al., 2002. Whole brain segmentation: automated labeling of neuroanatomical structures in the human brain. Neuron 33, 341–355.

Fischl, B., van der Kouwe, A.J.W., Destrieux, C., Halgren, E., Segonne, F., Salat, D.H., Busa, E., et al., 2004a. Automatically parcellating the human cerebral cortex. Cereb. Cortex 14, 11–22.

Fischl, B., Salat, D.H., van der Kouwe, A.J.W., Makris, N., Segonne, F., Quinn, B.T., Dale, A.M., 2004b. Sequence-independent segmentation of magnetic resonance images. Neuroimage 23, S69–S84.

Fortunato, Santo, 2010. Community detection in graphs. Phys. Rep. 486, 75–174.

Fox, M.D., Snyder, A.Z., Vincent, J.L., Corbetta, M., van Essen, D.C., Raichle, M.E., 2005. From the cover: the human brain is intrinsically organized into dynamic, anticorrelated functional networks. Proc. Natl. Acad. Sci. U. S. A. 102, 9673–9678.

Fox, M.D., Zhang, D., Snyder, A.Z., Raichle, M.E., 2009. The global signal and observed anticorrelated resting state brain networks. J. Neurophysiol. 101, 3270–3283.

Gasparovic, C., Yeo, R., Mannell, M., Ling, J., Elgie, R., Phillips, J, Doezema, D, Mayer, A.R., 2009. Neurometabolite concentrations in gray and white matter in mild traumatic brain injury: an ^{1}H-magnetic resonance spectroscopy study. J. Neurotrauma 26, 1635–1643.

Genovese, C.R., Lazar, N.A., Nichols, T.E., 2002. Thresholding of statistical maps in functional neuroimaging using the false discovery rate. Neuroimage 15, 870–878.

Greicius, M.D., Krasnow, B., Reiss, A.L., Menon, V., 2002. Functional connectivity in the resting brain: a network analysis of the default mode hypothesis. Proc. Natl. Acad. Sci. U. S. A. 100, 253–258.

Guimera, R., Amaral, L.A.N., 2005. Functional cartography of complex metabolic networks. Nature 433, 895–900.

Gujar, N., Yoo, S., Hu, P., Walker, M.P., 2010. The unrested resting brain: sleep deprivation alters activity within the default-mode network. J. Cogn. Neurosci. 22, 1637–1648.

Hagler, D.J., Saygin, A.P., Sereno, M.I., 2006. Smoothing and cluster thresholding for cortical surface-based group analysis of fMRI data. Neuroimage 33, 1093–1103.

Hagmann, P., Cammoun, L., Gigandet, X., Meuli, R., Honey, C.J., Wedeen, V.J., Sporns, O., 2008. Mapping the structural core of human cerebral cortex. PLoS Biol. 6, e159.
Hayasaka, S., Laurienti, P.J., 2010. Comparison of characteristics between region- and voxel-based network analyses in resting-state fMRI data. Neuroimage 50, 499–508.
He, Y., Chen, Z.J., Evans, A.C., 2007. Small-world anatomical networks in the human brain revealed by cortical thickness from MRI. Cereb. Cortex 17, 2407–2419.
He, Y., Wang, J., Wang, L., Chen, Z.J., Yan, C., Yang, H., Tang, H., et al., 2009. Uncovering intrinsic modular organization of spontaneous brain activity in humans. PLoS One 4, e5226.
Honey, C.J., Sporns, O., Cammoun, L., Gigandet, X., Thiran, J.P., Meuli, R., Hagmann, P., 2009. Predicting human resting-state functional connectivity from structural connectivity. Proc. Natl. Acad. Sci. U. S. A. 106, 2035–2040.
Horovitz, S.G., Braun, A.R., Carr, W.S., Picchioni, D., Balkin, T.J., Fukunaga, M., Duyn, J.H., 2009. Decoupling of the Brain's default mode network during deep sleep. Proc. Natl. Acad. Sci. U. S. A. 106, 11376–11381.
Jacobs, A., Put, E., Ingels, M., Put, T., Bossuyt, A., 1996. One-year follow-up of technetium-99m-HMPAO SPECT in mild head injury. J. Nucl. Med. 37, 1605–1609.
Jo, H.J., Lee, J., Kim, J., Shin, Y., Kim, I., Kwon, J.S., Kim, S.I., 2007. Spatial accuracy of fMRI activation influenced by volume- and surface-based spatial smoothing techniques. Neuroimage 34, 550–564.
Jo, H.J., Lee, J., Kim, J., Choi, C., Gu, B., Kang, D., Ku, J., Kwon, J.S., Kim, S.I., 2008. Artificial shifting of fMRI activation localized by volume- and surface-based analyses. Neuroimage 40, 1077–1089.
Johnson, B., Zhang, K., Gay, M., Neuberger, T., Horovitz, S., Hallett, M., Sebastianelli, W., Slobounov, S., 2012. Metabolic alterations in corpus callosum may compromise brain functional connectivity in MTBI patients: an ^{1}H-MRS study. Neurosci. Lett. 509, 5–8.
Johnstone, T., Walsh, K.S.O., Greischar, L.L., Alexander, A.L., Fox, A.S., Davidson, R.J., Oakes, T.R., 2006. Motion correction and the use of motion covariates in multiple-subject fMRI analysis. Hum. Brain Mapp. 27, 779–788.
Jovicich, J., Czanner, S., Greve, D., van der Elizabeth Haley, A.J.W., Kouwe, R., Gollub, D. Kennedy, et al., 2006. Reliability in multi-site structural MRI studies: effects of gradient non-linearity correction on phantom and human data. Neuroimage 30, 436–443.
Kasahara, M., Menon, D.K., Salmond, C.H., Outtrim, J.G., Taylor Tavares, J.V., Carpenter, T.A., Pickard, J.D., Sahakian, B.J., Stamatakis, E.A., 2010. Altered functional connectivity in the motor network after traumatic brain injury. Neurology 75, 168–176.
Larson-Prior, L.J., Zempel, J.M., Nolan, T.S., Prior, F.W., Snyder, A.Z., Raichle, M.E., 2009. Cortical network functional connectivity in the descent to sleep. Proc. Natl. Acad. Sci. U. S. A. 106, 4489–4494.
Latora, V., Marchiori, M., 2001. Efficient behavior of small-world networks. Phys. Rev. Lett. 87, 198701.
Levin, H.S., Wilde, E.A., Troyanskaya, M., Petersen, N.J., Scheibel, R., Newsome, M., Radaideh, M., et al., 2010. Diffusion tensor imaging of mild to moderate blast-related traumatic brain injury and its sequelae. J. Neurotrauma 27, 683–694.
Liang, X., Zou, Q., He, Y., Yang, Y., 2013. Coupling of functional connectivity and regional cerebral blood flow reveals a physiological basis for network hubs of the human brain. Proc. Natl. Acad. Sci. 110, 1929–1934.
Liao, Y., Tang, J., Fornito, A., Liu, T., Chen, X., Chen, H., Xiang, X., Wang, X., Hao, W., 2012. Alterations in regional homogeneity of resting-state brain activity in ketamine addicts. Neurosci. Lett. 522, 36–40.
Lin, A.P., Liao, H.J., Merugumala, S.K., Prabhu, S.P., Meehan, W.P., Ross, B.D., 2012. Metabolic imaging of mild traumatic brain injury. Brain Imaging Behav. 6, 208–223.
Lowe, M.J., Mock, B.J., Sorenson, J.A., 1998. Functional connectivity in single and multislice echoplanar imaging using resting-state fluctuations. Neuroimage 7, 119–132.
Mac Donald, C.L., Johnson, A.M., Cooper, D., Nelson, E.C., Werner, N.J., Shimony, J.S., Snyder, A.Z., et al., 2011. Detection of blast-related traumatic brain injury in U.S. military personnel. N. Engl. J. Med. 364, 2091–2100.
Marquez de la Plata, C.D., Garces, J., Kojori, E.S., Grinnan, J., Krishnan, K., Pidikiti, R., Spence, J., et al., 2011. Deficits in functional connectivity of hippocampal and frontal lobe circuits after traumatic axonal injury. Arch. Neurol. 68, 74–84.
Mayer, A.R., Mannell, M.V., Ling, J., Gasparovic, C., Yeo, R.A., 2011. Functional connectivity in mild traumatic brain injury. Hum. Brain Mapp. 32, 1825–1835.
Meunier, D., Achard, S., Morcom, A., Bullmore, E.T., 2009a. Age-related changes in modular organization of human brain functional networks. Neuroimage 44, 715–723.
Meunier, D., Lambiotte, R., Fornito, A., Ersche, K.D., Bullmore, E.T., 2009b. Hierarchical modularity in human brain functional networks. Front. Neuroinform. 3, 37.
Micheloyannis, S., Pachou, E., Stam, C.J., Breakspear, M., Bitsios, P., Vourkas, M., Erimaki, S., Zervakis, M., 2006. Small-world networks and disturbed functional connectivity in schizophrenia. Schizophr. Res. 87, 60–66.
Minka, T., 2000. Automatic choice of dimensionality for PCA. Massachusetts Inst. Technol., Cambridge, Tech. Rep. 514.
Murphy, K., Birn, R.M., Handwerker, D.A., Jones, T.B., Bandettini, P.A., 2009. The impact of global signal regression on resting state correlations: are anti-correlated networks introduced? Neuroimage 44, 893–905.
Nakamura, T., Hillary, F.G., Biswal, B.B., 2009. Resting network plasticity following brain injury. PLoS One 4, e8220.
Newman, M.E.J., 2004. Fast algorithm for detecting community structure in networks. Phys. Rev. E 69, 066133.
Newman, M., Girvan, M., 2004. Finding and evaluating community structure in networks. Phys. Rev. E 69, 026113.
Nichols, T.E., Holmes, A.P., 2001. Nonparametric permutation tests for functional neuroimaging: a primer with examples. Hum. Brain Mapp. 15, 1–25.
Niogi, S.N., Mukherjee, P., 2010. Diffusion tensor imaging of mild traumatic brain injury. J. Head Trauma Rehabil. 25, 241–255.
Niogi, S.N., Mukherjee, P., Ghajar, J., Johnson, C.E., Kolster, R., Lee, H., Suh, M., Zimmerman, R.D., Manley, G.T., McCandliss, B.D., 2008. Structural dissociation of attentional control and memory in adults with and without mild traumatic brain injury. Brain 131, 3209–3221.
Ojemann, J.G., Akbudak, E., Snyder, A.Z., McKinstry, R.C., Raichle, M.E., Conturo, T.E., 1997. Anatomic localization and quantitative analysis of gradient refocused echo-planar fMRI susceptibility artifacts. Neuroimage 6, 156–167.
Okie, Susan, 2006. Reconstructing lives—a tale of two soldiers. N. Engl. J. Med. 355, 2609–2615.
Pandit, A.S., Expert, P., Lambiotte, R., Bonnelle, V., Leech, R., Turkheimer, F.E., Sharp, D.J., 2013. Traumatic brain injury impairs small-world topology. Neurology 80, 1826–1833.
Peskind, E.R., Petrie, E.C., Cross, D.J., Pagulayan, K., McCraw, K., Hoff, D., Hart, K., et al., 2011. Cerebrocerebellar hypometabolism associated with repetitive blast exposure mild traumatic brain injury in 12 Iraq War veterans with persistent post-concussive symptoms. Neuroimage 54, S76–S82.
Ponten, S.C., Bartolomei, F., Stam, C.J., 2007. Small-world networks and epilepsy: graph theoretical analysis of intracerebrally recorded mesial temporal lobe seizures. Clin. Neurophysiol. 118, 918–927.
Power, J.D., Cohen, A.L., Nelson, S.M., Wig, G.S., Barnes, K.A., Church, J.A., Vogel, A.C., et al., 2011. Functional network organization of the human brain. Neuron 72, 665–678.
Power, J.D., Barnes, K.A., Snyder, A.Z., Schlaggar, B.L., Petersen, S.E., 2012. Spurious but systematic correlations in functional connectivity MRI networks arise from subject motion. Neuroimage 59, 2142–2154.
Raichle, M.E., MacLeod, A.M., Snyder, A.Z., Powers, W.J., Gusnard, D.A., Shulman, G.L., 2001. A default mode of brain function. Proc. Natl. Acad. Sci. U. S. A. 98, 676–682.
Rombouts, S.A.R.B., Stam, C.J., Kuijer, J.P.A., Scheltens, Ph., Barkhof, F., 2003. Identifying confounds to increase specificity during a 'no task condition': evidence for hippocampal connectivity using fMRI. Neuroimage 20, 1236–1245.
Rosvall, M., Bergstrom, C.T., 2008. Maps of random walks on complex networks reveal community structure. Proc. Natl. Acad. Sci. 105, 1118–1123.
Rubinov, M., Sporns, O., 2010. Complex network measures of brain connectivity: uses and interpretations. Neuroimage 52, 1059–1069.
Saad, Z.S., Reynolds, R.C., Argall, B., Japee, S., Cox, R.W., 2004. SUMA: an interface for surface-based intra- and inter-subject analysis with AFNI. 2004 2nd IEEE International Symposium on Biomedical Imaging: From Nano to Macro, Vols 1 and 2, pp. 1510–1513.
Saad, Z.S., Gotts, S.J., Murphy, K., Chen, G., Jo, H.J., Martin, A., Cox, R.W., 2012. Trouble at rest: how correlation patterns and group differences become distorted after global signal regression. Brain Connect. 2, 25–32.
Saatman, K.E., Duhaime, A., Bullock, R., Mass, A.I.R., Valadka, A., Manley, G.T., Workshop scientific team, advisory panel members, 2008. Classification of traumatic brain injury for targeted therapies. J. Neurotrauma 25, 719–738.
Salvador, R., Suckling, J., Coleman, M.R., Pickard, J.D., Menon, D., Bullmore, E.T., 2005. Neurophysiological architecture of functional magnetic resonance images of human brain. Cereb. Cortex 15, 1332–1342.
Satterthwaite, T.D., Wolf, D.H., Loughead, J., Ruparel, K., Elliott, M.A., Hakonarson, H., Gur, R.C., Gur, R.E., 2012. Impact of in-scanner head motion on multiple measures of functional connectivity: relevance for studies of neurodevelopment in youth. Neuroimage 60, 623–632.
Scheibel, R.S., Newsome, M.R., Troyanskaya, M., Lin, X., Steinberg, J.L., Radaideh, M., Levin, H.S., 2012. Altered brain activation in military personnel with one or more traumatic brain injuries following blast. J. Int. Neuropsychol. Soc. 18, 89–100.
Seeley, W.W., Menon, V., Schatzberg, A.F., Keller, J., Glover, G.H., Kenna, H., Reiss, A.L., Greicius, M.D., 2007. Dissociable intrinsic connectivity networks for salience processing and executive control. J. Neurosci. 27, 2349–2356.
Segonne, F., Dale, A.M., Busa, E., Glessner, M., Salat, D.H., Hahn, H.K., Fischl, B., 2004. A hybrid approach to the skull stripping problem in MRI. Neuroimage 22, 1060–1075.
Sharp, D.J., Beckmann, C.F., Greenwood, R., Kinnunen, K.M., Bonnelle, V., de Boissezon, X., Powell, J.H., Counsell, S.J., Patel, M.C., Leech, R., 2011. Default mode network functional and structural connectivity after traumatic brain injury. Brain 134, 2233–2247.
Shenton, M.E., Hamoda, H.M., Schneiderman, J.S., Bouix, S., Pasternak, O., Rathi, Y., Vu, M.-A., et al., 2012. A review of magnetic resonance imaging and diffusion tensor imaging findings in mild traumatic brain injury. Brain Imaging Behav. 6, 137–192.
Shumskaya, E., Andriessen, T.M.J.C., Norris, D.G., Vos, P.E., 2012. Abnormal whole-brain functional networks in homogeneous acute mild traumatic brain injury. Neurology 79, 175–182.
Slobounov, S.M., Gay, M., Zhang, K., Johnson, B., Pennell, D., Sebastianelli, W., Horovitz, S., Hallett, M., 2011. Alteration of brain functional network at rest and in response to YMCA physical stress test in concussed athletes: RsFMRI study. Neuroimage 55, 1716–1727.
Sponheim, S.R., McGuire, K.A., Kang, S.S., Davenport, N.D., Aviyente, S., Bernat, E.M., Lim, K.O., 2011. Evidence of disrupted functional connectivity in the brain after combat-related blast injury. Neuroimage 54, S21–S29.
Stam, C., Jones, B., Nolte, G., Breakspear, M., Scheltens, P., 2006. Small-world networks and functional connectivity in Alzheimer's disease. Cereb. Cortex 17, 92–99.
Tang, L., Ge, Y., Sodickson, D.K., Miles, L., Zhou, Y., Reaume, J., Grossman, R.I., 2011. Thalamic resting-state functional networks: disruption in patients with mild traumatic brain injury. Radiology 260, 831–840.
Taylor, P.A., Ford, C.C., 2009. Simulation of blast-induced early-time intracranial wave physics leading to traumatic brain injury. J. Biomech. Eng. 131, 061007.
Tucholka, A., Fritsch, V., Poline, J., Thirion, B., 2012. An empirical comparison of surface-based and volume-based group studies in neuroimaging. Neuroimage 63, 1443–1453.
Valencia, M., Pastor, M.A., Fernandez-Seara, M.A., Artieda, J., Martinerie, J., Chavez, M., 2009. Complex modular structure of large-scale brain networks. Chaos 19, 023119.
van den Heuvel, M.P., Stam, C.J., Boersma, M., Hulshoff Pol, H.E., 2008. Small-world and scale-free organization of voxel-based resting-state functional connectivity in the human brain. Neuroimage 43, 528–539.
van Dijk, K.R.A., Hedden, T., Venkataraman, A., Evans, K.C., Lazar, S.W., Buckner, R.L., 2010. Intrinsic functional connectivity as a tool for human connectomics: theory, properties, and optimization. J. Neurophysiol. 103, 297–321.

van Dijk, K.R.A., Sabuncu, M.R., Buckner, R.L., 2012. The influence of head motion on intrinsic functional connectivity MRI. Neuroimage 59, 431–438.
van Essen, D.C., Dierker, D., 2007. On navigating the human cerebral cortex: response to 'in praise of tedious anatomy'. Neuroimage 37, 1050–1054.
van Wingen, G.A., Geuze, E., Caan, M.W.A., Kozicz, T., Olabarriaga, S.D., Denys, D., Vermetten, E., Fernandez, G., 2012. Persistent and reversible consequences of combat stress on the mesofrontal circuit and cognition. Proc. Natl. Acad. Sci. U. S. A. 109, 15508–15513.
Vincent, J.L., Kahn, I., Snyder, A.Z., Raichle, M.E., Buckner, R.L., 2008. Evidence for a frontoparietal control system revealed by intrinsic functional connectivity. J. Neurophysiol. 100, 3328–3342.
Wang, J., Zuo, X., Gohel, S., Milham, M.P., Biswal, B.B., He, Y., 2011. Graph theoretical analysis of functional brain networks: test–retest evaluation on short- and long-term resting-state functional MRI data. PLoS One 6, e21976.
Warden, D.L., 2006. Military TBI during the Iraq and Afghanistan wars. J. Head Trauma Rehabil. 21, 398–402.
Watts, D.J., Strogatz, S.H., 1998. Collective dynamics of 'small-world' networks. Nature 393, 440–442.
Wig, G.S., Schlaggar, B.L., Petersen, S.E., 2011. Concepts and principles in the analysis of brain networks. Ann. NY Acad. Sci. 1224, 126–146.
Yeo, R.A., Gasparovic, C., Merideth, F., Ruhl, D., Doezema, D., Mayer, A.R., 2011a. A longitudinal proton magnetic resonance spectroscopy study of mild traumatic brain injury. J. Neurotrauma 28, 1–11.
Yeo, B.T.T., Krienen, F.M., Sepulcre, J., Sabuncu, M.R., Lashkari, D., Hollinshead, M., Roffman, J.L., et al., 2011b. The organization of the human cerebral cortex estimated by intrinsic functional connectivity. J. Neurophysiol. 106, 1125–1165.
Zhang, D., Snyder, A.Z., Fox, M.D., Sansbury, M.W., Shimony, J.S., Raichle, M.E., 2008. Intrinsic functional relations between human cerebral cortex and thalamus. J. Neurophysiol. 100, 1740–1748.

Title: Prospectively Assessed Clinical Outcomes in Concussive Blast vs. Non-blast Traumatic Brain Injury in Evacuated US Military Personnel.

Authors:

Christine L. Mac Donald PhD[1,2], Ann M. Johnson[1], Linda Wierzechowski RN[3], Elizabeth Kassner RN[3], Teresa Stewart RN[3], Elliot C. Nelson MD[1], Nicole J. Werner PhD[1], Col David Zonies MD[3], Col John Oh, MD[3], Col Raymond Fang MD[3, 4], and David L. Brody MD PhD[1]*

1. Washington University School of Medicine, St Louis, MO
2. Current address: University of Washington, Department of Neurosurgery, Seattle, WA
3. Landstuhl Regional Medical Center, Landstuhl, Germany
4. Current address: US Air Force Center for Sustainment of Trauma & Readiness Skills, R Adams Cowley Shock Trauma Center, University of Maryland, Baltimore MD

*To whom correspondence should be addressed at Washington University Department of Neurology, 660 S Euclid Ave, Box 8111, St Louis MO 63110, 314 362 1381 (tel) 314 362 3279 (fax) brodyd@neuro.wustl.edu

Funded by a grant from the Congressionally Directed Medical Research Program (PI: Brody)

Author Contact Information:

Christine L. Mac Donald, PhD
660 S Euclid Ave, CB8111
Saint Louis, MO 63110
Telephone: 314-362-1634
Fax: 314-362-3279
Email: macdonaldc@neuro.wustl.edu

Ann M. Johnson
660 S Euclid Ave, CB8009
Saint Louis, MO 63110
Telephone: 314-362-0881
Fax: 314-747-1404
Email: AJohnson22@WUSTL.EDU

Linda Wierzechowski RN
Trauma Research Coordinator
Landstuhl Regional Medical Center
Telephone: 06371-86-5186
Email: linda.wierzechowski@amedd.army.mil

Elizabeth Kassner RN
Trauma Research Coordinator
Landstuhl Regional Medical Center
Telephone: 06371-86-5186
Email: elizabeth.a.kassner.civ@mail.mil

Teresa Stewart RN
Trauma Research Coordinator
Landstuhl Regional Medical Center
Telephone: 06371-86-5186
Email: theresa.l.stewart4.civ@mail.mil

Elliot C. Nelson, MD
660 S Euclid Ave, CB8134
Saint Louis, MO 63110
Telephone: 314-286-2244
Fax: 314-286-2320
Telephone: 314-286-2244
Email: nelsone@wustl.edu

Nicole J. Werner, PhD
660 S Euclid Ave, CB8111
Saint Louis, MO 63110
Telephone: 314-286-1992
Fax: 314-454-7759
Email: schwarzen@WUSTL.EDU

David Zonies MD
Department of Surgery
Landstuhl Regional Medical Center
Telephone: 06371-86-5186
Email: david.h.zonies.mil@mail.mil

John Oh, MD
Department of Surgery
Landstuhl Regional Medical Center
Telephone: 06371-86-5186
Email: john.oh@amedd.army.mil

Raymond Fang, MD
22 South Greene Street
Baltimore, MD 21201
Telephone: 410-328-0398
Fax: 314-362-3279
Email: rfang@umm.edu

David Brody, MD, PhD
660 S Euclid Ave, CB8111
Saint Louis, MO 63110
Telephone: 314-362-1381
Fax: 314-362-3279
Email: brodyd@neuro.wustl.edu

ABSTRACT

Blast-related traumatic brain injury has been called a 'signature' injury of the wars in Iraq and Afghanistan. Clinical studies in military personnel with blast-related TBI have reported unique features when compared to civilian TBI of similar overall severity, most notably poor overall outcomes and high incidence of concomitant post-traumatic stress disorder and chronic pain. Furthermore, animal studies have reported histological effects of blast-related TBI that are substantially different from injury due to other mechanisms. However, the extent to which difference is clinical outcomes are due to the mechanism of injury (blast vs. other) as opposed to context (combat vs. civilian life) remain to be determined.

Here, we assessed four groups of active duty US Military personnel evacuated from Iraq or Afghanistan to Landstuhl Regional Medical Center, in Landstuhl, Germany: 1) blast-related TBI (n=52), 2) non-blast related TBI with injury due to other mechanisms (n=30), 3) blast-exposed controls evacuated for other medical reasons (n=26) 4) non-blast-exposed controls evacuated for other medical reasons (n=69). All subjects met Dept of Defense criteria for concussive ('mild') TBI. The subjects were evaluated 6-12 months after injury at Washington University in St Louis.

Surprisingly, we found that global outcomes, post-traumatic stress disorder severity, depression, headache severity, and neuropsychological performance were indistinguishable between the two TBI groups, independent of mechanism of injury. Both TBI groups had worse outcomes that the respective control groups. Self-reported combat exposure intensity was higher in the blast-related TBI than in non-blast related TBI subjects, and higher in blast-exposed controls than in non-blast-exposed controls. Interestingly, but combat exposure did not correlate with overall outcome, PTSD, depression, or headache severity. Overall outcomes were most strongly correlated with PTSD and headache severity, but a substantial fraction of the variance in overall outcome was not explained by any of the assessed measures.

One potential interpretation of these results is that TBI itself, independent of mechanism and combat exposure intensity, is the primary driver of adverse outcomes. However, many other factors may be unmeasured and adverse outcomes following war-time injuries still are difficult to fully explain.

Introduction: It has yet to be determined if specific mechanisms of concussive traumatic brain injury (TBI) will have unique effects on clinical outcome. In this prospective study of medically evacuated active-duty US military, blast TBI and non-blast TBI patients were enrolled 0-30 days post-injury and evaluated 6-12 months later. Two control groups were also enrolled, evacuated US military personnel with no history of blast exposure, and those with prior blast history but without clinical evidence of TBI. Global outcome assessed using the Glasgow Outcome Scale-Extended revealed moderate disability in 78% of blast TBI, 80% of non-blast TBI, 58% of blast control and 41% of non-blast control subjects. Impaired neuropsychological performance was found in 36% blast TBI, 33% of non-blast TBI, 19% of blast control, and 10% of non-blast control subjects. Significant neurobehavioral symptoms were identified with the Neurobehavioral Rating Scale-revised (NRS) in both TBI cohorts in comparison to non-blast controls ($p=0.00001$, MWU). Headache-related impairment was equally significant in both TBI groups in comparison to non-blast controls ($p=0.00001$, MWU). 42% of blast TBI and 53% of non-blast TBI subjects met all criteria for post-traumatic stress disorder while 23% of blast controls and only 7% of non-blast controls did as well. In contrast, intensity of combat exposure was found to be highest in blast-TBI and blast control subjects. Best fit logistic regression modeling identified global outcome modestly associated with headache severity, PTSD severity, poor neuropsychological performance and TBI diagnoses (Odd Ratio, 5.35, 95% CI -4.25 : -0.38). In general, there did not appear to be differential influence of mechanism of injury on outcome.

INTRODUCTION

Traumatic brain injury effects approximately 3.5 million individuals annually[1] and roughly 75% are due to mild or concussive like events[2]. In the military, it is estimated that roughly 20% of the current deployed force will suffer a head injury[3] in the wars in Iraq and Afghanistan; the majority of which will endure a mild-uncomplicated head injury or concussion[4]. Blast related TBI has become the 'signature injury' of these current conflicts, however little is known about what, if any, independent contributions blast exposure may have on overall patient outcome.

Previous studies have attempted to examine this question with evaluations based largely on self-reporting[5-12], retrospective medical records review [13-16], and at later stages following injury[17]. Findings from these studies vary regarding the similarity[5, 6, 14, 18, 19] or differences[13, 20] of blast and non-blast patients. Other studies have shown that self-reporting is poorly associated with actual performance on measures such as neuropsychological testing in the military[21, 22] motivating further research utilizing thorough clinical examinations in a prospective fashion.

In the current study, we prospectively enrolled and followed blast and non-blast TBI patients, injured in the wars in Iraq and Afghanistan, from a sub-acute time point following their injury (0-30 days) out to 6-12 months. Detailed clinical measures of outcome were collected at 6-12 months. Two control groups were also studied for comparison including a control group with prior blast exposure but no clinical diagnosis of brain injury as evaluated by trained medical personnel, and a control group with no history of blast exposure. The 'blast control' group was selected in order to explore whether blast exposures, not resulting in a diagnosis of TBI, could also contribute to outcome. These cohorts were enrolled from 2010-2013 as part of an ongoing

collaborative research effort at Landstuhl Regional Medical Center (LRMC), in Landstuhl, Germany. Results from previous cohorts, enrolled from 2008-2010, have been reported elsewhere[23-25].

MATERIALS and METHODS

Participants were enrolled at Landstuhl Regional Medical Center (LRMC) in Landstuhl, Germany following medical evacuation from theater. LRMC is the primary triage facility for all casualties of war originating from Iraq and Afghanistan.

Subjects: Inclusion criteria for the TBI group were as follows: 1) a positive screen for TBI at LRMC based on standard US military clinical criteria[26] including self-report of blast exposure or non-blast mechanism such as blunt trauma resulting in loss of consciousness, amnesia for the event, or change in neurological status, 2) injury from blast or non-blast mechanisms of injury within 30 days of enrollment, 3) US military, 4) ability to provide informed consent in person, 5) no contraindications to MRI such as retained metallic fragments, 6) no prior history of moderate to severe TBI based on Department of Defense criteria, 7) no prior history of major psychiatric disorder, 8) agreement to communicate by telephone or email monthly for 6-12 months and then travel to Washington University for in-person follow-up. Inclusion criteria for the control group were the same except for a negative screen for TBI at LRMC with or without a history of blast exposure. This comprised four groups of subjects : 1-non-blast control, 2-blast control, 3-blast TBI, 4-non-blast TBI (i.e. TBI from mechanisms other than blast).

The research protocol was approved by the Human Research Protection Office at Washington University, the Institutional Review Board for LRMC at Brooke Army Medical Center, and the Clinical Investigation Regulatory and Human Research Protection Offices of the U.S. Army Medical Research and Materiel Command. Written informed consent was obtained from all subjects in person at LRMC; no surrogate consent was allowed by the funding agency. Competence to provide informed consent was assessed in a standardized fashion based on responses to questions regarding the purpose of the study, expected requirements for participation, and potential risks. Additional written consent was obtained from the subjects at the time of follow-up at Washington University. Active duty military subjects were not paid for participation, though travel expenses to St Louis were covered. Subjects not on active military duty status at the time of follow-up in St Louis were paid $240 plus travel expenses for participation.

We enrolled 255 subjects, 97 non-blast control, 35 blast control, 44 non-blast TBI, and 79 blast TBI. Most subjects were young, white, male, enlisted, service members in the US Army (Table 1) as has been reported in previously cohorts enrolled at LRMC [25]. Medical evacuation of both control groups were mostly for gastrointestinal, dermatological, and women's health reasons. Orthopedic injuries from non-combat events such as broken bones resulting from recreational sports on time off or work-related accidents also comprised a subset of the control population. All clinical histories from the controls indicated no current or previous diagnoses of TBI with the blast control group endorsing previous history of blast exposure.

For the blast-TBI group, all available clinical histories indicated blast exposure plus another mechanism of head injury such as a fall, motor vehicle crash, or being struck by a blunt object. None suffered an isolated blast injury. The mechanisms of injury for the non-blast TBI

group were primarily falls, motor vehicle crashes, or being struck by a blunt object.that did not involve blast exposure. Diagnosis of TBI was typically made based on self-report of alteration of neurologic function either due to a blast or non-blast event[26]. Medical documentation regarding duration of loss of consciousness and post-traumatic amnesia was often not available or not reliable. All available clinical histories indicated change in level of consciousness or loss of consciousness for a few minutes and post-traumatic amnesia for less than 24 hours. The requirement for in-person informed consent made more severe TBI patients typically not eligible and none were enrolled. No intracranial abnormalities were detected on non-contrast head CT. Thus, all TBI subjects met the DoD criteria for uncomplicated 'mild' TBI. While previous literature has used the term 'mild' to describe TBI on the lower end of the spectrum of severity, we now prefer the term 'concussive' to describe these injuries.

All clinical histories were verified by study personnel taking additional clinical history and reviewing medical records. None that screened positive for TBI were determined not to have had a TBI upon further inspection.

Of these subjects, 177 followed up at Washington University 6-12 months after enrollment; 69 non-blast control, 26 blast control, 30 non-blast TBI, and 52 blast TBI (Table 1). Reasons for inability of subjects to follow-up at Washington University included redeployment to Afghanistan, reassignment to military position overseas, inability or unwillingness to travel to St. Louis , withdrawal of consent, and inability to maintain telephone or email contact.

Clinical Assessments: Initial records of clinical status in TBI subjects assessed at LRMC using the military acute concussion evaluation (MACE) [26] were reviewed. This brief cognitive

test assesses orientation, immediate verbal memory, concentration, and short term delayed verbal memory.

Overall clinical outcome was assessed using the Glasgow outcome scale extended (GOS-E) [27, 28] by telephone or email monthly for 6-12 months. The GOS-E is scored from 1-8: 1=dead, 2=vegetative, 3-4=severe disability, 5-6=moderate disability, 7-8=good recovery. Moderate disability (GOS-E = 5-6) is defined as one or more of the following: 1) inability to work to previous capacity 2) inability to resume the majority of regular social and leisure activities outside the home 3) psychological problems which have frequently resulted in ongoing family disruption or disruption of friendships. Severe disability is defined as reduced ability to perform activities of daily living such that supervision is required. Standardized, structured interviews were performed according to published guidelines [27]. The last assessment prior to in-person follow-up was considered the final outcome. Information was gathered separately from both the subject and a collateral source (typically a spouse, parent, or sibling) whenever possible. When information from the subject and the collateral source differed, the worse outcome was used.

The in-person clinical evaluations included a standardized neurological exam, neuropsychological test battery, and psychiatric evaluation. The neurological exam included a structured interview designed for TBI patients (Neurobehavioral Rating Scale-Revised [29]), two headache interviews to capture recent headache frequency and intensity (MIDAS, HIT-6)[30, 31] , and the Neurological Outcome Scale for TBI [32-34]. The Neurobehavioral Rating Scale – Revised was scored using a previously published 5 sub-domain model[35].

The neuropsychological test battery consisted of the Conner's Continuous Performance Test II [36], a computer-based assessment of attention, impulsivity, reaction time, and vigilance;

the California Verbal Learning Test II [37], an assessment of verbal declarative memory; the 25 hole grooved pegboard test [38], an assessment of upper extremity motor speed and coordination; a timed 25 foot walk; the Trail Making test [39], an assessment of visual scanning, coordination and mental flexibility; the Controlled Oral Word Association test [40], an assessment of verbal fluency; the Wechsler Test of Adult Reading [41] as an estimate of pre-injury verbal intelligence; the Iowa Gambling Test[42], a computer-based assessment of impulsivity and decision making; the D-KEFS Color-Word Interference Test [43], an multi-domain assessment of executive function similar to the Stroop test; and the Ruff-Light Trail Learning Test[44], an assessment of visual-spatial memory. A relatively easy forced choice test embedded in the California Verbal Learning Test was used to assess adequacy of effort.

The psychiatric evaluation included the Clinician-Administered PTSD Scale for DSM-IV (CAPS) [45], Montgomery-Asberg Depression Rating Scale (MADRS) [46], Combat Exposures Scale[47], the Michigan Alcohol Screening Test[48], and a general questionnaire devised in house regarding alcohol intake information for both current and lifetime use. The CAPS was scored using standard scoring rules from the Blake et al, National Center for Post-traumatic Stress Disorder, July 1998 revision.

The standardized neurological exam and interview required approximately 1 hour per subject. The psychiatric assessments required approximately 2 hours per subject, and the neuropsychological battery required approximately 2 hours per subject. Subjects took all medications as prescribed by their clinical providers. All tests were performed between 9 am and 5 pm in private, quiet, well-lighted rooms. All examiners were blinded to other clinical information and imaging results, though in the course of the interviews it often became clear whether the subjects were in the TBI or control group based off their endorsements of prior

events. All examiners were clinicians who underwent standardized training in administering the assessments.

Safety and Data Monitoring: Subjects were assigned a random 4 digit code number to protect confidentiality and all research data was identified by code number only. A board certified psychiatrist (Dr. Nelson) was immediately available in case the CAPS examination exacerbated PTSD symptoms. No exacerbations requiring medical intervention occurred, though additional support from study staff was required on several occasions.

For clinical evaluations, the principal investigator audited 1 in 10 randomly selected subjects' data sets to ensure that data was scored and entered correctly. These audits revealed only minor discrepancies in scoring criteria which were then corrected across the entire cohort of subjects.

Statistical Analyses: All data was analyzed using Statistica 6.0 (Statsoft Inc). Continuous variables have been summarized as mean ± standard deviation unless otherwise specified. The normal distribution of each continuous variable was assessed using the Shapiro-Wilk test. For normally distributed variables, Analysis of Variance and student's t tests were used to compare groups. For non-normally distributed variables, Kruskal-Wallis Test and Mann-Whitney U (MWU) tests were used. We pre-specified the hypothesis that TBI subjects would have worse outcomes than controls, but did not pre-specify any hypotheses regarding blast TBI vs non-blast TBI subjects. One-sided tests were used when hypotheses were pre-specified, and two-sided tests were used otherwise. Uncorrected p-values have been reported, but only considered significant if $p<0.05$ after Bonferroni correction for multiple comparisons within each class of variables. The 4 main comparisons of interest were: 1, Non-blast control vs Non-blast

TBI; 2, Non-blast control vs Blast control; 3, Blast control vs Blast TBI; 4, Blast TBI vs Non-blast TBI.

Logistic regression analysis was utilized to explore the relationship between measures of global outcome and measures of neurobehavioral impairment, psychiatric symptomatology, and neuropsychological performance. The NRS, the 5 NRS sub-domains, HIT-6, MIDAS, CAPS, MADRS, Combat Exposures Scale, and neuropsychological test measures were used as continuous predictors, along with TBI diagnoses as a categorical variable. The Statistica generalized linear/nonlinear model building software was used with the selection of the logit model that assumes a binomial distribution. The dependent variable was the dichotomized GOSE for good recovery or moderate to severe disability. Best subsets were summarized and ranked by Akaike IC score. The top combinations of variables were then run independently through the model building software again to determine odds ratio, confidence interval, and ROC curve for each model.

Clinical Trials Identifier: The study was registered at clinicaltrials.gov (NCT01313130).

RESULTS

Scores on the military acute concussion evaluation (MACE) completed after medical evacuation to Landstuhl, Germany did not significantly differ between non-blast and blast TBI subjects (25.32 ± 3.36 non-blast TBI, 24.8 ± 3.22 blast TBI, p=0.42, 2-sided Student's t) suggesting similar levels of initial concussion impairment in both TBI groups. Mean time from injury to enrolment was 11.58 ± 9.3 days (blast TBI) and 12.79 ± 9.9 days (non-blast TBI) with a total range of 0-30 days.

Global Outcomes

Global outcome was worse in both TBI groups than in either of the control groups (**Fig 1**). Non-blast TBI subjects were significantly more disabled than non-blast controls (p=0.00005, MWU). Likewise blast TBI subjects were significantly worse than blast control subjects (p=0.009, MWU); a finding replicated from our previous cohort (see Mac Donald etal, submitted. There were no differences in global outcome as evidenced by the GOS-E between the blast TBI vs. non-blast TBI groups (p=0.86, MWU), nor were there differences between the blast control vs. non-blast control groups (p=0.16, MWU). 39/50 blast TBI subjects (78%) and 24/30 non-blast TBI subjects (80%) had moderate to severe disability defined as GOS-E score of 6 or less. 15/26 blast controls (58%) and 28/69 non-blast controls (41%) also met this criteria. The subjects not available for in person follow-up 6-12 months after enrollment did not differ from those that were available for follow-up by group on the GOS-E (p-value range 0.46-0.85 across groups, MWU test per group).

Neuropsychological Testing

There were no substantial differences across groups on the neuropsychological testing (**Table 2**). Only a few exams identified differences and solely in the non-blast TBI group. Significantly worse performance was noted in the non-blast TBI group in comparison to the non-blast controls on the 25-foot walk (p=0.0037, MWU), Grooved Peg Board (p=0.002, MWU), and the assessment for proactive memory interference on the California Verbal Learning Test (p=0.0076, MWU). There were no differences in performance in the blast control vs. non-blast control, blast TBI vs. blast control, or blast TBI vs. non-blast TBI groups.

Further quantification of the number of neurospychological abnormalities per subject did yield more significant results (**Fig 2**). Abnormal performance was defined as a score that fell 2 standard deviations outside the mean non-blast control group in the direction of worse performance for each assessment (i.e. T-scores higher is better while timed tasks higher is worse). Both the non-blast TBI and blast TBI groups had higher number of subjects with abnormalities on neuropsychological performance in 2 or more assessments by Chi-Square comparison of the expected vs. observed distribution (non-blast TBI, p=0.0098; blast TBI p=0.0002). Blast controls did not differ from non-blast controls, nor did they differ from the expected binomial distribution for their group size. This result indicates that subsets of subjects in both the blast TBI and non-blast TBI groups were impaired in neuropsychological performance; even through the group means were generally not different from controls.

Neurobehavioral Assessment

The neurological assessments consistently showed greater impact of neurobehavioral deficits, for both TBI groups in comparison to non-blast controls (**Fig 3A-F**)**.** Non-blast TBI subjects showed significantly more neurobehavioral impairment than non-blast controls on the Neurological Rating Scale-Revised (p=0.00001, MWU) and each of the 5 subdomains with the exception of 'Positive Symptoms' **Fig 3E** (mood/affect p=0.000007 **Fig 3B**; executive/cognitive p=0.00003 **Fig 3C**; oral/motor p=0.00009 **Fig 3D**; negative symptoms p=0.0014 **Fig 3F,** all MWU). There was no difference between non-blast TBI and blast TBI groups (NRS p=0.66; mood/affect p=0.78; executive/cognitive p=0.48; oral/motor p=0.18; positive symptoms p=0.61; negative symptoms p=0.72, all MWU). Blast controls did differ from non-blast controls on the total NRS (p=0.003, MWU) and the mood/affect subdomain (p=0.003, MWU). No significant differences were observed comparing blast controls and blast TBI patients (NRS p=0.07;

mood/affect p=0.17; executive/cognitive p=0.23; oral/motor p=0.54; positive symptoms p=0.23; negative symptoms p=0.09, all MWU). The neurological outcome scale for traumatic brain injury (NOS-TBI) only identified significant impairment in the non-blast TBI group in comparison to the non-blast controls (p-0.006, MWU) (**Fig 4A**). No difference was observed on the NOS-TBI supplement across groups, an examination of gait and limb ataxia (**Fig 4B**).

Headache

Headache impairment was assessed using the MIDAS (**Fig 5**) and HIT6 (**Fig 6**). Non-blast TBI subjects scored significantly higher than non-blast controls on the MIDAS (p=0.000001, MWU) and each of its sub-scores (MIDAS grade p=0.000001, **Fig 5B**; MIDAS-A score for frequency p=0.000001, **Fig 5C**; MIDAS-B score for pain p=0.0004. **Fig 5D**, all MWU). There was no difference in non-blast TBI and blast TBI patients (MIDAS p=0.34; MIDAS grade p=0.23; MIDAS-A p=0.06; MIDAS-B p=0.59, all MWU). Blast controls did differ from non-blast controls on MIDAS-A, a measure of headache frequency (p=0.001, MWU). Similarly, non-blast TBI subjects showed significantly higher levels of headache impairment on the HIT-6 (p<0.0000001, MWU) and most of its weighted measures describing frequency (**Fig 6A-F**) (Never, p<0.0000001; Rarely, p=0.90; Sometimes, p=0.00007; Very often, p=0.00001; Always, p=0.00002. all MWU). There were no significant differences on the HIT-6 between non-blast TBI and blast TBI patients (HIT-6, p=0.14; Never, p=0.05; Rarely, p=0.52; Sometimes, p=0.14; Very often, p=0.37; Always, p=0.14, all MWU). Blast controls did differ from non-blast controls on the HIT-6 total (p=0.003, MWU) and the 'never' frequency measure (p=0.005, MWU). While 23% of non-blast controls were found to have impairment due to headache significant enough warrant suggested follow up with a physician by the HIT-6[31]

criteria, 46% of blast control, 64% of blast TBI, and 83% of non-blast TBI subjects also met this criterion.

Post-Traumatic Stress Disorder and Depression

Consistent with the neurobehavioral and headache evaluations, the psychiatric evaluations revealed worse severity of Depression and PTSD symptomatology in both TBI groups than controls (**Fig 7-8**). Total CAPS scores for PTSD severity were significantly increased in the non-blast TBI subjects in comparison to non-blast controls (p=0.000001, MWU) (**Fig 7A**). Of the three CAPS sub-severity scores, CAPS-D severity for increased arousal and hypervigilance (p=0.00001, MWU, **Fig 7D**) and CAPS-C severity for avoidance and numbing (p=0.00001, MWU, **Fig 7C**) were most impacted followed by CAPS-B severity for re-experiencing traumatic events (p=0.00007, MWU, **Fig 7B**). There was no difference in any of the PTSD severity scores between non-blast TBI and blast TBI subjects (CAPS total, p=0.68; CAPS-B, p=0.62; CAPS-C, p=0.23; CAPS-D, p=0.57; all MWU). Blast controls did significantly differ from non-blast controls on all of the measures (CAPS total, p=0.002; CAPS-B, p=0.0007; CAPS-C, p=0.007; CAPS-D, 0.008; all MWU).

Depression was also significantly worse in the non-blast TBI subjects in comparison to non-blast controls (p=0.000005, MWU) (**Fig 8**). Again no difference was observed comparing the blast TBI to non-blast TBI groups (p=0.26, MWU). There was a trend in blast controls towards worse depression than non-blast controls but it did not reach significance after correction for multiple comparisons (p=0.03, MWU).

Combat Exposure Intensity

Interestingly PTSD and depression severity were not solely related to combat exposure as the severity of combat exposure was highest in the blast controls and blast TBI subjects (**Fig 9**). It did not follow the same relationship as the CAPS scores for PTSD. Blast-controls had significantly higher levels of combat exposure than non-blast controls (p=0.0012, MWU) as did blast TBI in comparison to non-blast TBI subjects (p=0.00003, MWU).

Assessment for Alcohol Misuse

In contrast, there were no significant differences in the scores for any of the groups on the Michigan Alcohol Screening Test (p-value range 0.1-0.8 across groups, MWU test per group) (**Fig 10**). Self-reported alcohol use did not appear to be contributing to the clinical presentation of these patients at the time of follow up.

Impact of Poor Sleep

An index of poor sleep was taken from subsection D-1 of the CAPS comparing the number of hours of sleep reported to the number of hours sleep desired. This difference we refer to as poor sleep index and it was found to strongly correlate with total severity scores on the CAPS, MADRS, NRS, MIDAS, and HIT-6 (**Fig 11**). It did not correlate with any other metric of combat exposure, alcohol misuse, or neuropsychological testing performance.

Multivariate Predictors of Global Outcome

Logistic regression exploring the relationship between the GOS-E score as a measure of global outcome and the measures of neurobehavioral, headache, neuropsychological, and psychiatric impairment revealed only a modest interaction. Regression modeling identified the HIT-6 (headache), CAPS score (PTSD), number of neuropsychological abnormalities, and

'control' or 'TBI' distinction to have the strongest relation to a dichotomized measure of the GOS-E using good recovery as GOS-E 7-8, and bad recovery as GOS-E of 6 or less (Odd Ratio, 5.35, 95% CI -4.25 : -0.38). The results suggest that our current measures of impairment do not seem to completely explain global outcome.

DISCUSSION

In general worse global outcome was observed in both blast TBI and non-blast TBI patients in comparison to controls. Depression and PTSD symptomatology were more severe in both of the TBI groups unrelated to combat exposure. Neurobehavioral impairment was worse in the TBI groups with mood/affect appearing to drive much of this result. Significant impairment of headache was also worse in both TBI groups. Although there were very few group differences in the neuropsychological testing, on a single subject bases, poor performance in more than 2 assessments was significantly increased in both TBI groups in comparison to controls. These findings suggest a greater impact of concussive TBI on chronic outcome in active-duty US military deployed to war zones than previously appreciated that appears to be independent of mechanism of brain injury.

Blast controls did appear slightly worse on neurobehavioral, and psychiatric measures as well as headache impairment in comparison to non-blast controls. Neuropsychological test performance was no different than non-blast controls while combat exposure was significantly increased in comparison. This supports claims that increases in combat exposure can negatively influence outcome, although the contribution of concussive brain injury exacerbates this effect even when combat exposure is less as was the case for the non-blast TBI subjects.

Strengths of this study include the prospective design, direct comparison of blast and non-blast TBI patients, the addition of a blast exposed control group, and blinded clinical evaluations completed by trained personnel. Limitations include modest sample size, potential selection bias given these were all patients who were medically evacuated from theater, and lack of baseline clinical data for comparison. In addition, we were unable to get good measures of sleep disorders using approaches such as actigraphy due to limited resources and we were unable to control for medication and current interventions at the time of follow up. With regard to headache, we only globally collected headache information and did not thoroughly explore other potential contributions such as cervical segmental joint dysfunction, neck flexor endurance, or neck musculature tightness, among others that are commonly known to contribute to chronic post-traumatic headache[49].

In general our findings support previous work and expand upon the growing body of literature investigating different mechanisms of brain injury and their impact on outcome[6, 18]. The exacerbation of PTSD symptomatology following concussive brain injury is in line with prior studies that showed similar relationships specifically in blast TBI patients following loss of consciousness[17], self-report surveys in OIF/OEF veterans[22], and subjective complaint measures comparing pre and post-deployment[50]. Here we expand this to a prospective study of both blast and non-blast TBI subjects finding that both appear to have more severe PTSD symptomatology. Combat exposure did not solely account for this PTSD outcome and it appeared that brain injury contributed more to the exacerbation of this psychiatric symptomatology. It may be the case that injury to specific brain regions sustained in both TBI groups, is reducing the likelihood of the subject to extinguish traumatic combat memories and thus contributing to the chronic effects of post-traumatic stress[51]. The general lack of neuropsychological findings by group is also in line

with previous work[21, 22], although upon further inspection at the single subject level, we found significantly worse performance across measures in both TBI groups than would have been expected by chance (**Fig 2**) . The overall findings regarding headache impact were also consistent with prior reports although on the higher side of the very broad range of previously published prevalence following concussive brain injury[52]. While 23% of non-blast controls were found to have impairment due to headache significant enough warrant suggested follow up with a physician by the HIT-6[31] criteria, 46% of blast control, 64% of blast TBI, and 83% of non-blast TBI also met this criterion. This is higher than the 20% previously reported in the military following concussion[53], but within the broad range of 18-90% noted in prior studies of individuals with post-traumatic headache following 'mild' brain injury [52, 54-59].

Future work will be required to understand the underlying mechanism of how concussive brain injury contributes to poor psychiatric outcome and significant headache impairment in this population. It has been suggested by others that similar pathways involved in headache and PTSD exist[60, 61]. Prior work has identified very high levels of co-occurring post-traumatic headache and PTSD following 'mild' TBI in veterans[62-64]. It is likely that a better understanding of this relationship will lead to new treatments for both phenomena positively impacting outcome in these patients. Furthermore, the modest relationship between global outcome and the best fit models of logistic regression suggests that possibly new evaluations tools, specific for the concussive TBI population may be warranted. Development of novel methods for the evaluation of realms such as social and emotional intelligence may lead to a better understanding of overall outcome following this type of injury.

Acknowledgements: We would like to thank the participants, their families, commanding officers, and clinical providers for making this study possible. We are grateful for the assistance of the Washington University clinical assessment team including Leslie French, PhD, Justin Hampton, Erick Shumaker, PhD, Kathryn Salmo, Kathryn Stinson, Danielle Marinucci, April Reupke, Meghan Jenkins, Natasha Hilts, Christine Lakey, Amanda Hiesele and Laura Daigh.

The study was funded by the Congressionally Directed Medical Research Program (PT090444-PI: Brody). The views expressed in this article are those of the authors and do not reflect the official policy of the Department of the Army, Department of Defense, or U.S. Government.

Author Disclosure Statement:

The authors declare that there are no relevant financial relationships and no conflicts of interest.

REFERENCES

1. Coronado, V.G., McGuire, L.C., Sarmiento, K., Bell, J., Lionbarger, M.R., Jones, C.D., Geller, A.I., Khoury, N. and Xu, L. (2012). Trends in Traumatic Brain Injury in the U.S. and the public health response: 1995-2009. Journal of safety research 43, 299-307.
2. Centers for Disease Control and Prevention (CDC), N.C.f.I.P.a.C. (2003). Report to Congress on mild traumatic brain injury in the United States: steps to prevent a serious public health problem: Atlanta (GA): Centers for Disease Control and Prevention.
3. Taniellian, T. and Jaycox, L. (2008). Invisible Wounds of War: Psychological and Cognitive Injuries, Their Consequences, and Services to Assist Recovery. RAND Corporation.
4. Casscells, S. (2007). Traumatic Brain Injury: Definition and Reporting. In: Defense Aso, ed.: Department of Defense.
5. Kennedy, J.E., Leal, F.O., Lewis, J.D., Cullen, M.A. and Amador, R.R. (2010). Posttraumatic stress symptoms in OIF/OEF service members with blast-related and non-blast-related mild TBI. NeuroRehabilitation 26, 223-231.
6. Belanger, H.G., Proctor-Weber, Z., Kretzmer, T., Kim, M., French, L.M. and Vanderploeg, R.D. (2011). Symptom complaints following reports of blast versus non-blast mild TBI: does mechanism of injury matter? The Clinical neuropsychologist 25, 702-715.
7. Schneiderman, A.I., Braver, E.R. and Kang, H.K. (2008). Understanding sequelae of injury mechanisms and mild traumatic brain injury incurred during the conflicts in Iraq and Afghanistan: persistent postconcussive symptoms and posttraumatic stress disorder. American journal of epidemiology 167, 1446-1452.
8. Hoge, C.W., McGurk, D., Thomas, J.L., Cox, A.L., Engel, C.C. and Castro, C.A. (2008). Mild traumatic brain injury in U.S. Soldiers returning from Iraq. The New England journal of medicine 358, 453-463.
9. Polusny, M.A., Kehle, S.M., Nelson, N.W., Erbes, C.R., Arbisi, P.A. and Thuras, P. (2011). Longitudinal effects of mild traumatic brain injury and posttraumatic stress disorder comorbidity on postdeployment outcomes in national guard soldiers deployed to Iraq. Archives of general psychiatry 68, 79-89.
10. Thomas, J.L., Wilk, J.E., Riviere, L.A., McGurk, D., Castro, C.A. and Hoge, C.W. (2010). Prevalence of mental health problems and functional impairment among active component and National Guard soldiers 3 and 12 months following combat in Iraq. Archives of general psychiatry 67, 614-623.
11. Wilk, J.E., Herrell, R.K., Wynn, G.H., Riviere, L.A. and Hoge, C.W. (2012). Mild traumatic brain injury (concussion), posttraumatic stress disorder, and depression in U.S. soldiers involved in combat deployments: association with postdeployment symptoms. Psychosomatic medicine 74, 249-257.
12. Wilk, J.E., Thomas, J.L., McGurk, D.M., Riviere, L.A., Castro, C.A. and Hoge, C.W. (2010). Mild traumatic brain injury (concussion) during combat: lack of association of blast mechanism with persistent postconcussive symptoms. The Journal of head trauma rehabilitation 25, 9-14.
13. Kontos, A.P., Kotwal, R.S., Elbin, R.J., Lutz, R.H., Forsten, R.D., Benson, P.J. and Guskiewicz, K.M. (2013). Residual effects of combat-related mild traumatic brain injury. Journal of neurotrauma 30, 680-686.
14. Cooper, D.B., Chau, P.M., Armistead-Jehle, P., Vanderploeg, R.D. and Bowles, A.O. (2012). Relationship between mechanism of injury and neurocognitive functioning in OEF/OIF service members with mild traumatic brain injuries. Military medicine 177, 1157-1160.
15. Eskridge, S.L., Macera, C.A., Galarneau, M.R., Holbrook, T.L., Woodruff, S.I., MacGregor, A.J., Morton, D.J. and Shaffer, R.A. (2013). Influence of combat blast-related mild traumatic brain injury acute symptoms on mental health and service discharge outcomes. Journal of neurotrauma 30, 1391-1397.
16. Galarneau, M.R., Woodruff, S.I., Dye, J.L., Mohrle, C.R. and Wade, A.L. (2008). Traumatic brain injury during Operation Iraqi Freedom: findings from the United States Navy-Marine Corps Combat Trauma Registry. Journal of neurosurgery 108, 950-957.

17. Verfaellie, M., Lafleche, G., Spiro, A., 3rd, Tun, C. and Bousquet, K. (2013). Chronic postconcussion symptoms and functional outcomes in OEF/OIF veterans with self-report of blast exposure. J Int Neuropsychol Soc 19, 1-10.
18. Belanger, H.G., Kretzmer, T., Yoash-Gantz, R., Pickett, T. and Tupler, L.A. (2009). Cognitive sequelae of blast-related versus other mechanisms of brain trauma. J Int Neuropsychol Soc 15, 1-8.
19. Luethcke, C.A., Bryan, C.J., Morrow, C.E. and Isler, W.C. (2011). Comparison of concussive symptoms, cognitive performance, and psychological symptoms between acute blast-versus nonblast-induced mild traumatic brain injury. J Int Neuropsychol Soc 17, 36-45.
20. Maguen, S., Madden, E., Lau, K.M. and Seal, K. (2012). The impact of head injury mechanism on mental health symptoms in veterans: do number and type of exposures matter? Journal of traumatic stress 25, 3-9.
21. Spencer, R.J., Drag, L.L., Walker, S.J. and Bieliauskas, L.A. (2010). Self-reported cognitive symptoms following mild traumatic brain injury are poorly associated with neuropsychological performance in OIF/OEF veterans. Journal of rehabilitation research and development 47, 521-530.
22. Drag, L.L., Spencer, R.J., Walker, S.J., Pangilinan, P.H. and Bieliauskas, L.A. (2012). The contributions of self-reported injury characteristics and psychiatric symptoms to cognitive functioning in OEF/OIF veterans with mild traumatic brain injury. J Int Neuropsychol Soc 18, 576-584.
23. Mac Donald, C., Johnson, A., Cooper, D., Malone, T., Sorrell, J., Shimony, J., Parsons, M., Snyder, A., Raichle, M., Fang, R., Flaherty, S., Russell, M. and Brody, D.L. (2013). Cerebellar white matter abnormalities following primary blast injury in US military personnel. PloS one 8, e55823.
24. Han, K., Mac Donald, C.L., Johnson, A.M., Barnes, Y., Wierzechowski, L., Zonies, D., Oh, J., Flaherty, S., Fang, R., Raichle, M.E. and Brody, D.L. (2013). Disrupted modular organization of resting-state cortical functional connectivity in U.S. military personnel following concussive 'mild' blast-related traumatic brain injury. NeuroImage 84C, 76-96.
25. Mac Donald, C.L., Johnson, A.M., Cooper, D., Nelson, E.C., Werner, N.J., Shimony, J.S., Snyder, A.Z., Raichle, M.E., Witherow, J.R., Fang, R., Flaherty, S.F. and Brody, D.L. (2011). Detection of blast-related traumatic brain injury in U.S. military personnel. The New England journal of medicine 364, 2091-2100.
26. Dempsey, K.E., Dorlac, W.C., Martin, K., Fang, R., Fox, C., Bennett, B., Williams, K. and Flaherty, S. (2009). Landstuhl Regional Medical Center: traumatic brain injury screening program. Journal of trauma nursing : the official journal of the Society of Trauma Nurses 16, 6-7, 10-12.
27. Wilson, J.T., Pettigrew, L.E. and Teasdale, G.M. (1998). Structured interviews for the Glasgow Outcome Scale and the extended Glasgow Outcome Scale: guidelines for their use. Journal of neurotrauma 15, 573-585.
28. Pettigrew, L.E., Wilson, J.T. and Teasdale, G.M. (2003). Reliability of ratings on the Glasgow Outcome Scales from in-person and telephone structured interviews. The Journal of head trauma rehabilitation 18, 252-258.
29. Levin, H.S., High, W.M., Goethe, K.E., Sisson, R.A., Overall, J.E., Rhoades, H.M., Eisenberg, H.M., Kalisky, Z. and Gary, H.E. (1987). The neurobehavioural rating scale: assessment of the behavioural sequelae of head injury by the clinician. Journal of neurology, neurosurgery, and psychiatry 50, 183-193.
30. Stewart, W.F., Lipton, R.B., Whyte, J., Dowson, A., Kolodner, K., Liberman, J.N. and Sawyer, J. (1999). An international study to assess reliability of the Migraine Disability Assessment (MIDAS) score. Neurology 53, 988-994.
31. Kosinski, M., Bayliss, M.S., Bjorner, J.B., Ware, J.E., Jr., Garber, W.H., Batenhorst, A., Cady, R., Dahlof, C.G., Dowson, A. and Tepper, S. (2003). A six-item short-form survey for measuring headache impact: the HIT-6. Quality of life research : an international journal of quality of life aspects of treatment, care and rehabilitation 12, 963-974.
32. McCauley, S.R., Wilde, E.A., Kelly, T.M., Weyand, A.M., Yallampalli, R., Waldron, E.J., Pedroza, C., Schnelle, K.P., Boake, C., Levin, H.S. and Moretti, P. (2010). The Neurological Outcome Scale for

Traumatic Brain Injury (NOS-TBI): II. Reliability and convergent validity. Journal of neurotrauma 27, 991-997.
33. Wilde, E.A., McCauley, S.R., Kelly, T.M., Weyand, A.M., Pedroza, C., Levin, H.S., Clifton, G.L., Schnelle, K.P., Shah, M.V. and Moretti, P. (2010). The Neurological Outcome Scale for Traumatic Brain Injury (NOS-TBI): I. Construct validity. Journal of neurotrauma 27, 983-989.
34. Wilde, E.A., McCauley, S.R., Kelly, T.M., Levin, H.S., Pedroza, C., Clifton, G.L., Robertson, C.S., Valadka, A.B. and Moretti, P. (2010). Feasibility of the Neurological Outcome Scale for Traumatic Brain Injury (NOS-TBI) in adults. Journal of neurotrauma 27, 975-981.
35. McCauley, S.R., Levin, H.S., Vanier, M., Mazaux, J.M., Boake, C., Goldfader, P.R., Rockers, D., Butters, M., Kareken, D.A., Lambert, J. and Clifton, G.L. (2001). The neurobehavioural rating scale-revised: sensitivity and validity in closed head injury assessment. Journal of neurology, neurosurgery, and psychiatry 71, 643-651.
36. Conners, C. and Staff., M. (2000). Conners' Continuous Performance Test II: Computer program for Windows technical guide and software manual. Multi-Health Systems: North Tonwanda, NY.
37. Delis D, Kramer J, Kaplan E and B, O. (2000). California Verbal Learning Test Manual: Second Edition, Adult Version. Psychological Corporation: San Antonio, Tx.
38. Matthews C and Kløve, H. (1964). Instruction manual for the Adult Neuropsychology Test Battery. University of Wisconsin Medical School: Madison, WI.
39. Reitan, R. (1992). Trail Making Test manual for administration and scoring. Reitan Neuropsychology Laboratory: Tuscon, AZ.
40. Benton A, Hamsher K and A, S. (1983). Multilingual Aphasia Examination (3rd ed.). AJA Associates: Iowa City, Ia.
41. Wechsler, D. (2001). Wechsler Test of Adult Reading (WTAR) Manual. Psychological Corporation: New York.
42. Bechara, A., Damasio, A.R., Damasio, H. and Anderson, S.W. (1994). Insensitivity to future consequences following damage to human prefrontal cortex. Cognition 50, 7-15.
43. Delis, D.C., Kaplan, E. & Kramer, J.H. (2001). Delis-Kaplan Executive Function System (D-KEFS): *Examiner's manual*. The Psychological Corporation: San Antonio, TX.
44. Ruff, R., Light, R. and Parker, S. (1996). Visuospatial learning: Ruff Light Trail Learning Test. Archives of clinical neuropsychology : the official journal of the National Academy of Neuropsychologists 11, 313-327.
45. Weathers, F.W., Keane, T.M. and Davidson, J.R. (2001). Clinician-administered PTSD scale: a review of the first ten years of research. Depression and anxiety 13, 132-156.
46. Montgomery, S.A. and Asberg, M. (1979). A new depression scale designed to be sensitive to change. The British journal of psychiatry : the journal of mental science 134, 382-389.
47. Keane, T., Fairbank, J., Caddell, J., Zimering, R., Taylor, K. and Mora, C. (1989). Clinical evaluation of a measure to assess combat exposure. Psychological Assessment, 53-55.
48. Selzer, M.L. (1971). The Michigan Alcoholism Screening Test (MAST): The quest for a new diagnostic instrument. American Journal of Psychiatry, 1653-1658.
49. Treleaven, J., Jull, G. and Atkinson, L. (1994). Cervical musculoskeletal dysfunction in post-concussional headache. Cephalalgia : an international journal of headache 14, 273-279; discussion 257.
50. Vasterling, J.J., Brailey, K., Proctor, S.P., Kane, R., Heeren, T. and Franz, M. (2012). Neuropsychological outcomes of mild traumatic brain injury, post-traumatic stress disorder and depression in Iraq-deployed US Army soldiers. The British journal of psychiatry : the journal of mental science 201, 186-192.
51. Myers, K.M. and Davis, M. (2007). Mechanisms of fear extinction. Molecular psychiatry 12, 120-150.
52. Theeler, B., Lucas, S., Riechers, R.G., 2nd and Ruff, R.L. (2013). Post-traumatic headaches in civilians and military personnel: a comparative, clinical review. Headache 53, 881-900.

53. Theeler, B.J., Flynn, F.G. and Erickson, J.C. (2012). Chronic daily headache in U.S. soldiers after concussion. Headache 52, 732-738.
54. Lucas, S., Hoffman, J.M., Bell, K.R., Walker, W. and Dikmen, S. (2012). Characterization of headache after traumatic brain injury. Cephalalgia : an international journal of headache 32, 600-606.
55. Lew, H.L., Lin, P.H., Fuh, J.L., Wang, S.J., Clark, D.J. and Walker, W.C. (2006). Characteristics and treatment of headache after traumatic brain injury: a focused review. American journal of physical medicine & rehabilitation / Association of Academic Physiatrists 85, 619-627.
56. Nampiaparampil, D.E. (2008). Prevalence of chronic pain after traumatic brain injury: a systematic review. JAMA : the journal of the American Medical Association 300, 711-719.
57. Hoffman, J.M., Lucas, S., Dikmen, S., Braden, C.A., Brown, A.W., Brunner, R., Diaz-Arrastia, R., Walker, W.C., Watanabe, T.K. and Bell, K.R. (2011). Natural history of headache after traumatic brain injury. Journal of neurotrauma 28, 1719-1725.
58. O'Neil, M., Carlson, K. and Storzbach, D. (2012). Complications of Mild Traumatic Brain Injury in Veterans and Military Personnel: A Systematic Review. Vol Project #05-225. Department of Veterans Affairs Health Services Research & Development Service: Washington, DC.
59. Keidel, M. and Diener, H.C. (1997). [Post-traumatic headache]. Der Nervenarzt 68, 769-777.
60. Ressler, K.J., Mercer, K.B., Bradley, B., Jovanovic, T., Mahan, A., Kerley, K., Norrholm, S.D., Kilaru, V., Smith, A.K., Myers, A.J., Ramirez, M., Engel, A., Hammack, S.E., Toufexis, D., Braas, K.M., Binder, E.B. and May, V. (2011). Post-traumatic stress disorder is associated with PACAP and the PAC1 receptor. Nature 470, 492-497.
61. Syed, A.U., Koide, M., Braas, K.M., May, V. and Wellman, G.C. (2012). Pituitary adenylate cyclase-activating polypeptide (PACAP) potently dilates middle meningeal arteries: implications for migraine. Journal of molecular neuroscience : MN 48, 574-583.
62. Ruff, R.L., Riechers, R.G., 2nd, Wang, X.F., Piero, T. and Ruff, S.S. (2012). A case-control study examining whether neurological deficits and PTSD in combat veterans are related to episodes of mild TBI. BMJ open 2, e000312.
63. Ruff, R.L., Riechers, R.G., 2nd, Wang, X.F., Piero, T. and Ruff, S.S. (2012). For veterans with mild traumatic brain injury, improved posttraumatic stress disorder severity and sleep correlated with symptomatic improvement. Journal of rehabilitation research and development 49, 1305-1320.
64. Ruff, R.L., Riechers, R.G. and Ruff, S.S. (2010). Relationships between mild traumatic brain injury sustained in combat and post-traumatic stress disorder. F1000 medicine reports 2, 64.

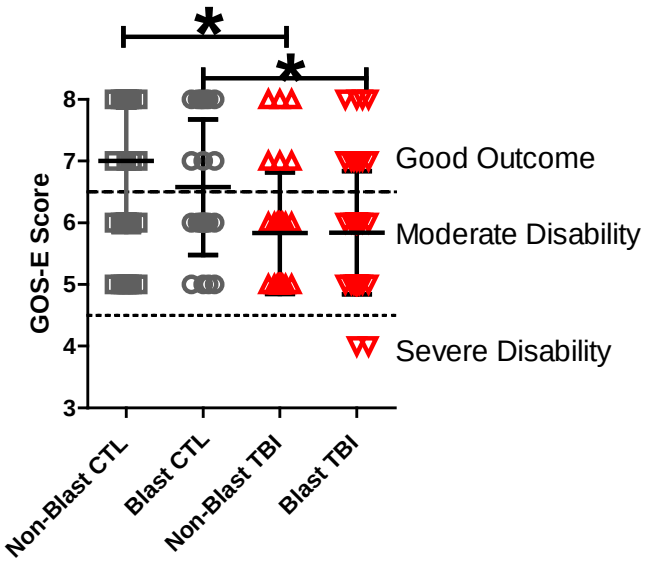

FIG 1: Global outcome in US military personnel. Glasgow Outcome Scale – Extended Results assessed 6-12 months after enrollment. * indicates significant group differences by 1-tailed Mann-Whitney U after correction for multiple comparisons.

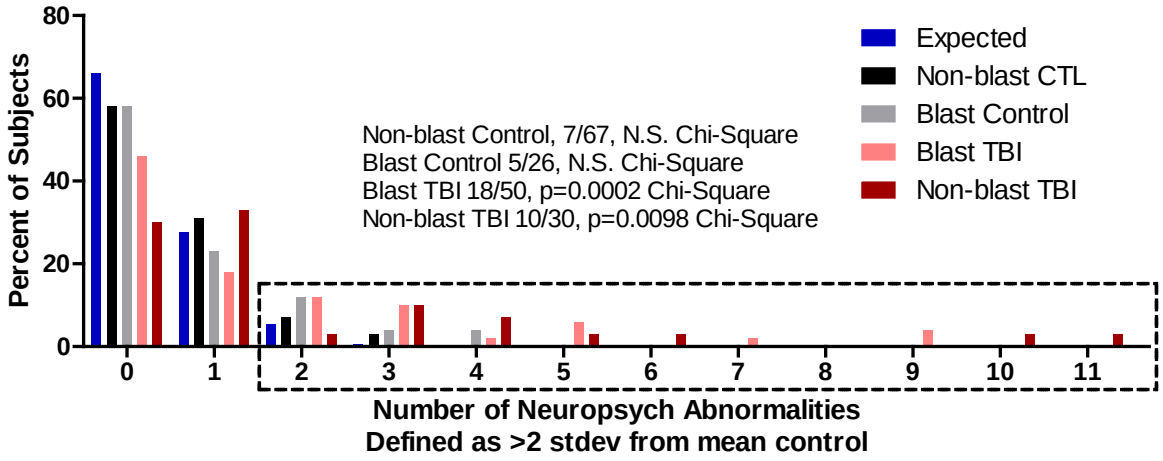

FIG 2: Neuropsychological abnormalities detected across groups. The number of subjects with neuropsychological test abnormalities are displayed by group in comparison to what would be expected by chance (blue bars). Percent of subjects is displayed to account for the differences in the number of subjects across groups. Dotted box indicates the group of subjects who had poor performance on 2 or more of the 18 neuropsychological assessments. P-value calculated using the chi-square test by group.

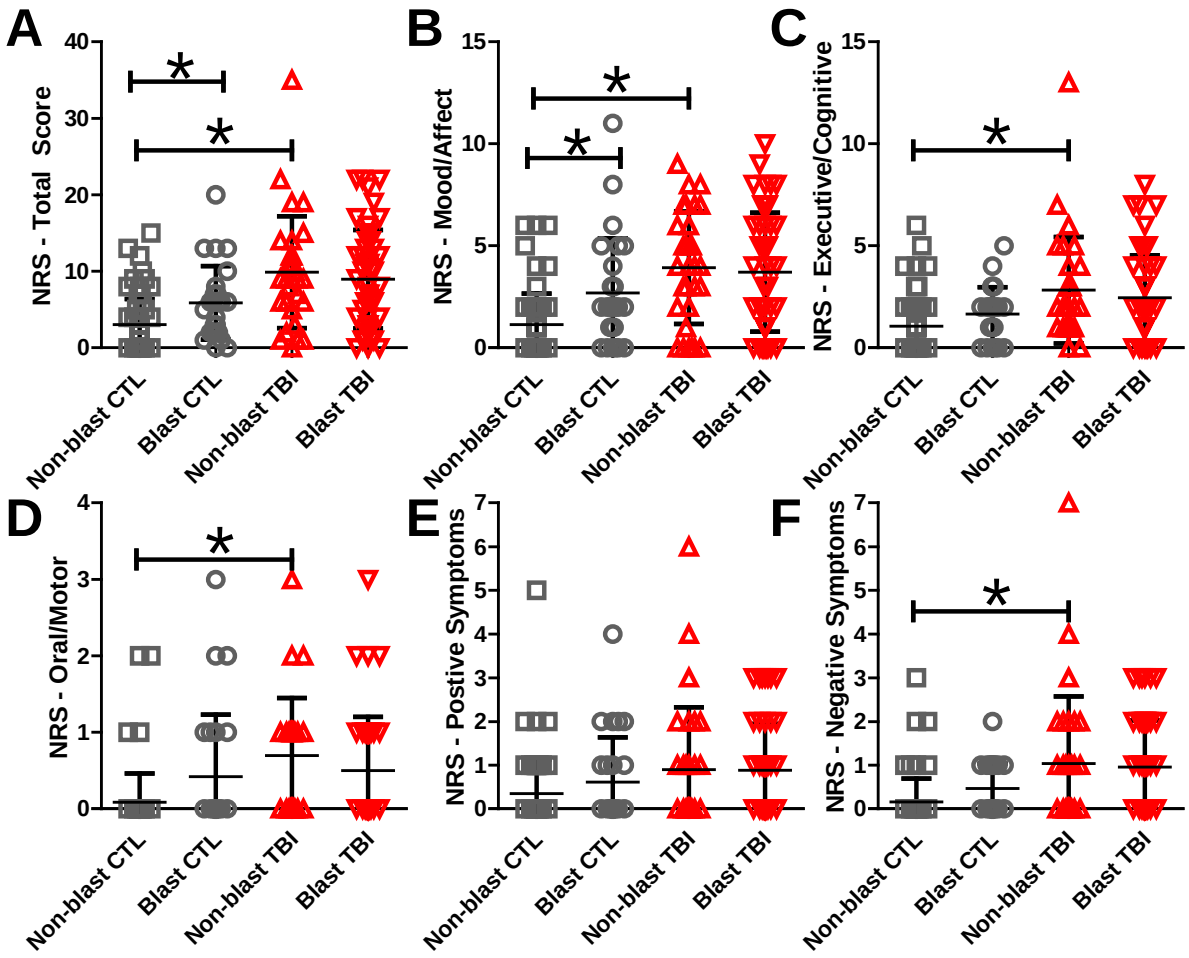

FIG 3: Neurobehavioral measures of outcome. **A.** Neurobehavioral outcome assessed using the Neurological Rating Scale-Revised Total Score: (Max xx),. **B.** Mood/affect domain. **C.** Executive/Cognitive domain. **D.** Oral/motor domain. **E.** Positive Symptoms domain. **F.** Negative Symptoms domain. Higher scores on all of the measures indicate worse impairment. * indicates significant group differences by 1-tailed Mann-Whitney U after correction for multiple comparisons.

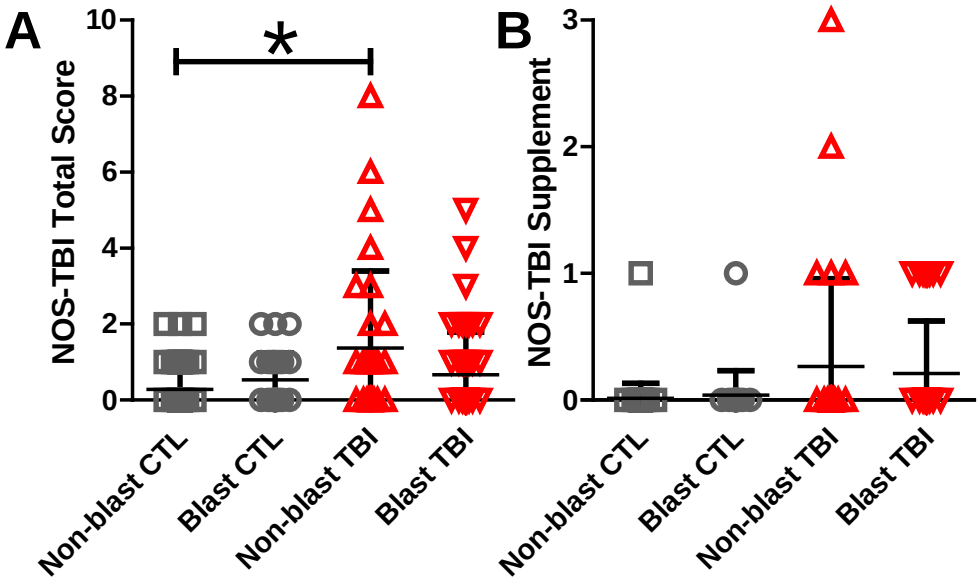

FIG 4: Neurological outcome measures for TBI. A. Neurological outcome for traumatic brain injury assessed using the NOS-TBI. **B.** NOS-TBI Supplement. Higher scores on both measures indicate worse impairment. * indicates significant group differences by 1-tailed Mann-Whitney U after correction for multiple comparisons.

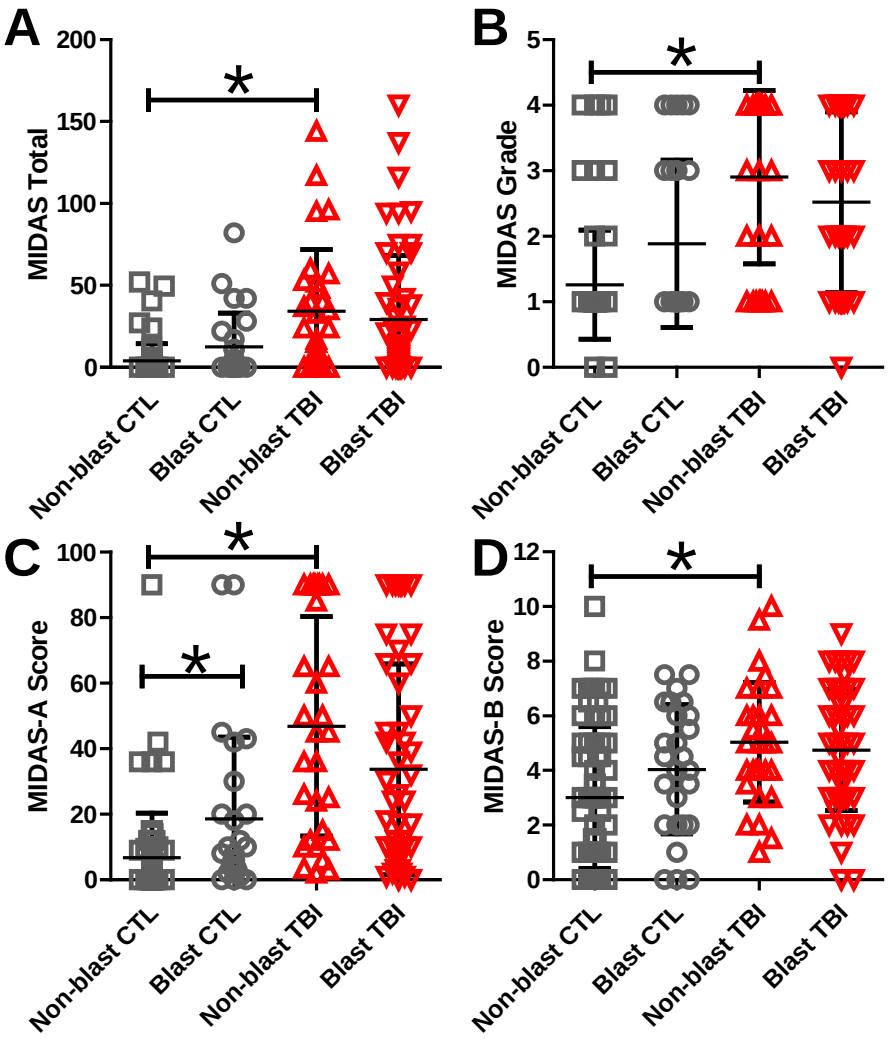

FIG 5: Migraine Disability Assessment. **A.** Headache impairment assessed by the migraine disability assessment test (MIDAS). **B.** Total grade score. **C.** MIDAS-A assessment for frequency. **D.** MIDAS-B assessment for pain. Higher scores on all of the measures indicate worse impairment. * indicates significant group differences by 1-tailed Mann-Whitney U after correction for multiple comparisons.

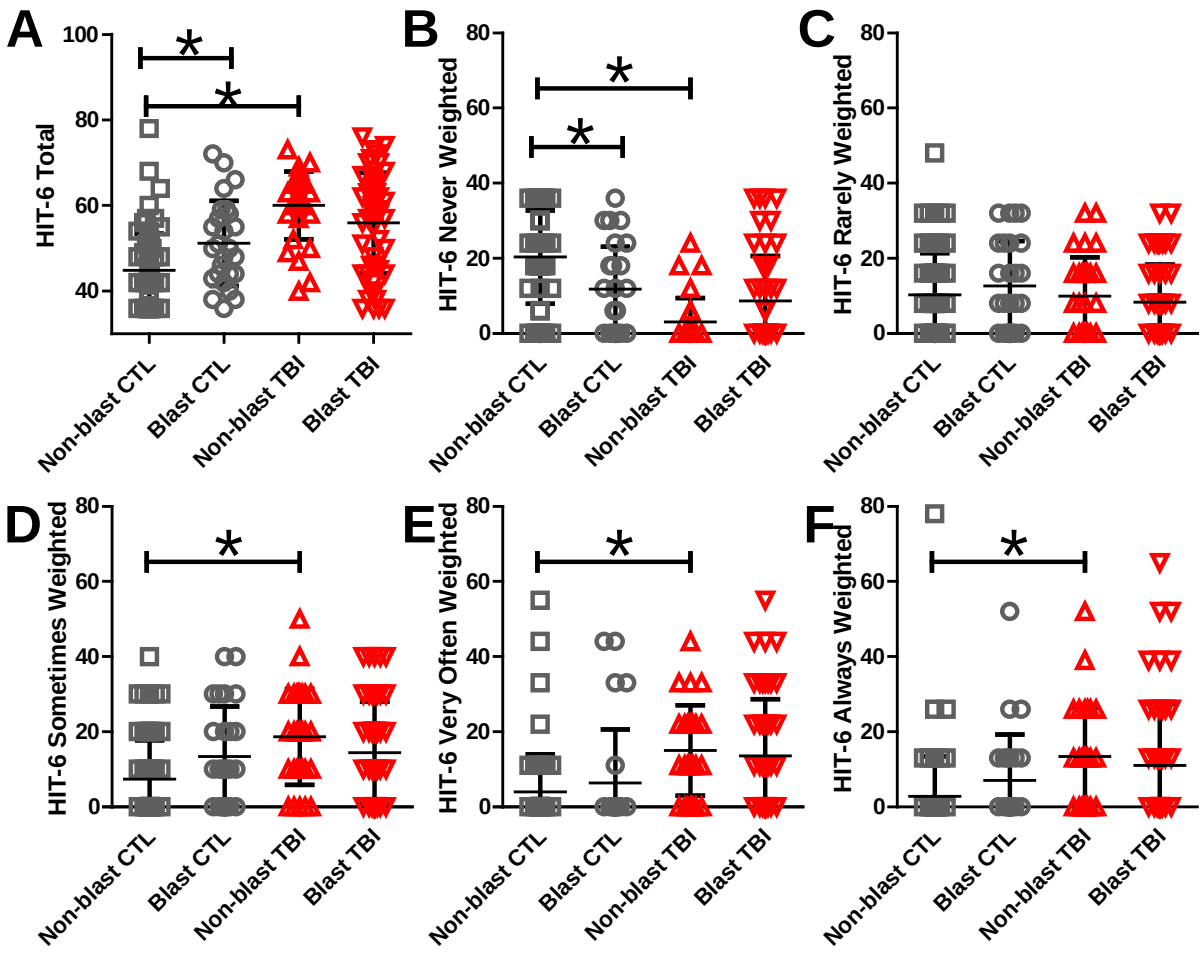

FIG 6: Headache Impairment. **A.** Headache impairment assessed by the headache impact test (HIT-6). **B.** 'Never' as a weighted frequency measure of impairment. **C.** 'Rarely' as a weighted frequency measure of impairment. **D.** 'Sometimes' as a weighted frequency measure of impairment. **E.** 'Very often' as a weighted frequency measure of impairment. **F.** 'Always' as a weighted frequency measure of impairment. Higher scores on all of the measures indicate worse impairment. * indicates significant group differences by 1-tailed Mann-Whitney U after correction for multiple comparisons.

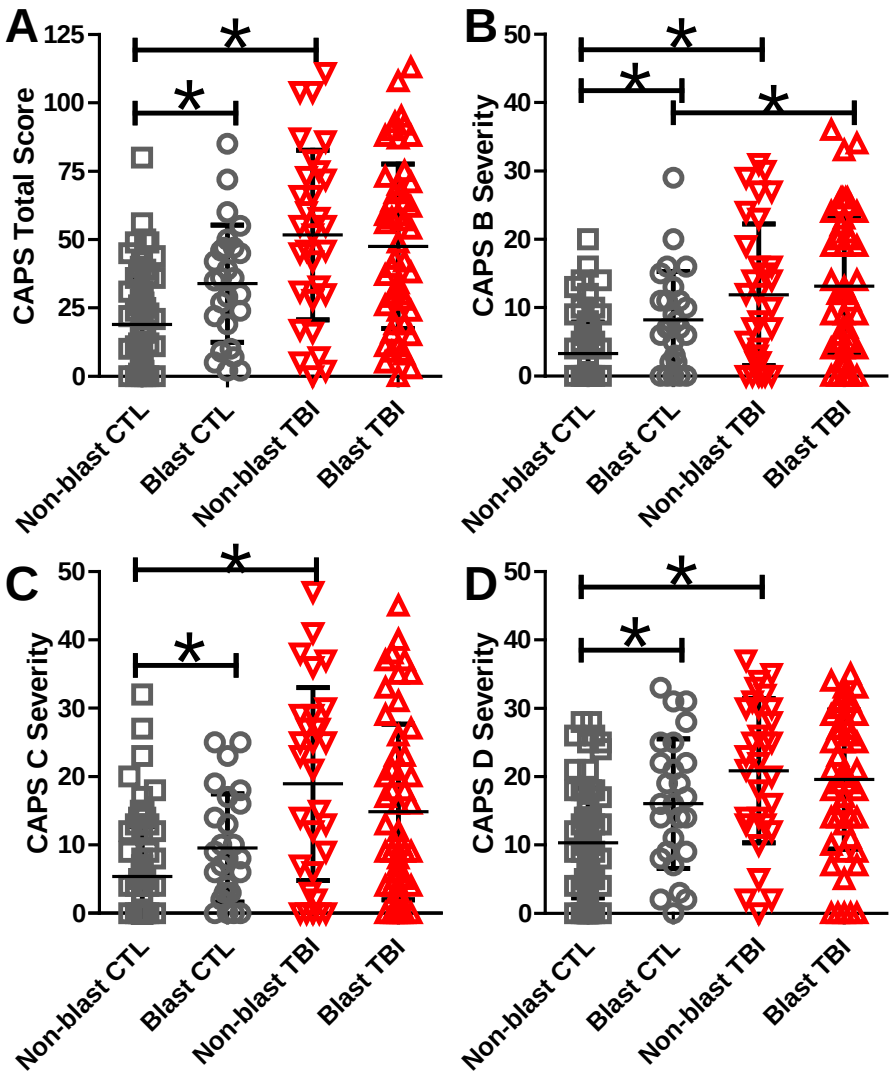

FIG7: Post-Traumatic Stress Disorder Severity. **A.** PTSD severity assessed by the Clinician administered PTSD scale for DSM IV (CAPS). **B.** CAPS B Severity – Re-experiencing. **C.** CAPS C Severity – Avoidance and Numbing. **D.** CAPS D Severity – Increased Arousal and hypervigilance. Higher scores on all of the measures indicate worse impairment. * indicates significant group differences by 1-tailed Mann-Whitney U after correction for multiple comparisons.

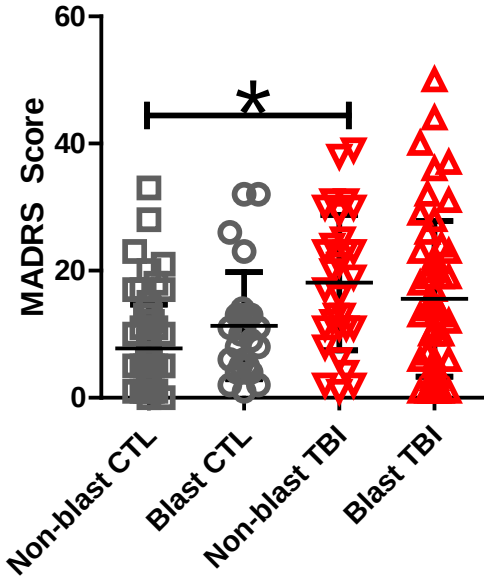

FIG8: Depression Severity. Depression severity assessed by the Montgomery Asberg depression rating scale (MADRS). Higher scores indicate worse impairment. * indicates significant group differences by 1-tailed Mann-Whitney U after correction for multiple comparisons.

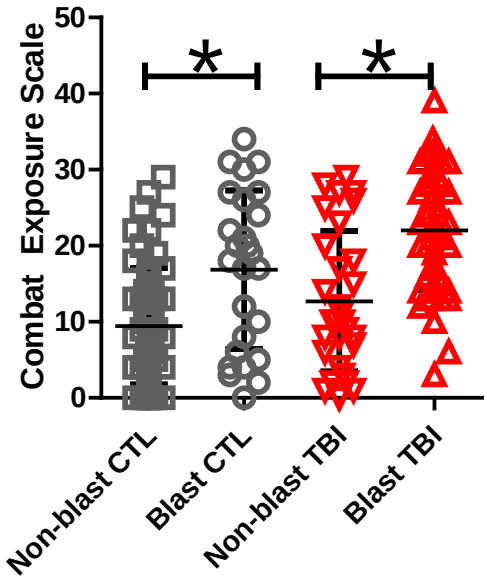

FIG9: Intensity of Combat Exposure. Combat intensity was assessed by the combat exposures scale (CES). Higher scores indicate great combat exposure. * indicates significant group differences by 1-tailed Mann-Whitney U after correction for multiple comparisons.

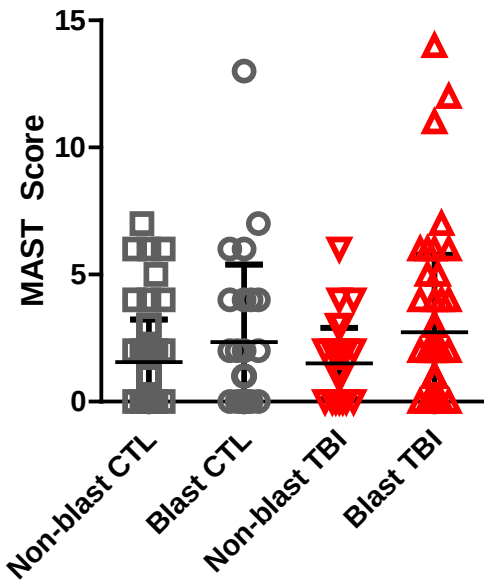

FIG10: Alcohol Misuse. Alcohol misuse was assessed using the Michigan Alcohol Screening Test (MAST). No differences were observed across groups.

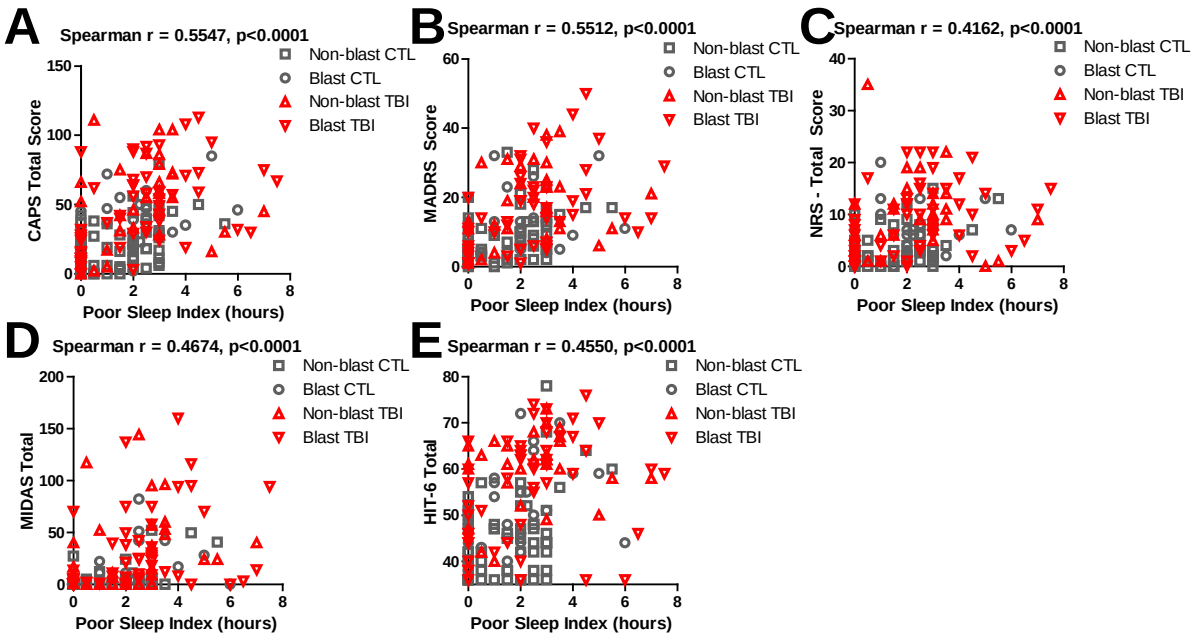

FIG11: Correlations between self-reported poor sleep index (number of hours desired minus number of hours reported) and measures of clinical evaluation. A. Positive correlation with CAPS total severity for PTSD. **B.** Positive correlation with MADRS total severity for depression. **C.** Positive correlation with Neurobehavioral Rating Scale (NRS) for overall neurobehavioral outcome. **D.** Positive correlation with MIDAS for migraine disability. **E.** Positive correlation with HIT-6 for headache impact. Higher scores indicate worse impairment on all of the measures.

Table 1. Characteristics of Study Participants

Characteristic	Non Blast CTL (n=69)	Blast CTL (n=26)	Non Blast TBI (n=30)	Blast TBI (n=50)
Age in years: median (range)	31 (21-49)	33.5 (22-46)	28.5 (20-50)	26 (19-47) [A]
Education in years: median (range)	14 (9-23)	13 (10-18)	14 (9-18)	12 (12-18)
Gender - no (%)				
Male	63 (91.3%)	24 (92.3%)	26 (86.7%)	48 (96%)
Female	6 (8.7%)	2 (7.7%)	4 (13.3%)	2 (4%)
Race/ethnicity* - no (%)				
White	48 (69.6%)	20 (76.9%)	18 (60%)	37 (75.5%)
African American	18 (26.1%)	3 (11.5%)	8 (26.7%)	3 (6.1%)
Hispanic/Latino	3 (4.3%)	2 (7.7%)	3 (10%)	7 (14.3%)
Asian	0	1 (3.9%)	1 (3.3%)	2 (4.1%)
Branch of Service - no (%)				
US Army	55 (79.7%)	23 (88.5%)	27 (90%)	44 (89.8%)
US Air Force	11 (15.9 %)	0	2 (6.7%)	1 (2%)
US Marine Corps	3 (4.3%)	3 (11.5%)	1 (3.3%)	3 (6.1%)
US Navy	0	0	0	1 (3.1%)
Duty Status - no (%)				
Active Duty	43 (62.3%)	18 (69.2%)	20 (66.6%)	36 (72%)
National Guard	23 (33.3%)	7 (26.9%)	5 (16.7%)	10 (20%)
Reserve	3 (4.4%)	1 (3.9%)	5 (16.7%)	4 (8%)
Military Rank - no (%)				
Enlisted	64 (92.7%)	23 (88.5%)	28 (93.3%)	50 (100%)
Officer	5 (7.3%)	3 (11.5%)	2 (6.7%)	
Theatre of Operation - no (%)				
Afghanistan	55 (79.7%)	20 (76.7%)	18 (60%)	47 (94%)
Iraq	14 (20.3%)	6 (23.3%)	12 (40%)	3 (6%)

Superscripted letters indicate significance after correction for multiple comparisons ($p<0.0125$).
Uncorrected p-values are reported.
[A] Blast control v Blast TBI – Mann-Whitney U, $p=0.000026$

Table 2. Neuropsychological Test Performance

Test	Non Blast CTL (n=69)	Blast CTL (n=26)	Non Blast TBI (n=30)	Blast TBI (n=50)
25-Foot Walk (seconds)				
(Motor Strength, Balance, Coordination)	4.00 ± 0.82	4.22 ± 0.66	4.76 ± 1.16 [A]	4.59 ± 1.17
Conners' Continuous Performance Test II				
Omission Errors (T-score):				
(*Attention Lapses*)	49.05 ± 12.17	47.53 ± 7.51	53.30 ± 15.11	51.52 ± 19.8
Commission Errors (T-score):				
(*Impulsivity*)	50.73 ± 10.60	50.34 ± 8.19	52.56 ± 9.81	54.47 ± 10.6
Hit Rate (T-score):				
(*Reaction Time*)	49.24 ± 11.72	49.9 ± 8.67	52.67 ± 12.22	47.66 ± 8.63
Hit Rate Block Change (T-score):				
(*Sustained Vigilance)*	52.03 ± 10.62	48.01 ± 8.82	50.94 ± 13.75	48.23 ± 12.0
Iowa Gambling Test (T-score)				
(Impulsivity)	49.52 ± 10.40	47.62 ± 9.65	46.3 ± 9.91	48.9 ± 11.1
Ruff-Light Trail Learning Test (T-score)				
Trials Correct *(Visual Memory)*	49.53 ± 11.10	52.58 ± 6.54	50.17 ± 10.10	49.02 ± 10.85
Wechsler Test of Adult Reading (Standard Score)				
(Estimate of Pre-injury Verbal Intelligence)	101.88 ± 14.55	100.08 ± 10.99	97.7 ± 11.10	99.32 ± 11.66
California Verbal Learning Test II				
Long-Delay Free Recall (Standard Score)				
(Verbal Memory)	-0.27 ± 1.10	-0.14 ± 0.95	-0.32 ± 1.27	-0.62 ± 1.21
Total Intrusions (Standard Score)				
(Falsely Recalled Items)	0.28 ± 1.00	0.23 ± 0.95	0.52 ± 1.42	0.46 ± 1.38
List B vs. Trial 1 List A (Z-Score)				
(Proactive Memory Interference)	0.07 ± 0.87	-0.13 ± 0.89	0.58 ± 1.03 [B]	-0.17 ± 1.12
Grooved Pegboard				
(Motor Speed & Coordination)				
Average Dom & Non-Dom Time (seconds)	69.78 ± 17.7	68.96 ± 10.56	76.58 ± 15.85 [C]	75.81 ± 15.52
Trail Making Test				
Trails A time (seconds)				
(Visual Scanning, Coordination)	23.16 ± 8.61	24.42 ± 7.41	28.12 ± 14.10	28.97 ± 16.69
Trails B time (seconds)				
(Trails A + Mental Flexibility)	59.61 ± 24.77	57.62 ± 14.97	66.14 ± 31.28	61.37 ± 21.40
Controlled Oral Word Association				
Total Score: *(Verbal Fluency)*	41.3 ± 10.18	40.76 ± 9.05	37.2 ± 9.98	38.16 ± 9.30
D-KFES Color-Word Interference Test				
(Executive Function)				
Color & Word Naming (summed scaled score)	20.45 ± 4.98	18.46 ± 5.85	18.03 ± 7.25	18.70 ± 6.95
Inhibition (scaled score)	10.42 ± 3.02	10.12 ± 2.92	9.17 ± 4.57	9.71 ± 3.39
Inhibition/Switching (scaled score)	10.25 ± 2.88	9.27 ± 3.17	8.86 ± 4.16	9.37 ± 3.20

Superscripted letters indicate significance after correction for multiple comparisons ($p<0.0125$).
Uncorrected p-values are reported.

[A] Non-blast control v Non-blast TBI – Mann-Whitney U, p=0.0037

[B] Blast TBI v Non-blast TBI – Mann-Whitney U, p=0.0076

[C] Non-blast control v Non-blast TBI – Mann-Whitney U, p=0.002